

**METABOLISM AND CELL-TO-CELL INTERACTIONS OF ANAEROBIC
SYNTROPHIC CLOSTRIDIA CO-CULTURES**

by

Hannah Elizabeth Streett

A thesis submitted to the Faculty of the University of Delaware in partial fulfillment
of the requirements for the degree of Master of Science in Biological Sciences

Winter 2019

© 2019 Hannah Elizabeth Streett
All Rights Reserved

**METABOLISM AND CELL-TO-CELL INTERACTIONS OF ANAEROBIC
SYNTROPHIC CLOSTRIDIA CO-CULTURES**

by

Hannah Elizabeth Streett

Approved: _____
Eleftherios Terry Papoutsakis, Ph.D.
Professor in charge of thesis on behalf of the Advisory Committee

Approved: _____
E. Fidelma Boyd, Ph.D.
Interim Chair of the Department of Biological Sciences

Approved: _____
John A. Pelesko, Ph.D.
Interim Dean of the College of Arts and Sciences

Approved: _____
Douglas J. Doren, Ph.D.
Interim Vice Provost for Graduate and Professional Education

ACKNOWLEDGMENTS

I would first like to thank my advisor, E. Terry Papoutsakis, Ph.D., for his patience, guidance, and support throughout my M.S., and look forward to remaining in the Papoutsakis Lab for my Ph.D.. I would also like to thank my committee members, Dr. Boyd and Dr. Neunuebel, for their support, advice, and feedback on my project, as well as Dr. Selva for her advice and guidance regarding classes and our department.

I would also like to thank the entire Papoutsakis lab for their support and feedback throughout my project. I would like to in particular thank Dr. Kyle Bennett for his advice and expertise in bacterial cloning, Chen-Yuan Kao for his guidance regarding fluorescence microscopy and flow cytometry, and Kamil Charubin for his endless advice and expertise regarding *Clostridium spp.* and anaerobic chambers. All three of whom have helped me to become a better scientist and feel like I belong in the Papoutsakis Lab. I would also like to thank my friend and former lab member, Erica Winter, for her support and encouragement in both classes and the Papoutsakis Lab.

I would like to thank my family for their love and support throughout my M.S. and my life, in particular my dad, who doesn't always understand what I am doing but still supports me in everything that I do. His advice and guidance throughout the last few years has meant more to me than I ever thought it would. I would also like to thank my mom for raising me to be the woman I am today, and I know if she were here, she would be proud of what I have accomplished. I would also like to thank my sisters, Emily and Evelyn for being there for me when I need them.

I finally like to thank my boyfriend, Kevin Failor, for his endless love and support of everything I do, and for his encouragement in pursuing graduate school. Without you I would have never made it so far and accomplished so much. I have infinite gratitude for all that you do for me.

TABLE OF CONTENTS

LIST OF TABLES.....	viii
LIST OF FIGURES	ix
ABSTRACT.....	xii
Chapter	
1 INTRODUCTION	1
1.1 <i>Clostridia spp.</i> of Note and Their Respective Metabolic Pathways	1
1.1.1 <i>Clostridium acetobutylicum</i> and Acetone-Butanol-Ethanol Fermentation	1
1.1.2 <i>Clostridium ljungdahlii</i> and the Wood-Ljungdahl Pathway	5
1.1.3 <i>Clostridium kluyveri</i> and Fatty Acid Chain-elongation	8
1.2 The Importance of Co-cultures and Recent Advances in Microbial Co- cultures.....	11
1.3 Reporter Systems in <i>Clostridium spp.</i>	16
1.4 Gene Promoters in <i>Clostridium spp.</i>	25
1.5 Fluorescence in Anaerobic Microbes.....	28
1.6 Fluorescence-Activating and Absorption-Shifting Tag (FAST) Could be a Promising Fluorescent System for Anaerobes	33
2 SYNTROPHIC INTERACTIONS IN CLOSTRIDIA CO-CULTURES....	38
2.1 Introduction.....	38
2.2 Materials and Methods.....	40
2.2.1 Chemicals.....	40
2.2.2 Bacterial Strains, Media and Growth Conditions	40
2.2.3 High Performance Liquid Chromatography	41
2.2.4 Scanning Electron Microscopy	41
2.3 Results & Discussion	42
2.3.1 <i>C. kluyveri</i> consumes acetate and ethanol and produces butyrate and hexanoate in monoculture	42
2.3.2 Co-culture of <i>C. kluyveri</i> and <i>C. acetobutylicum</i> displays a culture phenotype similar to that of pure <i>C. acetobutylicum</i> and produces no hexanoate	43
2.3.3 <i>C. kluyveri</i> can use butanol as the primary source of alcohol for chain elongation	46

2.3.4	Increasing the ratio of <i>C. kluyveri</i> to <i>C. acetobutylicum</i> in co-culture does not enable the co-culture to produce hexanoate .	48
2.3.5	A co-culture of <i>C. acetobutylicum</i> , <i>C. ljungdahlii</i> and <i>C. kluyveri</i> produces hexanoate	49
2.3.6	Scanning electron microscopy (SEM) of co-cultures of <i>C. acetobutylicum</i> and <i>C. ljungdahlii</i> show potential fusion events, but similar cell shape and surface texture in SEM makes it difficult to distinguish the two species	52
3	ENGINEERING A FLUORESCENT REPORTER SYSTEM AND VIEWING PROTEIN LOCALIZATION WITH FAST IN <i>Clostridium acetobutylicum</i>	65
3.1	Introduction.....	65
3.2	Materials and Methods.....	67
3.2.1	Chemicals.....	67
3.2.2	Bacterial Strains, Media and Growth Conditions	67
3.2.3	Genetic Manipulation.....	68
3.2.4	Vector Transformations	69
3.2.5	Flow Cytometry	69
3.2.6	SpectraMax i3x Microplate Reader	70
3.2.7	Confocal Microscopy.....	71
3.2.8	Statistical Analysis.....	71
3.3	Results.....	72
3.3.1	<i>E. coli</i> FAST shows promising fluorescence intensity using flow cytometry, microplate reader, and confocal microscopy	72
3.3.2	Expression of FAST in <i>C. acetobutylicum</i> using the native thiolase promoter (<i>Pthl</i>) results in low HMBR-dependent fluorescence but using a strong mutant <i>Pthl</i> promoter improves fluorescent signal	73
3.3.3	Development of a FAST-based Fluorescent Reporter System for <i>Clostridium acetobutylicum</i>	74
3.3.4	<i>C. acetobutylicum</i> <i>adc</i> FAST and <i>C. acetobutylicum</i> <i>adc</i> ^{mod} FAST promoters show highest fluorescence activity compared to other <i>C. acetobutylicum</i> FAST promoters	81
3.3.5	Development of a Successful Bacterial Cell Division Fusion Protein using FAST and HMBR.....	82
3.4	Discussion.....	83
4	CONCLUSIONS AND FUTURE DIRECTIONS	102

4.1 Overall Conclusions.....	102
4.2 Recommendations for Future Work.....	106
REFERENCES	108
Appendix	
A SYNTROPHIC INTERACTIONS IN CLOSTRIDIA CO-CULTURES..	121
B ENGINEERING A FLUORESCENT REPORTER SYSTEM AND VIEWING PROTEIN LOCALIZATION WITH FAST IN <i>Clostridium</i> <i>acetobutylicum</i>	122

LIST OF TABLES

Table A.1 Strains and plasmids used in this study.....	121
Table B.1 Strains and Plasmids used in this study.....	122
Table B.2 Primers used in this study. Binding regions are indicated by uppercase. Homology regions are indicated by lowercase.....	123

LIST OF FIGURES

Figure 1.1 - Primary metabolism of the solventogen <i>C. acetobutylicum</i> for the ABE fermentation [5].	4
Figure 1.2 - Primary metabolism of the acetogen, <i>C. ljungdahlii</i> , using the Wood-Ljungdahl Pathway (WLP), glycolysis, and the pentose phosphate pathway [2].	8
Figure 1.3 - Ethanol and acetate fermentation by the chain-elongating <i>C. kluyveri</i> [13].	11
Figure 2.1 - <i>C. kluyveri</i> shows a similar growth pattern in the co-culture medium Turbo CGM compared to <i>C. kluyveri</i> growth medium DSMZ 52.	53
Figure 2.2 - <i>C. kluyveri</i> and <i>C. acetobutylicum</i> co-culture shows a similar metabolite profile to pure <i>C. acetobutylicum</i> co-culture and produces no hexanoate after 20ml of spun down <i>C. kluyveri</i> (~OD ₆₀₀ 0.3) is added to 20ml active <i>C. acetobutylicum</i> culture (~OD ₆₀₀ 4.5).	55
Figure 2.3 - <i>C. kluyveri</i> and <i>C. acetobutylicum</i> co-culture shows a similar metabolite profile to pure <i>C. acetobutylicum</i> co-culture and produces no hexanoate after 40ml of spun down <i>C. kluyveri</i> (~OD ₆₀₀ 0.3) is added to 20ml active <i>C. acetobutylicum</i> culture (~OD ₆₀₀ 4.5).	57
Figure 2.4 - <i>C. kluyveri</i> can grow on acetate and butanol and utilize butanol as the primary alcohol in chain elongation.	59
Figure 2.5 - <i>C. kluyveri</i> and <i>C. acetobutylicum</i> co-culture shows a similar metabolite profile to pure <i>C. acetobutylicum</i> co-culture and produces no hexanoate after 50ml of spun down <i>C. kluyveri</i> (~OD ₆₀₀ 0.6) is added to 5ml of active <i>C. acetobutylicum</i> culture (~OD ₆₀₀ 5.0) and 5 ml of <i>C. acetobutylicum</i> culture supernatant.	61
Figure 2.6 - <i>C. kluyveri</i> , <i>C. ljungdahlii</i> and <i>C. acetobutylicum</i> co-culture shows a metabolite profile consistent with growth of all three organisms and produces hexanoate.	63
Figure 2.7 - Possible fusion events between <i>C. ljungdahlii</i> and <i>C. acetobutylicum</i> cells in co-culture using Scanning electron microscopy.	64
Figure 3.1 - <i>E. coli</i> thlFAST shows promising fluorescence using flow cytometry and microplate reader.	88

Figure 3.2 - <i>E. coli</i> thlFAST shows stable linear fluorescence expression pattern in exponential and stationary phases of growth, shows higher fluorescence intensity in stationary phase of growth (red) compared to exponential phase of growth, and shows bright fluorescence using confocal microscopy.....	89
Figure 3.3 - <i>C. acetobutylicum</i> thl ^{sup} FAST shows improved fluorescence when compared to <i>C. acetobutylicum</i> thlFAST and <i>C. acetobutylicum</i> ATCC 824 using flow cytometry.	90
Figure 3.4 - <i>C. acetobutylicum</i> thl ^{sup} FAST shows improved fluorescence when compared to <i>C. acetobutylicum</i> thlFAST and <i>C. acetobutylicum</i> ATCC 824 using confocal microscopy.....	92
Figure 3.5 - <i>C. acetobutylicum</i> thl ^{sup} FAST shows improved fluorescence over time compared to <i>C. acetobutylicum</i> thlFAST using flow cytometry and both <i>C. acetobutylicum</i> thl ^{sup} FAST and <i>C. acetobutylicum</i> thlFAST show a fluorescence pattern consistent with promoter growth phase activity.	93
Figure 3.6 - Histograms of thlFAST and thl ^{sup} FAST over time show improvement in fluorescence shift over time.....	94
Figure 3.7 - <i>C. acetobutylicum</i> adc ^{mod} FAST shows improved fluorescence over time compared to <i>C. acetobutylicum</i> adcFAST using flow cytometry and both <i>C. acetobutylicum</i> adc ^{mod} FAST and <i>C. acetobutylicum</i> adcFAST show a fluorescence pattern consistent with promoter growth phase activity.	95
Figure 3.8 - Histograms of adcFAST and adc ^{mod} FAST over time show slight improvement in fluorescence shift over time.	96
Figure 3.9 - <i>C. acetobutylicum</i> ptb ^{mod} FAST shows improved fluorescence over time compared to <i>C. acetobutylicum</i> ptbFAST using flow cytometry and both <i>C. acetobutylicum</i> ptb ^{mod} FAST and <i>C. acetobutylicum</i> ptbFAST show a fluorescence pattern consistent with promoter growth phase activity.	97
Figure 3.10 - Histograms of ptbFAST and ptb ^{mod} FAST over time show little difference in fluorescence shift over time.....	98

Figure 3.11 - *C. acetobutylicum* adc^{mod}FAST and *C. acetobutylicum* adcFAST show strongest activity compared to *C. acetobutylicum* thlFAST, *C. acetobutylicum* thl^{sup}FAST, *C. acetobutylicum* ptbFAST, and *C. acetobutylicum* ptb^{mod}FAST using flow cytometry and microplate reader. 99

Figure 3.12 - FAST and HMBR are an efficient system to view protein localization within *E. coli* cells. *E. coli* ZapA-FAST with 20uM HMBR (left) differential interference contrast (middle) and merge (right) using confocal microscopy. 100

Figure 3.13 - FAST and HMBR are an efficient system to view protein localization within *C. acetobutylicum* cells. *C. acetobutylicum* ZapA-FAST with 20uM HMBR (left) differential interference contrast (middle) and merge (right) using confocal microscopy. 101

ABSTRACT

The greenhouse gas, CO₂, in Earth's atmosphere is a threat to our planet and a cause of global warming. Utilizing CO₂ industrial waste gases as fermentation feedstock for biofuel production is a promising technology for the reduction of industrial waste. One of the notable genera of bacteria that can accomplish this is the genus *Clostridium*. *Clostridium spp.* are Gram-positive, anaerobic Firmicutes that can metabolize a diverse amount of substrates, including sugars, acids, alcohols, and gases like CO₂, H₂, and CO. Engineering non-acetogenic clostridia to efficiently consume waste as feedstock has been the subject of many recent studies, but using multiple species of *Clostridium* in co-culture has been shown to be an achievable and economical option for optimizing fermentation carbon recoveries and production of non-natural products.

Many different co-cultures between *Clostridium spp.* have been studied, but one pair that has not been investigated previously is between the chain elongating *C. kluyveri*, and the well-studied solventogen, *C. acetobutylicum*. Our lab has previously established a co-culture between *C. acetobutylicum* and the CO₂ fixing acetogen, *C. ljungdahlii*, and this co-culture has been shown to improve carbon efficiency of clostridia fermentation when compared to mono-culture. The addition of a third organism, *C. kluyveri*, to the co-culture could potentially use the products of syntrophic interactions between *C. ljungdahlii* and *C. acetobutylicum* to produce medium-chain fatty acids that can be converted to biofuels.

In this study, we examined the possibilities of *C. acetobutylicum* and *C. kluyveri* in co-culture as well as a triple organism co-culture between *C.*

acetobutylicum, *C. ljungdahlii*, and *C. kluyveri*. This triple organism co-culture has the potential to use sugars for syntrophic production acids and alcohols, which would be further converted to of medium-chain fatty acids by *C. kluyveri*. *C. acetobutylicum* and *C. kluyveri* co-cultures were shown to be need further optimization due to pH discrepancies between species, but the addition of *C. ljungdahlii* to the culture was able to produce the medium-chain fatty acid, hexanoate from additional acetate and ethanol in co-culture. In order to further understand syntrophic interactions between *Clostridium spp.*, we designed an anaerobic, highly-fluorescent reporter system using the fluorescence activating protein, FAST, and the fluorogenic ligand, HMBR. Commonly used fluorescent proteins reporters require oxygen for chromophore maturation, and anaerobic fluorescent proteins lack brightness comparable to aerobic fluorescent proteins. FAST does not require oxygen, and fluoresces instantaneously when the fluorogenic ligand, HMBR, is added. In addition to being a successful fluorescent reporter, FAST was also used to successfully tag and view protein localization of the cell division protein, ZapA, in live *C. acetobutylicum* cells. This fluorescent system opens the door for research on other *Clostridium spp.* and other anaerobes to study protein interactions with oxygen-independent fluorescence. FAST could be used in the future for further investigation of protein localization, particularly shedding light on localization of proteins that may be involved in syntrophic co-cultures.

Chapter 1

INTRODUCTION

1.1 *Clostridia* spp. of Note and Their Respective Metabolic Pathways

Organisms of the genus *Clostridium* are rod shaped, Gram-positive, endospore-forming, non-sulfate reducing Firmicutes. *Clostridium* species can produce a variety of metabolites including organic acids and alcohols from a diverse number of substrates. Some of these substrates include carbohydrates, alcohols, amino acids, purines, and steroids, and some species can even fix atmospheric nitrogen. Most species of *Clostridium* are obligate anaerobes, with only few able to tolerate low levels of oxygen [1-3].

1.1.1 *Clostridium acetobutylicum* and Acetone-Butanol-Ethanol Fermentation

C. acetobutylicum stains Gram-positive in early growing cultures, while staining Gram-negative in later cultures. Endospores in *C. acetobutylicum* are oval and subterminal, and slightly swell the cell. Granulose is produced by most strains [1] and has a pH range of 5.0-6.5 in industrial fermentations [4]. *C. acetobutylicum* is a member of the group called solventogens. Solventogenic *Clostridium* spp. can produce solvents like acetone, butanol, and ethanol from a variety of different substrates, particularly mono-saccharide, di-saccharide and poly-saccharide sugars (Figure 1.1). These solvents are produced through the anaerobic ABE (acetone-butanol-ethanol) fermentation, which was the primary industrial source of butanol and acetone before the 1950s [5]. ABE producing *Clostridium* spp. show a biphasic growth pattern where

in the early growth phase, acidogenesis, *C. acetobutylicum* produces acids like acetate and butyrate. Once *C. acetobutylicum* reaches stationary growth phase it switches to solventogenesis, during which acids are reabsorbed and converted to solvents along with any remaining sugar substrates [6]. It is suggested that the acids produced by acidogenesis quickly reduce the pH of the medium, causing the switch to solventogenesis, and the fermentation comes to an end when the solvent concentration becomes too high to support growth and the metabolism is halted [7]. While *C. acetobutylicum* can produce high titers of butanol in ABE fermentation, the high concentrations inhibit cell growth and lead to cell death unless the cells sporulate. It has been suggested that repeated fed-batch fermentations could improve butanol production without any strain modification, and that creating more butanol tolerant *Clostridium* strains could be more favorable economically. It has also been suggested that eliminating sporulation and degradation as well as reduction in the production of acetone and ethanol could help improve production of biobutanol [5].

In ABE fermentation, glucose is broken down into 2 pyruvate molecules through glycolysis, and pyruvate is oxidized to form acetyl-CoA. During acidogenesis, acetate is produced from acetyl-CoA via the phosphotransacetylase (PTA) and acetate kinase (AK) enzymes. Two acetyl-CoA molecules are condensed to form acetoacetyl-CoA via thiolase (THL). Acetoacetyl-CoA is then converted to butyryl-CoA via the beta-hydroxybutyryl dehydrogenase (BHBD), crotonase (CRO), and butyryl-CoA dehydrogenase (BCD) enzymes. Butyrate is formed from butyryl-CoA using the phosphotransbutyrylase (PTB) and butyrate kinase (BK) enzymes. During solventogenesis, acetate and butyrate previously produced are converted back to acetyl-CoA and butyryl-CoA, respectively, via the CoA Transferase (CoAT) enzyme.

Acetyl-CoA can be also converted to acetaldehyde and then to ethanol via the alcohol/aldehyde dehydrogenase (AAD), while butyryl-CoA can be converted to butyraldehyde and butanol via AAD [5].

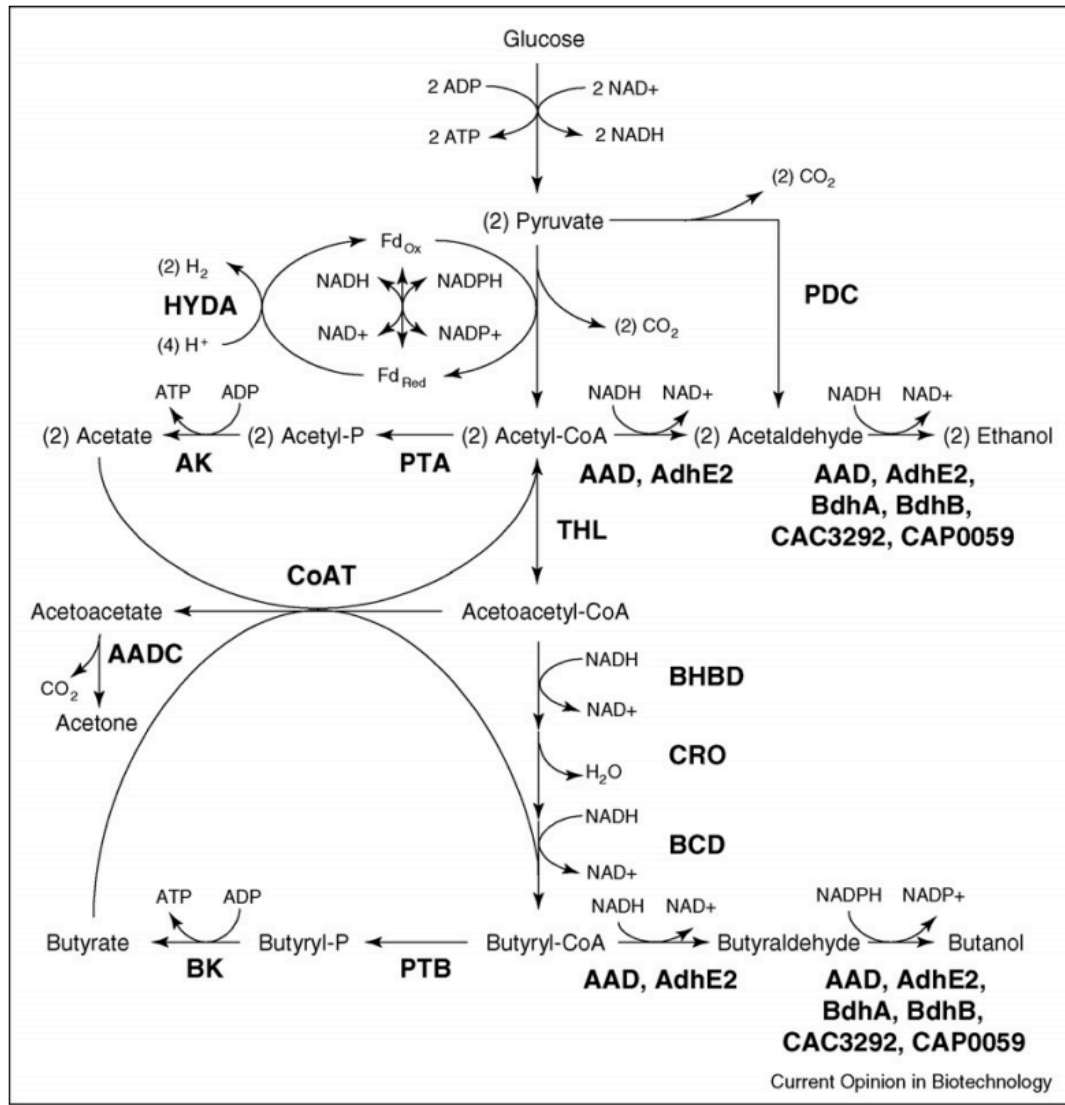


Figure 1.1 - Primary metabolism of the solventogen *C. acetobutylicum* for the ABE fermentation [5]. Enzymes in pathway are abbreviated as follows: hydrogenase (HYDA); pyruvate decarboxylase (PDC); acetate kinase (AK); phosphotransacetylase (PTA); alcohol/aldehyde dehydrogenase (AAD); thiolase (THL); CoA Transferase (CoAT); acetoacetate decarboxylase (AADC); Beta-hydroxybutyryl dehydrogenase (BHBD); crotonase (CRO); butyryl-CoA dehydrogenase (BCD); butyrate kinase (BK); phosphotransbutyrylase (PTB). In addition to the main butanol and ethanol forming enzyme, AAD, other enzymes that carry out these reactions also exist in *C. acetobutylicum* (AdhE1 and 2, BdhA, BdhB, CAC3292, CAP0059). Figure taken from Papoutsakis 2008.

1.1.2 *Clostridium ljungdahlii* and the Wood-Ljungdahl Pathway

C. ljungdahlii cells stain Gram-positive and rarely form spores. *C. ljungdahlii* also has a growth pH range of 4.0-7.0, but optimal growth occurs at a pH of 6.0 [1]. *C. ljungdahlii* belongs to the group known as acetogens. Acetogens can fix CO₂ by using an electron donor, such as H₂, or fix CO as a sole carbon source. It is estimated that about 20% of the CO₂ on earth is fixed by acetogens, which could help to utilize the carbon lost as waste in other fermentations as CO₂ [8]. Some acetogens can also utilize other one carbon compounds like formate and methanol [9]. Acetogens like *C. ljungdahlii* do this by utilizing the Wood-Ljungdahl pathway (WLP) for autotrophic growth, which consists of a carbonyl, or Western, branch and a methyl, or Eastern, branch. Through the carbonyl branch of the WL pathway, one CO₂ molecule is reduced to CO by the CO Dehydrogenase/Acetyl-CoA synthase complex (CODH/ACS). Through the methyl branch, the formate dehydrogenase (FDH) enzyme reduces CO₂ to formate, which eventually is further reduced to a methyl-group. Both the carbonyl and methyl branches together utilize ACS to form Acetyl-CoA, which can be used in the formation of ATP through acetate production, or reduced to ethanol. However, due to no net ATP being produced by the WL pathway, the cells must pair the WL pathway with a proton gradient to create the necessary ATP [2]. *C. ljungdahlii* also grows heterotrophically on fructose and other pentose sugars like xylose, arabinose and ribose [10] via glycolysis and the pentose phosphate pathway, which produces ATP through substrate-level phosphorylation and the phosphotransacetylase/acetate kinase reaction. *C. ljungdahlii* contains an Rnf-complex which uses reduced ferredoxin to generate a proton gradient and NADH, and pairs with an H⁺F₁F₀ ATP synthase complex to create a proton motive force to generate ATP [2, 11]. The development of genetic tools to utilize this ability to consume waste

gases to produce valuable metabolites are underway, and it is also suggested that acetogens could be ideal partners for solventogens in syntrophic systems in order to maximize fermentation product yields [8].

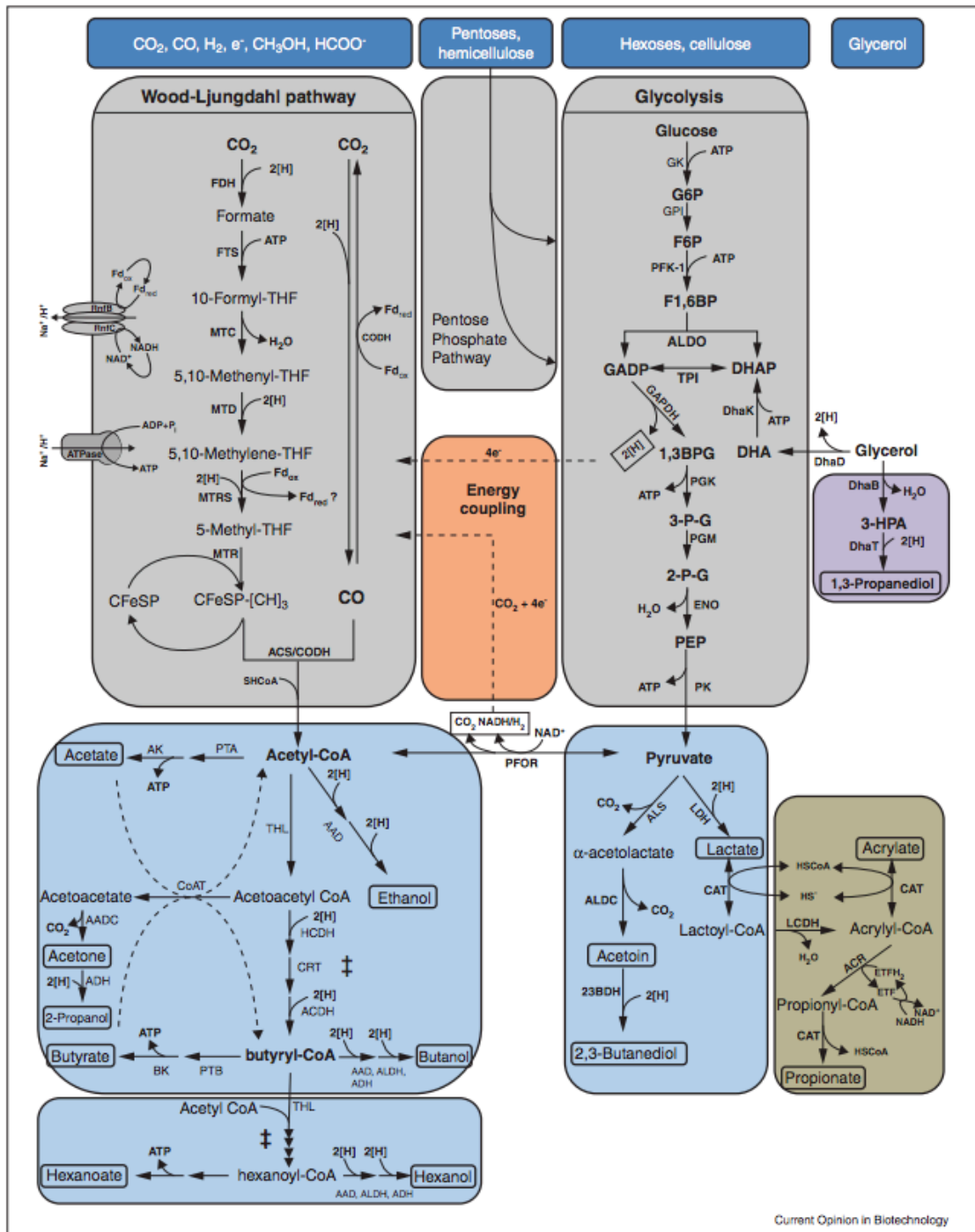


Figure 1.2 - Primary metabolism of the acetogen, *C. ljungdahlii*, using the Wood-Ljungdahl Pathway (WLP), glycolysis, and the pentose phosphate pathway [2]. WLP, glycolysis and the pentose phosphate pathway are shown in gray, substrates used for each pathway are shown in dark blue, products are circled in black, pathways used in the conversion of acetyl-CoA and pyruvate are shown in light blue, production pathways for propionate and acrylate are shown in brown, and energetic coupling between glycolysis, pyruvate:ferredoxin oxidoreductase, and WLP is shown in orange. Enzymes are abbreviated as follows: 2,3-butanediol dehydrogenase (23BDH); alcohol/aldehyde dehydrogenase (AAD); acetoacetate decarboxylase (AADC); acyl-CoA dehydrogenase (ACDH); acrylyl-CoA reductase (ACR); acetyl-CoA synthase/CO dehydrogenase (ACS/CODH); alcohol dehydrogenase (ADH); acetate kinase (AK); acetolactate decarboxylase (ALDC); aldehyde dehydrogenase (ALDH); fructose biphosphate aldolase (ALDO); acetolactate synthase (ALS); butyrate kinase (BK); CoA transferase (CAT); corrinoid iron-sulfur protein (CFeSP); crotonase (CRT); glycerol dehydratase (DhaB); glycerol dehydratase (DhaD); DHA kinase (DhaK); 1,3-propanediol oxidoreductase (DhaT); enolase (ENO); electron-transferring flavoprotein (Etf,); ferredoxin (Fd); formate dehydrogenase (FDH); formyl-THF synthase (FTS); glyceraldehyde phosphate dehydrogenase (GAPDH); hexokinase (GK); phosphoglucose isomerase (GPI); 3-hydroxyacyl-CoA dehydrogenase (HCDH); lactoyl-CoA dehydrogenase (LCDH); lactate dehydrogenase (LDH); methenyl-THF cyclohydrolase (MTC); methylene-THF dehydrogenase (MTD); methyl transferase (MTR); methylene-THF reductase (MTRS); phosphofructokinase (PFK-1); pyruvate:ferredoxin oxidoreductase (PFOR); phosphoglycerate kinase (PGK); phosphoglycerate mutase (PGM); pyruvate kinase (PK); phosphotransacetylase (PTA); phosphotransbutyrylase (PTB); thiolase (THL); triosephosphate isomerase (TPI). Figure taken from Tracy *et al.* 2012.

1.1.3 *Clostridium kluyveri* and Fatty Acid Chain-elongation

C. kluyveri is an obligate anaerobe with a pH growth range from 6.0 to 7.5 [12]. *C. kluyveri* stains weakly Gram-positive, quickly becoming Gram-negative over time. Endospores are oval, can be terminal or subterminal, and swell the cell when forming [1]. *C. kluyveri* ferments ethanol and acetate to butyrate, caproate (hexanoate) and H₂ and had become a model organism for the study of fatty acid synthesis and

fatty acid oxidation in the 1950s. [13]. It has also been suggested that *C. kluyveri* can further extend the carbon chain length of fatty acids to form caprylate (octanoate) [14].

The metabolism of ethanol and acetate by *C. kluyveri* has been illustrated by Seedorf and colleagues in a study shedding light on the complex metabolic features discovered by the *C. kluyveri* genome sequence [13]. In this process, ethanol is oxidized to acetyl-CoA by an NAD-dependent ethanol dehydrogenase (Adh) and a NAD(P)-dependent acetaldehyde dehydrogenase (Ald). *C. kluyveri* can then convert acetyl-CoA to butyryl-CoA utilizing an acetoacetyl-CoA thiolase (Thl), an NAD- and NADP-dependent 3-hydroxybutyryl-CoA dehydrogenase (Hbd), a 3-hydroxybutyryl-CoA dehydratase (Crt) and an NAD-dependent butyryl-CoA dehydrogenase complex (Bcd/EtfAB). Butyryl-CoA can then interact with acetate, resulting in the formation of acetyl-CoA and butyrate by the butyryl-CoA: acetate CoA transferase (Cat3) [13]. Reverse beta oxidation can further extend the length of carboxylic acids by extending the chain length by 2 carbons at a time by adding an acetyl-CoA molecule, converting acetate to butyrate, butyrate to caproate, and caproate to caprylate respectively [15]. There are two membrane associated complexes that *C. kluyveri* also utilizes. The first complex is the energy-converting NADH: ferredoxin oxireductase (RnfA-G) and the second is the ATP sythase (AtpA-E) which create a proton/sodium gradient across the membrane thus generating ATP [13, 15].

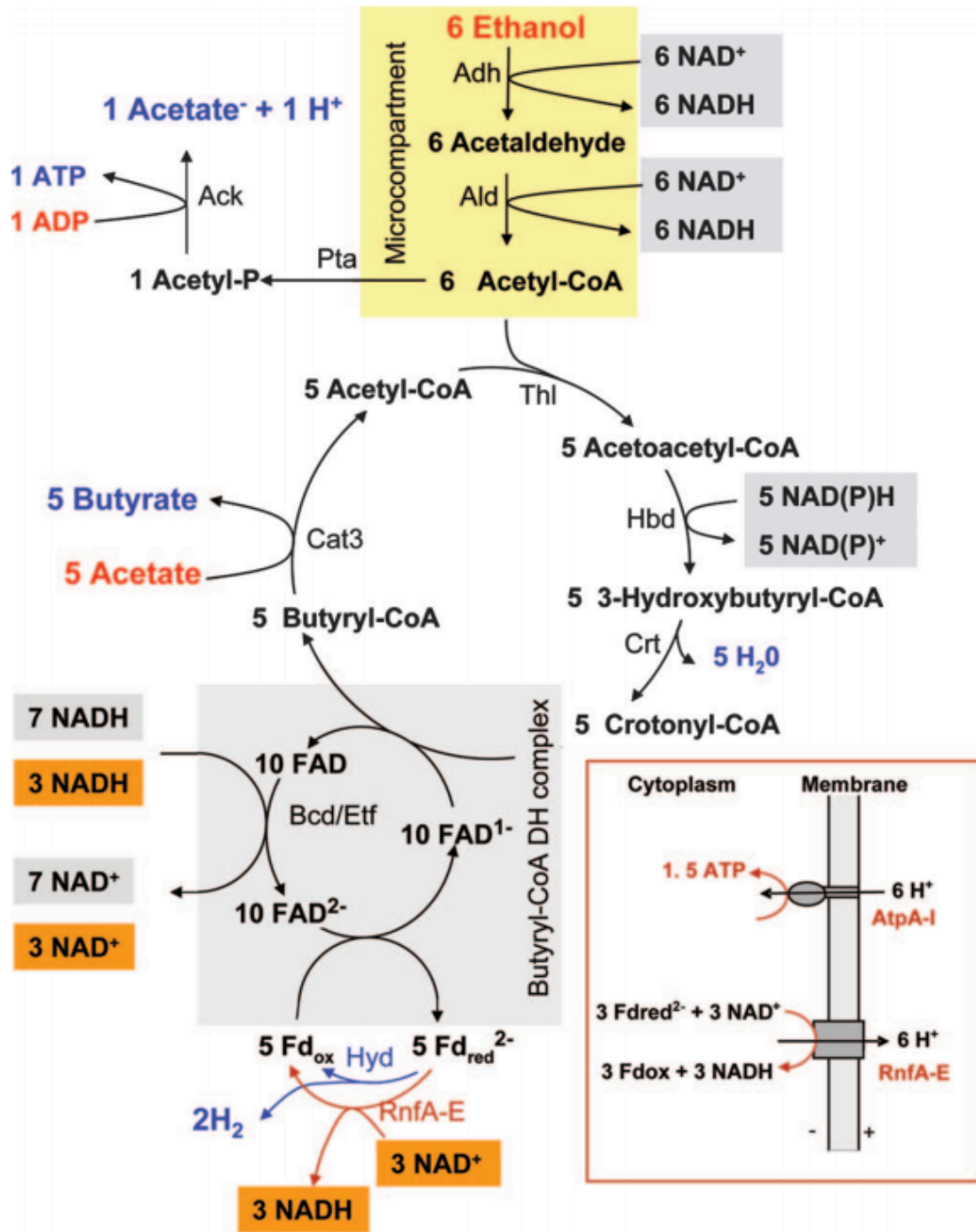


Figure 1.3 - Ethanol and acetate fermentation by the chain-elongating *C. kluyveri* [13]. This figure shows only butyrate, acetate, and H₂ as fermentation products, but hexanoate and octanoate have also been shown to be formed in fermentations [13]. Red box indicates the two membrane-associated, energy-converting enzyme complexes involved in the fermentation: ferredoxin:NAD oxidoreductase (RnfA-E) and ATP synthase (AtpA-I). Yellow shaded area indicates microcompartment. Other enzymes are abbreviated as follows: NAD-dependent ethanol dehydrogenase (Adh); NAD(P)-dependent acetaldehyde dehydrogenase (Ald); acetate kinase (Ack), phosphotransacetylase (Pta); thiolase (Thl); NAD- and NADP-dependent 3-hydroxybutyryl-CoA dehydrogenase (Hbd); 3-hydroxybutyryl-CoA dehydratase (Crt); NAD-dependent butyryl-CoA dehydrogenase complex (Bcd/EtfAB); acetate CoA transferase (Cat3); hydrogenase (Hyd). Figure taken from Seedorf *et al.* 2008.

1.2 The Importance of Co-cultures and Recent Advances in Microbial Co-cultures

Using co-cultures to study and develop novel metabolite producing systems is a promising method to reduce complicated engineering of a single organism. In a recent review by Charubin and colleagues about engineering *Clostridium* it is mentioned that both syntrophic and non-syntrophic co-cultures can be used to produce pharmaceuticals, gases, alcohols, and varying-length acids[8]. Charubin and colleagues have also highlighted several important syntrophic clostridia co-cultures that have been recently reported in publications. Syntrophic co-cultures can allow microbes to thrive and coexist while one or more of the microbes utilizes the products from the other or others [8]. *Clostridium* co-cultures can be particularly useful due to the extremely diverse number of metabolites produced by each species.

Salimi and Mahadevan have developed a clostridial co-culture system involving the cellulolytic *Clostridium cellulolyticum*, and the solventogenic *C. acetobutylicum* and suggest a synergistic relationship between the two organisms [16].

C. cellulolyticum showed increased growth rate in co-culture, based on qPCR data, while the co-culture exhibited high cellulolytic activity that surpassed the activity of *C. cellulolyticum* mono-culture in optimal conditions [16]. Diender and colleagues have recently established a synthetic co-culture between the syngas fermenting *C. autoethanogenum* and the medium-chain fatty acid synthesizing *C. kluyveri*. This study shows the ability of this co-culture to convert CO or syngas to the medium-chain fatty acids, butyrate and caproate, as well as butanol and hexanol. However, toxicity of caproate in co-culture as well as a small range of compatible pH range between *C. autoethanogenum* and *C. kluyveri* were shown to be limiting [17]. Richter and colleagues have recently established a co-culture system with *C. kluyveri*, but with the syngas fermenting acetogen *C. ljungdahlii* in a continuous fermentation. In this study, it was shown that *C. kluyveri* and *C. ljungdahlii* compete for carboxylate intermediates resulting in butanol, hexanol, as well as the first detection of octanol from syngas fermentation. However, this study also highlights that the pH discrepancy between each strain is a limiting factor in this co-culture, and that a chain-elongating strain with an growth optimal pH between 5 and 5.5 would be superior [18]. A co-culture with *C. autoethanogenum* as *C. kluyveri* was also developed by Haas and colleagues to create an anaerobic conversion of syngas produced by a CO₂ electrolyser to produce butanol and hexanol, and proposed a model for scaling up fermentations for industrial production via artificial photosynthesis [19].

Another recent application for the study of co-cultures is to observe and characterize cell-to-cell interactions between different species of bacteria. *Geobacter metallireducens* consumes ethanol while *Geobacter sulfurreducens* cannot. Summers and colleagues created a strain of *G. sulfurreducens* that could not consume hydrogen

due to the deletion of a hydrogenase subunit. *Geobacter metallidreducens* and *Geobacter sulfurreducens* in co-culture were able to metabolize ethanol, and cells were shown to aggregate to an electrically conductive environment. It was shown that a mutation leading to enhanced production of c-type cytochrome (OmcS) in the extracellular electron transport chain occurred in cells from aggregates. Summers and colleagues suggest that this mutation enhanced the ability of different species to exchange electrons. Fluorescence in situ hybridization (FISH) with species specific probes showed distinct clusters of each *Geobacter* spp. within aggregates. It is suggested that OmcS of *G. sulfurreducens* can accept electrons from *G. metallidreducens* allowing *G. sulfurreducens* to grow without consuming hydrogen. [20].

Dubey and Ben-Yehuda have found that *Bacillus subtilis* can exchange fluorescent molecules between adjacent cells and can even exchange antibiotic resistance genes through non-hereditary transfer rather than through conjugation. A GFP reporter and fluorescent microscopy were used to show a gradient of gained fluorescence between *gfp+* and *gfp-* *B. subtilis*. In addition to GFP, the cytoplasmic fluorophore, calcein was used. The acetoxymethylester (AM), calcein-AM, is non-fluorescent, but upon interaction with esterases within the cytoplasm it becomes fluorescent and hydrophilic, allowing calcein to remain within the stained cells. *B. subtilis* was also shown to form nanotubes to interact with adjacent *B. subtilis* cells and was visualized through high-resolution scanning electron microscopy (HR-SEM). *B. subtilis* was also shown to interact with the Gram-positive *Staphylococcus aureus* as well as the distantly related, Gram-negative *E. coli* in co-culture through nanotube formation, as well as to exchange GFP between the two species [21].

Pande and colleagues have shown nanotube interactions in *Acinetobacter baylyi* and *E. coli*. In this study, it was shown that *E. coli*, but not *A. baylyi*, can exchange nutrients through these nanotubes when histidine (His) and tryptophan (Trp) biosynthesis pathways were altered. This created strains of *E. coli* and *A. baylyi* that depended on each other by one strain overproducing the amino acid, while the other strain cross-feeds to utilize the missing amino acid synthesis. Nanotubes were observed in *A. baylyi* and *E. coli* co-culture through SEM microscopy, and confocal microscopy was used to visualize the exchange of cellular materials between mCherry tagged *A. baylyi* and EGFP tagged *E. coli*. This implies hollow nanotubes that are large enough for fluorescent proteins to pass through. The lipophilic dye, DiO was used to stain cell membranes. DiO was able to stain the nanotubes, indicating nanotubes have a lipid composition [22]. This study shows that engineering auxotrophic bacteria to complement each other could be another way to create and study beneficial syntrophic co-cultures.

Benomar and colleagues have also observed interspecies interactions but between two anaerobic bacteria associated with biomass degradation, *C. acetobutylicum* and *Desulfovibrio vulgaris*. This study showed that under conditions of nutrient starvation, *D. vulgaris* will use cell-to-cell interactions between species to exchange cytoplasmic materials. It was first determined that *D. vulgaris* and *C. acetobutylicum* need direct contact to exchange cellular materials, which was shown through the use of dialysis bags separating the two species. It was shown that, when separated, there was no growth of *D. vulgaris* or increase in H₂ production in the culture, but when combined in co-culture with the glucose metabolizing *C. acetobutylicum*, *D. vulgaris* was shown to be able to grow in the absence of the

necessary metabolites (lactate and sulfate). Using SEM, it was shown that *D. vulgaris* interacts directly with *C. acetobutylicum*. *C. acetobutylicum* was also stained using calcein dye and showed direct exchange of cytoplasmic material to *D. vulgaris*. *D. vulgaris* was then labeled with mCherry, and *C. acetobutylicum* was stained with calcein and exchange of cytoplasmic molecules was shown as yellow fluorescence. Control co-culture of *E. coli* and *C. acetobutylicum* were not shown to exchange material between species because both had enough nutrients from glucose. There was also a substantial increase of H₂ in *C. acetobutylicum* and *D. vulgaris* co-culture, which was suggested to be the result of increased expression of the enzyme related to the production of pyruvate, pyruvate ferredoxin oxidoreductase (*pfor*), and the decrease in expression of lactate dehydrogenase (*ldh*) [23].

Most recently, a study has been done to show syntrophic interactions between the acetogen, *C. ljungdahlii*, and the solventogen, *C. acetobutylicum* [24]. This co-culture was shown to fix CO₂ produced by *C. acetobutylicum* through the WLP in *C. ljungdahlii* and improve carbon recoveries of *C. acetobutylicum* fermentation products. In this study it was shown that *C. acetobutylicum* and *C. ljungdahlii* produce isopropanol and 2,3-butanediol in co-culture, which is not found in either pure monoculture. High glucose concentrations can be toxic to *C. ljungdahlii* [24] so *C. ljungdahlii* was also adapted to high glucose concentrations, and showed an even higher improvement in carbon recovery. This study also proposes a model for cell-to-cell interactions in order to exchange metabolites in co-culture [24]. In a recent review by Lovley, it is suggested that the use of direct interspecies electron transfer (DIET) could allow for improvement in the already efficient and large-scale consumption of organic wastes by anaerobic organisms [25]. Tracy and colleagues have highlighted

that *Clostridium spp.* can utilize a broad spectrum of carbon substrates, possess many diverse pathways in order to produce biotechnologically useful metabolites, as well as are tolerant to metabolites that may be too toxic for other systems [2]. Charubin and Papoutsakis have also highlighted that *C. acetobutylicum* and *C. ljungdahlii* appear to exchange electrons in co-culture [24]. Utilizing the already efficient metabolic capabilities of *C. acetobutylicum*, *C. ljungdahlii*, *C. kluyveri* and potentially other *Clostridium spp.* in co-culture could potentially be used to produce useful biofuels in addition to the use of industrial wastes.

1.3 Reporter Systems in *Clostridium spp.*

Genetic reporters offer an opportunity to observe and measure processes in a cell that were previously unobservable. Joseph and colleagues suggest that an ideal reporter system for gene expression and screening should have: (1) high sensitivity and specificity, (2) a dynamic range of detection, and (3) low endogenous levels of the reporter in the bacterial strain of interest [26]. In addition to being used for gene expression, genetic reporters are often used to observe the activity and strength of promoters. Some of the most common reporters used when studying gene expression are enzymatic, colorimetric, luminescent and fluorescent reporters. Enzymatic reporters catalyze reactions in vivo or in vitro and the specific activity of these enzymes is calculated to estimate protein levels and concurrently gene expression. Enzymatic reporters also require specific substrates and cofactors as well as the isolation of cell lysate to measure this enzymatic activity. This method is often used in organisms that grow in an anaerobically since most fluorescent proteins require O₂ for fluorophore activation [6]. Colorimetric reporters also offer opportunities to observe gene expression without the need for an aerobic environment.

One of the first enzyme-based reporter assays developed for *Clostridium spp.* was chloramphenicol acetyltransferase. Bacteria that are resistant to the antibiotic chloramphenicol most often inactivate the antibiotic by the enzyme chloramphenicol acetyltransferase (CAT), which causes the antibiotic to not bind to bacterial ribosomes to inhibit peptide elongation [27]. *Clostridium perfringens* was found to have a transferable antibiotic resistant plasmid pIP401 [28] and Steffen and Matzura determined the nucleotide sequence of this *cat* gene [29]. Bullifent and colleagues used this enzyme to construct a reporter system to study gene expression in *C. perfringens*. This study shows the expression of the alpha-toxin gene (*plc*) in *C. perfringens* by inserting the chloramphenicol acetyltransferase gene (*catP*) and comparing the alpha-toxin and CAT production under the *C. perfringens* NCTC8237 alpha-toxin promoter [30]. However, *catP* reporter systems may not be ideal for certain *Clostridium spp.* that have natural chloramphenicol resistance [31].

An important enzyme-based reporter assay used in *Clostridium spp.* is beta-galactosidase. The *lacZ* gene encodes the beta-galactosidase enzyme which cleaves lactose to glucose and galactose and can be further metabolized through glycolysis [32]. Burchhardt and Bahl first analyzed a beta-galactosidase-encoding gene from *Thermoanaerobacterium thermosulfurogenes* EM1 and predicted that this *lacZ* gene could be used for other *Clostridium spp.* with a G + C content too low for *E. coli lacZ* [33]. Tummala and colleagues then developed a gene expression reporter system (pHT3) in *Clostridium acetobutylicum* ATCC 824. This study developed a reporter system using the *lacZ* gene from *T. thermosulfurogenes* described by Burchhardt and Bahl and used promoters from 3 different metabolic pathways in *C. acetobutylicum* [34]. The first promoter tested by Tummala and colleagues was for the *ptb* gene,

which codes for phosphotransbutyrylase, which interconverts butyryl coenzyme A (butyryl-CoA) and butyryl phosphate and works together with butyrate kinase to produce butyrate in *C. acetobutylicum* [35]. Tummala and colleagues also used the promoter from the *thl* gene, which codes for thiolase, or acetyl-coenzyme A [CoA] acetyltransferase, which carries out a condensation reaction between two acetyl-CoA molecules to form acetoacetyl-CoA [36]. The last gene promoter used by Tummala and colleagues was *adc*, or acetoacetate decarboxylase. Acetoacetate decarboxylase is the enzyme in *C. acetobutylicum* which catalyzes the decarboxylation acetoacetate to acetone during solvent production [37]. Through this study, Tummala and colleagues show that the *ptb* and *thl* promoters are active through exponential growth and are early-growth associated promoters, with *thl* being the stronger of the two, while the *adc* promoter is active in both the solventogenic phase as well as the acidogenic phase of growth [34].

Yang and colleagues also used the beta-galactosidase assay as well as the reporter gene *catP* to create a dual-reporter system in order to generate a synthetic strong promoter library. Using the already strong *thl* promoter (*Pthl*) for *C. acetobutylicum*, Yang and colleagues generated a randomized mutant library of the *Pthl* promoter in three different regions of the promoter sequence. The strength of these mutants was measured with beta-galactosidase, and the strongest *Pthl* mutant yielded a 0.4-fold increase in activity to the native *Pthl* promoter. For further engineering of the *Pthl* promoter, the length and the sequence of the region between the RBS and the start codon was modified, allowing the previous strongest promoter mutant (1200-9) to have over a 10-fold increase in *Pthl* promoter activity (1200-9-9),

which was shown to work well in both *C. acetobutylicum* and *Clostridium ljungdahlii* [38].

Adcock and Saint have used beta-galactosidase activity to identify the pathogen, *C. perfringens* using colorimetric detection of the hydrolysis of ortho-nitrophenyl-beta-D-galactopyranoside (ONPG). The product resulting from hydrolysis of ONPG is ortho-nitrophenol, which is chromogenic. This study also utilized the metabolite 4-methylumbelliferyl phosphate (MUP), which the enzyme acid phosphatase in *C. perfringens* can convert to 4-methylumbelliferone that fluoresces under ultraviolet light (365nm). Using these chromogenic and fluorogenic substrates, Adcock and Saint created the liquid MUP-ONPG assay for the rapid detection of *C. perfringens* in water samples. With this assay, it was determined that MUP and acid phosphatase yielded many false positives and was an unreliable detection method alone, but in combination with ONPG, results could be obtained within 4 hours, and in an aerobic environment [39]. Tan and colleagues also have used beta-galactosidase activity using ONPG in combination with RNA-seq to determine what pathways in *C. acetobutylicum* involve a carbon storage regulator protein (CsrA), and found that CsrA is involved in flagella assembly, oligopeptide transport, iron uptake, and central carbon metabolism [40].

The beta-glucuronidase (*gusA*) gene fusion system is another important reporter of *Clostridium* gene expression. First developed by Jefferson and colleagues, the beta-glucuronidase enzyme system catalyzes the hydrolysis of a variety of glucuronides [41, 42]. Ravagnani and colleagues have used the *gusA* reporter gene transcriptionally fused to mutagenized promoters to show that the *adc* and *ptb* genes are under the control of the Spo0A transcription factor in *C. beijerinckii* and *C.*

acetobutylicum [43]. Girbal and colleagues similarly created a *gusA* reporter system in *C. acetobutylicum* and demonstrated the effectiveness of *gusA* by showing the activity of different promoters during acidogenesis and solventogenesis [44]. Mani and colleagues have also used the *gusA* reporter system to study transcriptional regulation in *C. difficile*. This study uses a *gdh* promoter fusion to *gusA* to measure its activity anaerobically in *C. perfringens* and showed that it was highly activated in the absence of glucose and repressed when present in the culture and show the ability of *C. difficile* promoters to be utilized in another host [45]. Dong and colleagues created an inducible gene expression (ICE) system in *C. acetobutylicum* using an anhydrotetracycline (aTc) inducible *cat* gene expression cassette as well as *gusA* gene expression using the *Pthl* promoter controlling a TetR repressor. Using the Pcm promoter for CAT to construct a tetracycline regulatory system using GusA (pGusA2-2tetO1) was shown to be the best optimized system for *C. acetobutylicum* gene expression reporting [46].

The luciferase enzyme has also been used as a bioluminescent reporter in several *Clostridium spp.* Luciferase catalyzes the oxidation of reduced flavin mononucleotide and a long-chain aliphatic aldehyde by oxygen. The alpha subunit of the luciferase enzyme is coded for by the *luxA* gene, while the beta subunit is coded by the *luxB* gene [47]. Phillips-Jones first developed a *luxA-luxB* construct for the aerotolerant *C. perfringens* using the *luxA* and *luxB* genes from *Vibrio fischeri*. This study showed that *luxA* and *luxB*, using the alpha-toxin gene promoter, can be used to observe bioluminescence in an anaerobic organism [48]. Phillips-Jones also has shown this *luxA-luxB* system can be used to study the real-time expression of genes in *C. perfringens*. This study determined that the use of this *lux* reporter system in *C.*

perfringens shows sensitivity in agreement with other studies observing the expression of alpha-toxin genes [49].

In addition to using the *luxA* and *luxB* genes (luciferase) from *V. fischeri*, Davis and colleagues also used the *lacZ* gene from *T. thermosulfurogenes* to construct a reporter system for the botulinum toxin genes of *C. botulinum*. This study shows that *lacZ* can be used accurately to show the production of botulinum toxin but that further studies on the sensitivity of *lacZ* in *C. botulinum* are needed [50]. Because maximal intensity of luciferase occurs after exposing cells to oxygen for 3 hours, they concluded that oxygenation of cells expressing luciferase is needed in order to be able to use *lux*-gene products as reporters in clostridia [50]. These data suggest that luciferase from the *lux* genes may not provide a timely and efficient reporter system for *Clostridium spp.* that are not aerotolerant.

Feustel and colleagues also used the *lacZ* gene from *T. thermosulfurogenes* and the *lucB* gene (firefly luciferase) from *Photinus pyralis* to examine promoter expression in *C. acetobutylicum*. They examined the expression of the promoters of the *bdhA* (butanol dehydrogenase A) gene, of the *sol* operon (containing the genes for the bifunctional butyraldehyde/butanol dehydrogenase E and the two genes of the Coenzyme A transferase) and the *bdhB* (butanol dehydrogenase B) gene in early growth phase. It was found that *lucB* is not affected by background activity and can be used in clostridia that contain a beta-galactosidase. This study also shows that the light emission from LucB can be increased 10-fold by adding 25mM of ATP to the reaction. Washing the *C. acetobutylicum* cells with potassium phosphate buffer and vigorous shaking of the sample to saturate with oxygen was shown to be necessary for accurate measurement of expression. This was due to a red shift in bioluminescence from

culture acidification. It was also shown that while luciferase initially showed bright luminescence, the luminescence decreased rapidly after five minutes, and stayed stable for only half an hour after. It is suggested that while luciferase can be expressed in *Clostridium spp.*, the expression is low and the appropriate enzyme needs to be determined for each strain being studied. [31].

The amylase protein enables the breakdown of starch in culture and has been used as an enzyme reporter in *Clostridium spp.* expressing the amylase protein. Sabathé and colleagues utilized the extracellular alpha-amylase produced by *C. acetobutylicum* to show that the expression of the *amyP* gene is transcriptionally regulated. Northern blot analyses of total RNA isolated from *C. acetobutylicum* cells showed that the *amyP* gene is transcribed in pH controlled solventogenic chemostat culture (pH 4.4) but not during pH controlled acidogenic (pH 6.5) chemostat cultures. This study also showed that the *amyP* gene in *C. acetobutylicum* is coded on the megaplasmid (pSOL1) that is lost during the process of strain degeneration upon serial subculturing. *C. acetobutylicum* strain degeneration involves attenuated solvent production possibly leading to a total loss of solvent production. Using this information, Sabathé and colleagues used the *amyP* gene to characterize the degeneration process of *C. acetobutylicum*, which previously has been poorly understood. Wild-type *C. acetobutylicum* and a mutant strain that had lost pSOL1 (DGI) were spread on 2% starch agar plates and stained with iodine to reveal starch hydrolysis. While the Wild-type *C. acetobutylicum* had high starch hydrolysis the DGI mutant still showed a small halo of starch hydrolysis. This showed that there are other alpha-amylase genes present on the chromosome. A second experiment was performed on 2% starch 0.2% glucose agar plates using the same strains and iodine staining

method, and it was shown that the DGI mutant produced no starch hydrolysis halo, showing that these other alpha-amylase genes are catabolically repressed by glucose while *amyP* is not. This shows that the loss of *amyP* activity can be used to identify strains that have lost the pSOL1 megaplasmid due to *amyP* not being catabolically repressed [51].

Paiva and colleagues constructed two novel secreted promoters that enable screening of gene expression in *Clostridioides difficile*. *C. difficile* was shown to not have amylase activity, so one of the reporters developed was an engineered *B. subtilis* alpha-amylase gene (*amyE*) which was used to create a fusion protein with one of the most secreted proteins by *C. difficile*, zinc metalloprotease PPEP-1. A luciferase reporter was also designed (*sLuc^{opt}*), and used to determine the activity of the toxin A gene (*tcdA*) over time using cell lysates and diluted culture supernatants [52].

A few other enzyme-based reporter assays have been used in *Clostridium spp.* Quixley and Reid developed a reporter system using an endoglucanase gene (*eglA*) from *C. acetobutylicum* P262 to demonstrate that the *C. beijerinckii* glutamine synthase (*glnA*) gene has a strong promoter [53]. Oh and colleagues have constructed several expression vectors using a variety of bacterial promoters, each using the *Pseudomonas fluorescens* thermostable lipase (*tilA*) gene as a reporter for expression in *C. beijerinckii*. It was shown that the *Ralstonia eutropha* promoter *phaP* (pKBE45-TliA) exhibited the highest expression and TliA activity. The metabolic engineering capabilities of these new strains were also tested using the *C. beijerinckii* DSM 6423 secondary alcohol dehydrogenase (2Adh). The expression vector with the *C. beijerinckii pta* promoter (pKBE411-CB2Adh) showed the highest 2-propanol production. This study shows that pairing the right promoter to the target gene is

crucial for development of expression vectors and these newly identified promoters are valuable as tools to other researchers who may have struggled with previously established *C. beijerinckii* promoters. [54].

Another useful colorimetric reporter assay in *Clostridium spp.* is using the alkaline phosphatase gene from *Enterococcus faecalis* (*phoZ*). While the *E. coli* alkaline phosphatase (*phoA*) gene has been studied extensively in Gram-negative bacteria, PhoA shows reduced activity in Gram-positive bacteria possibly due to the lack of an enzyme with the disulfide bond-forming activity required for PhoA in defined periplasms [55]. Lee and colleagues have previously characterized *E. faecalis* PhoZ protein for use in Gram-positive bacteria and used PhoZ as a reporter in *Streptococcus agalactiae*, *S. pyogenes* and in *E. faecalis* [56]. Edwards and colleagues recently developed an alkaline phosphatase reporter assay using the *E. faecalis* PhoZ protein in *C. difficile*. It was determined that *C. difficile* has no native alkaline phosphatase activity, and that the *phoZ* gene can be used as an anaerobic reporter. Edwards and colleagues then used the strong promoter *PdltD* and the nisin-inducible promoter *Pcpr* along with qRT-PCR to determine that inducible alkaline phosphatase activity correlated with native gene expression [57]. However, it was suggested that use of this reporter in solventogenic *Clostridium* organisms like *C. acetobutylicum* could be limiting due to native phosphatase activity [6].

Dave and colleagues have also developed a useful colorimetric assay to detect *C. perfringens* in canned food by detecting para nitrophenyl produced during the hydrolysis of paranitrophenyl phosphetidyl choline (PNPC) by phospholipase C (lecithinase). This rapid colorimetric assay shows specificity for *C. perfringens* and can be quickly preformed to test canned-food contamination. However, a color change

was also detected in the presence of *C. botulinum* and *C. tetani* in certain growth media and culture conditions [58].

While these reporter assays are useful in the study of gene expression in *Clostridium spp.*, a sensitive, simple and quick reporter assay for anaerobic organisms is still needed. Enzyme reporter assays have been used for many years, but often require the addition of substrates and cofactors, as well as lysing cells [6], which can be tedious. A fluorescent reporter, however, can be used for real-time measurement and do not require the addition of substrates [26]. The need for a fluorescent reporter system in anaerobes as well as a way to observe cellular gene expression with fluorescence microscopy could lead to many advances in the understanding of cell-to-cell interactions in co-cultures as well as localization of proteins with *Clostridium* organisms.

1.4 Gene Promoters in *Clostridium spp.*

Promoters are one of the most simple tools for controlling the expression of a gene of interest, however the available promoters for *Clostridium spp.* do not always transfer to non-native clostridial hosts [26]. A recent review has gone into detail about the promoters that have been previously used in engineering *C. acetobutylicum* [6]. Here we will discuss some of the major promoters available to *Clostridium spp.*

Native gene promoters are often used to control gene expression in *Clostridium spp.* *C. acetobutylicum* native promoters thiolase (*Pthl*), phosphotransbutyrylase (*Pptb*), and acetoacetate decarboxylase (*Padc*) are the most widely used native promoters [31, 34]. These central metabolism genes have been used extensively in *C. acetobutylicum* and other *Clostridium spp.* [59]. When ClosTron was developed by Heap and colleagues, the *Clostridium pasteurianum* ferredoxin promoter was used in

combination with downstream *E. coli LacZ* operon, creating *Pfac*, and IPTG was used to induce gene expression in *C. botulinum*, *C. sporogenes*, and *C. difficile* [60]. Later, the *C. sporogenes* ferredoxin promoter, *Pfdx*, was used and IPTG was no longer needed to induce the promoter [61]. Nariya and colleagues have also used a ferredoxin promoter for the construction of a suicide vector for gene knockout in *C. perfringens* [62]. Nakayama and colleagues have used the butanol dehydrogenase promoter (*Pbdh*) from *C. saccharoperbutylacetonicum* in order to control hydrogenase activity with antisense RNA [63]. Tolonen and colleagues have also used a metabolic-gene promoter, *C. phytofermentans* pyruvate ferredoxin oxidoreductase (*cphy3558*)(*Ppfo*), in order to investigate the role of *Cphy3558* in degradation of cellulosic biomass [64]. Several non-native *Clostridium* promoters have been used for promoter characterization and screening in *C. cellulolyticum* [65]

Another recent application of *Clostridium spp.* promoters is the design of synthetic mutant promoter libraries. Yang and colleagues have created a mutant library of *Pthl* promoters by optimizing both the core promoter region and the spacer between the RBS and start codon (ATG). The *Pthl* mutant 1200-9-9 was shown to have a 10-fold higher activity when compared to the native *Pthl*. This mutant promoter was shown to work in both *C. acetobutylicum* and *C. ljungdahlii* [38]. Mordaka and Heap have also recently developed a mutant *Pthl* promoter library by randomizing 39 bases around the -35 and -10 elements in *Pthl*. This study looked at 3 oxygen independent reporter assays, with the glucuronidase enzyme assay being the most accurate. Higher promoter-activity mutants in *C. acetobutylicum* were created when certain areas of the promoter sequence were conserved between native and mutant *Pthl*. These promoter libraries were also shown to be portable between *Clostridium spp.*, showing a linear

correlation of glucuronidase activity between *C. acetobutylicum* and *C. sporogenes* [66]. Interestingly, Mordaka and Heap proposed that the strongest promoter in this study, was 30% stronger than the strongest promoter designed by Yang and colleagues [38, 66].

Another type of promoter that is particularly useful for protein fusions in *Clostridium spp.* is an inducible promoter. Pyne and colleagues have listed several inducible promoters that have been used over the years in a review on genetic advances in *Clostridium* organisms [59]. One of the first inducible promoters designed for *C. acetobutylicum* were the radiation inducible promoters, *PrecA* and *PrecN*. The hypoxic environment of tumors can be targeted with *Clostridium* spores, and this study created promoters that can activate genes when induced with ionizing radiation [67]. Girbal and colleagues have developed a xylose-inducible promoter for *C. acetobutylicum* based on the *Staphylococcus xylosus* xylose operon promoter-repressor regulatory system (*PxyIA*) for use in characterizing a the glucuronidase reporter system for *C. acetobutylicum* [44]. A lactose inducible promoter (*PbgaL*) was developed by Hartman and colleagues for the control of gene expression in the pathogen *C. perfringens* [68] This lactose inducible promoter was also used by Al-Hinai and colleagues for creating KOs and KIs in *C. acetobutylicum* [69]. This promoter was also used by Banerjee and colleagues for inducing genes for enzymes involved in diverting *C. ljungdahlii* away from acetate production and toward more desirable metabolic products [70]. Dong and colleagues have previously developed an anhydrotetracycline-inducible chloramphenicol acetyltransferase promoter (*PcatP*) for regulation of gene expression in *C. acetobutylicum* [46]. An arabinose inducible

promoter has recently been developed for *C. cellulolyticum* using the AraR-regulon from *C. acetobutylicum* and the *Pptk* [71].

1.5 Fluorescence in Anaerobic Microbes

Fluorescent proteins (FPs) like GFP and mCherry have been used as gene reporters and tags in both prokaryotes and eukaryotes and are essential molecular biology research tools. Fluorescent proteins and fluorescent tags can be used as both gene reporters and for cell physiology and probing molecular interactions with microscopy. However, despite the robust applications for traditional GFP and mCherry proteins, the use of these proteins to study anaerobic organisms is limited as they all require molecular oxygen for fluorophore activation.

GFP is a β -barrel shaped FP derived from *Aequorea victoria* that contains a Ser-Tyr-Gly amino acid sequence, which goes through cyclization and oxidation to form a p-hydroxybenzylideneimidazolidinone fluorophore [72, 73]. Red fluorescence proteins are derivatives of the tetrameric protein, DsRed, which was originally derived from *Discosoma* sp.. The red chromophore is a result of a post-translational modification of Gln-Tyr-Gly residues go through during imidazolidinone cyclization with p-hydroxybenzylidene and acylimine substituents [74, 75]. The mRFP is a monomeric variant of DsRed and was further optimized to the most-widely used red FP, mCherry. The mCherry protein is a rapidly maturing, bright and more stable variant of the FP mRFP [75, 76].

Although traditional FPs cannot be observed in an anaerobic environment, one way to combat this limitation is through aerobic fluorescence recovery. Zhang and colleagues cloned GFP into the facultative anaerobe, *Enterobacter aerogenes*, to

quantify the bacterial concentration and production of hydrogen under anaerobic conditions and developed a method of aerobic fluorescence recovery (AFR) of the anaerobically expressed GFP. This method involves the production of the non-fluorescent form of GFP anaerobically and inducing fluorescence by exposing the cells to air [77]. Ransom and colleagues have also recently used AFR, but with mCherry in the obligate anaerobe *C. difficile*. In this study, they used a codon optimized cyan fluorescent protein (CFP_{opt}) as well as a codon optimized form of mCherry (mCherryOpt). It was found that mCherryopt had a faster acquisition of fluorescence than CFP_{opt}, and mCherryopt can be used as a reporter for the *pdaV* operon coding for lysozyme resistance. It was shown that after 1 hour treatment with lysozyme, cell fixation, and overnight aerobic incubation to mature the chromophore the fluorescence could be quantified using a plate reader, however, it was determined that mCherry underreports induction when results were compared to qRT-PCR [78]. Pinilla-Redondo and colleagues have also recently used AFR on mCherry and a GFP mutant (GFPmut3) in anaerobically grown *E. coli* to demonstrate detection and quantification of horizontal gene transfer in anaerobic environments like the gastrointestinal tract. The GFPmut3 cells were able to recover fluorescence within 1 hour and mCherry containing cells were able to recover some fluorescence within 2 hours of aerobic incubation. [79]. However, the long maturation time it takes for AFR to occur as well as testing AFR on organisms that can grow both aerobically and anaerobically, like *E. coli*, is limiting in the study of aerobic fluorescent protein use in strict anaerobes.

A SNAP-tagTM covalent labeling method described by Keppler and colleagues has shown promising results in low oxygen environments. The SNAP-tagTM is an evolved human DNA repair protein O6-alkylguanine-DNA alkyltransferase (AGT)

and works by transferring a benzyl group from O6-benzylguanine (BG) to a cysteine residue, allowing for irreversible labeling when using the biotin (BGBT) and fluorescein (BGAF) BG derivatives. This study describes an oxygen-independent method whereby SNAP-tagTM is used to detect fusion proteins in AGT-deficient cells [80]. Regoes and Hehl also described a method for using a SNAP-tagTM showing that it can be used in place of oxygen dependent GFP in organisms grown in an anaerobic environment. This study used SNAP-tagTM to detect the localization of reporter proteins in the microaerotolerant parasite, *Giardia intestinalis*, and proposed that this method could be used for other microaerotolerant organisms or possibly anaerobic organisms [81]. Nicolle and colleagues have also demonstrated SNAP-tag-mediated cell labeling in the anaerobic periodontal pathogen *Porphyromonas gingivalis* [82].

Los and colleagues have also developed a protein labeling system called HaloTag. HaloTag is a modified haloalkane dehalogenase designed to covalently bind to its synthetic HaloTag ligands and can be used for a variety of protein labeling and cellular signaling methods [83]. Martincova and colleagues have used the HaloTag to label hydrogenosomes and mitosomes in microaerotolerant parasitic protists *Trichomonas vaginalis* and *G. intestinalis*, showing that this technology can be used to study mitochondrial adaptations in anaerobic organisms [84]. However, with the SNAP-tag protein being 20 kDa and the Halo-tag being a 33 kDa protein, a smaller protein or tag would be more useful when creating fusion proteins in cell labeling [85].

Another promising fluorescent system for anaerobic environments are flavin mononucleotide (FMN)-based fluorescent reporter systems, which contain light-oxygen-voltage-sensing (LOV) domains [86]. Drepper and colleagues developed a set of flavin mononucleotide (FMN)-based fluorescent proteins (FbFPs) for in vivo

labeling and detection in both anaerobic and aerobic environments. This study utilized FbFPs from *Bacillus subtilis* YtvA (BsFbFP) and *Pseudomonas putida* SB2 (PpFbFP) in which photoactive cysteine residues were substituted for alanine by site-directed mutagenesis. These proteins were then expressed in *E. coli* and *Rhotobacter capsulatus*. Drepper and colleagues also created a truncated gene of only the photoactive LOV domain and cloned the gene into *E. coli*, creating a higher intensity FP (EcFbFP) [86]. Drepper and colleagues also have shown that the FbFP is more a stable and reliable reporter than GFP-derived yellow fluorescent protein (YFP) [87]. Lobo and colleagues have also shown that Drepper's modified protein, BS2, can be used to study in vitro and in vivo gene expression in the anaerobic bacterium, *Bacteroides fragilis*, which is found in the normal microflora of the human digestive system [88]. While this study showed that FbFPs can work in oxygen limited environments, it is important to study the efficiency of FbFPs in a strict anaerobic environment in other organisms.

Potzkei and colleagues have also developed a Forster resonance energy transfer (FRET)-based biosensor called fluorescent protein-based biosensor for oxygen (FluBO). FRET works by transferring energy between chromophores of a donor domain, and an acceptor domain where the acceptor quenches fluorescence of the donor. FluBO contains both a yellow fluorescent protein (YFP) that is sensitive to oxygen depletion and a hypoxia-tolerant FbFP and was used for real-time monitoring changing O₂ levels in cell cytoplasm. In this study YFP works as the FRET acceptor, and FbFP works as the FRET donor. When oxygen is present YFP efficiently quenches FbFP, but when FRET efficiency is low in low oxygen environments, FbFP is not quenched due to the immature YFP and loss of FRET coupling. However, it was

determined that further investigation is needed in cells with lower metabolic activity than *E. coli* cells. [89].

These FbFPs are trademarked as “evoglow” [6], but are no longer available commercially [8]. Landete and colleagues have used this anaerobic form of GFP (Evoglow-Pp1) in addition to aerobic GFP to create a non-invasive reporter system for the tracking of *Bifidobacterium sp.* in vivo. This study showed how the reporter vector pNZ:Tu-GFPana can be used to track probiotic species in food and intestinal microbiota to assess the ability to successfully colonize [90]. Landete and colleagues have also created a cyan-green based (evoglow-Pp1) fluorescent system to track lactic acid bacteria (LAB; *Lactococcus*, *Lactobacillus*, and *Enterococcus*) of probiotic interest, and show that this system works as a successful reporter system in a low oxygen environment [91]. The variants Bs1 (monomeric BsFbFP), Bs2 (Dimeric BsFbFP), and Pp1 (PpFbFP) are also now available for *Clostridium* species from Evocatal [6].

In addition to the FbFPs developed by Drepper and colleagues, Chapman and colleagues developed a FP system that also involves a LOV-domain based fluorescence. Chapman and colleagues developed a FP derived from the molecular evolution of plant-derived LOV domains, called improved LOV (iLOV), in order to track virus infection in plant cells [92]. Christie and colleagues further engineered the iLOV protein to develop a photostable iLOV (phiLOV), which constrains the FMN fluorophore and yields improved photochemical properties in *E. coli* [93].

These oxygen independent FPs have the potential to further advance molecular and physiological studies of *Clostridium* organisms. Teng and colleagues have utilized the *P. putida* FbFP and the *Pthl* promoter from *C. acetobutylicum* to construct a

fluorescence reporter system for screening promoters in *Clostridium cellulolyticum* [65]. Buckley and colleagues have used a codon-optimized phiLOV FP from Christie and colleagues to fluorescently label *C. difficile*, *C. sordellii*, and *C. acetobutylicum*, and have also created fusion proteins with the *C. difficile* cell division FtsZ protein and the flagella subunit FliC [94]. Seo and colleagues have also recently used FbFPs in creating a fluorescent reporter system in *C. beijerinckii*. This study utilized the *B. subtilis* YtvA variant EcFbFP to develop a codon-optimized FbFP for *C. beijerinckii* (CbFbFP) and used FACS to isolate high CbFbFP expressing *C. beijerinckii* and determine mutations in the plasmid. Using the CbFbFP mutant plasmid, Seo and colleagues were able to apply real-time fluorescence measurement to *C. beijerinckii* [95]. Mordaka and Heap have tested several oxygen-independent reporter assays and found that in *E. coli*, the FbFPs CreiLOV and PhiLOV2.1 showed high fluorescence compared to the background, but in *C. acetobutylicum* fluorescence if these two proteins was indistinguishable from background fluorescence. Other fluorescent protein systems are needed to further expand the resources available and could potentially allow the use of multiple FPs in anaerobic bacterial imaging.

1.6 Fluorescence-Activating and Absorption-Shifting Tag (FAST) Could be a Promising Fluorescent System for Anaerobes

One promising way to combat the ineffectiveness of traditional fluorescent proteins in *Clostridium spp.* is using fluorogen-activating proteins (FAPs), which only fluoresce when bound to a specific fluorogenic chromophore. In a recent fluorogen-based reporter review, Jullien and Gautier suggest that using a fluorogen-based system provides high contrast due to the chromophore being non-fluorescent on its own, but displaying very bright fluorescence when bound to the target [96]. Plamont and

colleagues have recently developed the Fluorescence-Activating absorption-Shifting Tag, or FAST, as an alternative to traditional FPs like GFP. FAST is an engineered variant of the small Photoactive Yellow Protein. In their study, 2 fluorogens for FAST were tested, 4-hydroxybenzylidene-rhodanine (HBR) and 4-hydroxy-3-methylbenzylidene-rhodanine (HMBR). Both HBR and HMBR fluoresce green when bound to FAST under blue light excitation, which allows rapid, high contrast fluorescence even in the presence of excess fluorogen [97].

Plamont and colleagues showed that FAST paired with the fluorogen, HMBR showed comparable brightness and photostability to other fluorescent proteins like GFP. FAST is also promising due to the variety of cells that can use the FAST-HMBR system, from mammalian cells to microorganisms like *E. coli* and *Saccharomyces cerevisiae*. FAST and the HMBR fluorogen also show the ability to fluoresce instantaneously once the protein is folded, and does not require the long maturation time of GFP in aerobic conditions of up to 1 hour, which is may be problematic for real-time monitoring [97]. Plamont and colleagues also suggest that FAST can be used in FRET measurements with FAST being an acceptor, allowing other fluorescence to be quenched when the fluorogen is added, or decrease quenching by washing away the fluorogen. Their study also suggests that FAST would make an ideal system for super-resolution imaging in live cells, showing that the FAST system can be used for a diverse number of techniques and can further advance the field of fluorescence based reporters as well as microscopy [97]. Using a system like FAST and HMBR would provide an excellent fluorescent reporter system in *Clostridium spp.* as well as shed light on cell physiology that could not be shown with previous oxygen-dependent fluorescent protein systems in clostridia.

Recently, Li and colleagues have presented new analogous fluorogens developed for FAST to offer even more experimental versatility. Their study shows the fluorogen 4-hydroxy-3,5-dimethoxybenzyliden rhodamine (HBR-3,5DOM) in particular forms a tight complex with the FAST protein, allowing red fluorescence under green light excitation. This study demonstrates that by creating complimentary protein fusions, FAST and the fluorogen, HMBR, with mCherry or FAST and the fluorogen, HBR-3,5DOM, with EGFP, and using a dual 488/543 nm excitation and variable spectral detection, with an appropriate ligand, the FAST protein could be distinguished from its fusion. [98].

The FAST system has already been used successfully in a variety of studies. Pimenta and colleagues have recently published a study that attempts to combat photobleaching in fluorogen-binding tags like FAST. In this study it was found that FAST can be optimized by mutating specific amino acid residues to reduce photo damage or by minimizing the electron donating properties of nearby amino acids and by chemical modifications of the fluorogenic ligand [99]. Emanuel and colleagues have created a FAST mutant library to identify brighter and more photostable variants. This study looked for mutants with slower decay of the biphasic photobleaching behavior of this system. They used an image-based screening approach in order to view the photobleaching effects and thus identify slower photobleaching mutants. [100]. Kim and colleagues used the FAST system to create new fluorogens that can be used with the FAST protein. This study found that gallol-containing compounds such as gallic aldehyde-rhodanine (GA-Rho) and 3-methylcatechol aldehyde-rhodanine (mCA-Rho) showed similar red-shifted fluorescence emission wavelengths as the

original fluorogen HBR and successfully used the new fluorogens in *E. coli* and in eukaryotic cells [101].

Li and colleagues have also recently shown that the FAST system can be used to monitor membrane protein trafficking. This study introduced a membrane-impermeant FAST fluorogen HBR by adding a negatively charged carboxymethyl group to the rhodamine head and varied the substituents on the aromatic ring. The HBR substituent chosen for this study was HBRAA-3E which was shown to be non-toxic to mammalian cells, and FAST was fused to the C-terminus of the platelet derived growth factor receptor (PDGFR) transmembrane domain (sFASTtml) in HeLa cells in order to evaluate cell surface labeling. This study was able to use both HMBR and HBRAA-3E to quantify the total amount of surface proteins and the total amount of proteins through flow cytometry [102].

Most recently, Monmeyran and colleagues have used the FAST system in order to study bacterial biofilm complexity where the oxygen dependency of GFP-like FPs cannot be utilized. In this study it was shown that the fluorescence of GFP-like FPs is dependent on the oxygen distribution throughout the biofilm and that fluorescence levels were not an accurate measurement of gene expression. However, fluorogens that bind to the FAST protein can quickly disperse through bacterial biofilms and still tightly complex. To compare FAST fluorescence to GFP, a biofilm was constructed with MG1655-gfp-F cells expressing both GFP and FAST, and the orange/red fluorogen HBR-3,5-DOM was added at 2 μ M concentration. It was shown that the GFP signal was saturated after 5 hours, but FAST fluorescence increased exponentially over 20 hours. A similar test was also done to compare FAST:HBR-2.5-DM to mCherry using MG1655-F cells with an mCherry-FAST fusion. Similarly,

FAST continued to increase saturation after the maturation of the mCherry protein. While the oxygen dependent fluorescent protein signals were lower in the bacterial biofilm, it was determined that the low oxygen concentration did not alter the growth of the biofilm. This study has successfully shown that FAST is superior to GFP and mCherry in the low oxygen environments of bacterial biofilms [103].

Chapter 2

SYNTROPHIC INTERACTIONS IN CLOSTRIDIA CO-CULTURES

2.1 Introduction

Fossil fuel availability and greenhouse gas emissions have pushed scientists to find sustainable and carbon neutral energy systems. One viable option for reduction of greenhouse gas emissions is the utilization of industrial waste gases like CO₂, H₂, and CO, also known as syngas [18]. Acetogens like *C. ljungdahlii* can consume syngas as the only source of carbon, but the small amount of ATP generated and limited growth rate of acetogens due to high acetate production can limit the productivity of these fermentations [2]. Attempts to engineer clostridia to optimize utilization of syngas in addition to glucose, fructose and other substrates are increasingly successful, however, limitations persist in easy to use recombineering methods and efficient transformation protocols. However, using syntrophic clostridial consortia in co-culture could achieve the carbon utilization outcomes that traditional monoculture cannot achieve alone [8].

Pairing the solventogen, *C. acetobutylicum*, with the acetogen *C. ljungdahlii* has been shown to allow a sugar consuming bacteria to release large amounts of CO₂ during anaerobic fermentation, allowing *C. ljungdahlii* to consume these gases to increase production of acetate [24]. *C. acetobutylicum* can then use this acetate to produce other useful metabolites like acetone, butyrate, and butanol using ABE fermentation. Recent co-culture studies have taken interest in the chain-elongating *C. kluyveri* as another potential partner for *C. ljungdahlii* to pair with in syntrophic co-culture. Diender and colleagues have recently paired *C. ljungdahlii* and *C. kluyveri* in co-culture, allowing *C. ljungdahlii* to consume syngas (CO, H₂, and CO₂) to produce acetate and ethanol. *C. kluyveri* can then use these metabolites and create butyrate,

hexanoate and octanoate using chain-elongation. The co-culture was also found to produce butanol, hexanol, and was the first clostridial co-culture to report the production of octanol [17]. Another clostridial co-culture that could be of potential interest is the pairing of *C. acetobutylicum* with *C. kluyveri*. The ability for *C. acetobutylicum* to consume large amounts of sugars like glucose to produce solvents like ethanol, and butanol could pair well with the chain-elongating capabilities of *C. kluyveri*. *C. kluyveri* requires ethanol and acetate to grow and perform chain-elongation, both of which are produced by *C. acetobutylicum*. *C. acetobutylicum* produces acetate and butyrate during the acidogenic phase of growth, and ethanol during solventogenesis. *C. kluyveri* should be able to utilize these chemicals to potentially increase the amount of butyrate formed by the culture, potentially allowing for the production of hexanoate from chain-elongation of butyrate. These fatty acids could then be converted to large quantities of butanol and hexanol. In addition to pairing *C. acetobutylicum* with *C. kluyveri*, the addition of a third bacterium, *C. ljungdahlii*, could increase the efficiency of the co-culture even further, allowing the waste gases produced by *C. acetobutylicum* (H_2 and CO_2), and *C. kluyveri* (H_2) to increase the carbon utilization of the co-culture. This novel pairing of *C. acetobutylicum* and *C. kluyveri*, and the triplicate co-culture of *C. acetobutylicum*, *C. kluyveri* and *C. ljungdahlii* could potentially produce novel metabolites not found in previously reported clostridial co-cultures.

2.2 Materials and Methods

2.2.1 Chemicals

All chemicals were purchased from Sigma-Aldrich (St. Louis, MO) unless noted otherwise.

2.2.2 Bacterial Strains, Media and Growth Conditions

All strains used in this study are listed in Table A.1 of Appendix A. *C. acetobutylicum* ATCC 824 was grown anaerobically at 37°C in either liquid 2xYTG medium (16 g/L tryptone, 10 g/L yeast extract, 4 g/L NaCl, and 5g/L glucose[pH 5.2]), solid 2xYTG medium (pH 5.8), Turbo CGM clostridial growth medium [24]. *C. acetobutylicum* strains were grown on 2xYTG for at least 5 days, colonies were inoculated in 10 mL of Turbo CGM and heat shocked for 10 minutes at 70-80 °C to kill vegetative cells that may have lost the megaplasmid pSOL1. *C. ljungdahlii* was grown anaerobically at 37°C in liquid Turbo CGM medium. Entire glycerol stocks were thawed and inoculated in 10 mL of Turbo CGM and passaged to fresh Turbo CGM medium at 20% inoculum after 48 hours of growth. *C. kluyveri* was grown anaerobically in either liquid DSMZ 52 medium (DSMZ) or liquid Turbo CGM medium. Entire glycerol stocks were thawed and inoculated in 10 mL of medium and allowed to grow for ~5 days before passaging active culture into fresh medium. Optical Density was determined at a wavelength of 600 nm (OD₆₀₀) using a Beckman-Coulter DU370 spectrophotometer.

2.2.3 High Performance Liquid Chromatography

Metabolite concentrations were measured via high performance liquid chromatography (HPLC; Agilent 1200 series) with an Aminex HPX-87H column (Bio Rad) as described [24, 104-106].

2.2.4 Scanning Electron Microscopy

Culture samples were fixed with 2% glutaraldehyde (Electron Microscopy Sciences, EM grade) at 4°C overnight. 1:10 dilution of poly-L-lysine was incubated for 5 minutes on silicon chips. Poly-L-lysine was removed from silicon chip and chip was allowed to air dry overnight. Culture samples on silicon chips were added to a 12 well plate covered in fume hood and were incubated on poly-L-lysine coated silicon chips for 1 hour, then rinsed 3 times 5 minutes each using 1X PBS. Samples were incubated with 1 mL 1% OsO₄ solution for 1 hour and rinsed 3 times 5 minutes each with nanopore H₂O. Samples were dehydrated using 200 proof ethanol, incubating for 10 minutes each at 25%, 50%, 75%, 95% and 100% ethanol. After 100% incubation, samples were left in 100% ethanol at 4°C overnight in 12 well plate wrapped in parafilm. A second 10 minute 100% ethanol incubation was completed before critical point drying with Autosamdri-815B Critical Point Dryer (Tousimis), and samples were coated with platinum using a Benchtop Turbo III Sputter Coater (Denton Vacuum). Electron images were collected using Field-Emission Scanning Electron Microscope (Hitachi 54700) at a working distance of 7.0-8.9 mm and a voltage of 3.0kV.

2.3 Results & Discussion

2.3.1 *C. kluyveri* consumes acetate and ethanol and produces butyrate and hexanoate in monoculture

C. kluyveri has been shown previously to consume ethanol and acetate (as well as a small number of other substrates) to produce carboxylic acid butyrate and hexanoate through chain elongation pathway [12, 13, 17, 107]. To examine the ability for *C. kluyveri* to grow in the Turbo CGM co-culture medium, *C. kluyveri* was grown in DSMZ 52 medium (DSMZ) as well as Turbo CGM co-culture medium over 48 hours. *C. kluyveri* consumed 44 ± 12.4 mM of ethanol and 32 ± 20.5 mM of acetate (Figure 2.1A) and produced 9.9 ± 0.3 mM of butyrate and 22.5 ± 1.7 mM of hexanoate growing in DSMZ 52 medium over 48 hours (Figure 2.1B). In comparison, *C. kluyveri* consumed 40.1 ± 6.1 mM of ethanol and 20.4 ± 0.7 mM of acetate over 48 hours (Figure 2.1C) and produced 14.8 ± 0.4 mM of butyrate and 18.3 ± 0.9 mM of hexanoate growing in Turbo CGM medium (Figure 2.1D). It grew to a maximum OD_{600} of 0.39 ± 0.02 at 48 hours of growth in DSMZ 52 medium, while reaching a maximum OD_{600} of 0.34 ± 0.02 at 48 hours of growth in Turbo CGM co-culture medium (Figure 2.1E). Growth in the DSMZ 52 medium displayed a more neutral pH, with a maximum pH of 6.91 ± 0.04 at 22.5 hours and a minimum pH of 6.54 ± 0.04 at 48 hours of growth. In Turbo CGM, *C. kluyveri* growth resulted in a slightly more acidic pH profile, with a maximum pH at the start of the culture of 6.5 ± 0.06 , and a minimum pH of 6.00 ± 0.05 at 48 hours (Figure 2.1E). Here we confirm that *C. kluyveri* consumes acetate and ethanol to form butyrate and hexanoate in DSMZ 52 medium. We also show that *C. kluyveri* can successfully grow in Turbo CGM co-culture medium when supplemented with 100mM of ethanol. Because of this, *C.*

kluyveri should be able to grow in Turbo CGM along with *C. acetobutylicum* in co-culture.

2.3.2 Co-culture of *C. kluyveri* and *C. acetobutylicum* displays a culture phenotype similar to that of pure *C. acetobutylicum* and produces no hexanoate

Pure *C. kluyveri* control was spun down at 5000 rpm and added to 20 mL of fresh Turbo CGM, and *C. acetobutylicum* pure control was inoculated into fresh Turbo CGM ~15 hours previously ($OD_{600} \sim 0.1$) and allowed to grow overnight to an OD_{600} of ~ 4.0 . The same amount of *C. kluyveri* and *C. acetobutylicum* were used in the co-culture. To generate a synthetic *C. kluyveri* – *C. acetobutylicum* co-culture, 20 mL of *C. kluyveri* overnight culture ($OD_{600} \sim 0.3$) was spun down at 5000 rpm and added to 20 mL of active *C. acetobutylicum* culture and the co-culture was allowed to grow for 48 hours. Actively growing *C. acetobutylicum* should allow *C. kluyveri* to utilize metabolites like ethanol that have already been produced by *C. acetobutylicum*. In pure culture, *C. kluyveri* reached a maximum OD_{600} of 0.42 ± 0.07 at 6 hours of growth due to higher initial inoculation OD_{600} , had a maximum pH of 6.4 at the start of the culture, and reached a pH of 5.87 ± 0.02 at 48 hours (Figure 2.2A). In the pure culture control, *C. kluyveri* consumes 27 ± 0.38 mM acetate and 59.9 ± 1.22 mM of ethanol and produced 10.8 ± 0.39 mM of butyrate and 27.7 ± 3.12 mM of hexanoate over 48 hours (Figure 2.2B). The *C. kluyveri* and *C. acetobutylicum* co-culture showed exponential growth until it reached a maximum OD_{600} of 11.6 ± 0.07 after 26 hours of growth, with a pH drop to 4.95 ± 0.007 which was then adjusted with 1M NaOH to above a pH of 5 and reached a maximum pH of 5.65 at 48 hours of growth (Figure 2.2C). In co-culture, 275.5 ± 0.8 mM of glucose, 12.7 ± 0.4 mM of fructose was consumed, while 36.2 ± 2.2 mM of ethanol, and 163.4 ± 0.2 mM of butanol was

produced, but no production of hexanoate was detected (Figure 2.2D). The pure *C. acetobutylicum* control showed exponential growth until a maximum OD₆₀₀ was reached of 9.95 ± 0.63 after 28 hours. Pure *C. acetobutylicum* showed a minimum pH of 4.85 ± 0.04 after 4 hours of growth which was then adjusted with 1M NaOH to above 5. The culture reached a maximum pH of 5.44 ± 0.13 after 48 hours (Figure 2.2E). The pure *C. acetobutylicum* control consumed 275.3 ± 24.1 mM of glucose, 12.8 ± 1.2 mM of fructose, and produced 40.2 ± 10.4 mM of ethanol, and 168.6 ± 28 mM of butanol (Figure 2.2F). Here we show that the co-culture metabolite profile is similar to the metabolite profile of pure *C. acetobutylicum*, leading us to believe *C. acetobutylicum* is the dominant participant in the co-culture in both metabolite production and growth. It is unclear whether *C. kluyveri* is active at all in the co-culture due to no detection of hexanoate. While *C. kluyveri* also produces butyrate, *C. acetobutylicum* produces butyrate and converts it to butanol. Because the metabolite profile of *C. acetobutylicum* is so similar to the co-culture, it is unclear whether *C. kluyveri* contributes to butyrate production. It is also possible that *C. acetobutylicum* does not produce enough ethanol to support *C. kluyveri* growth, producing only 36.2 ± 2.2 mM of ethanol after 48 hours (Figure 2.2D). The addition of more *C. kluyveri* and possibly supplementing the co-culture with additional ethanol could encourage production of hexanoate.

To encourage more *C. kluyveri* growth in co-culture, 40 ml of active *C. kluyveri* culture (OD₆₀₀ ~0.4) was spun down at 5000 rpm and was added to 20 mL of active *C. acetobutylicum* culture (OD₆₀₀ ~4.5) and was allowed to grow for 48 hours. Pure *C. acetobutylicum* was inoculated 15.5 hours before passaging into 20 mL of fresh Turbo CGM at a 10% inoculum. 40 mL of pure *C. kluyveri* (OD₆₀₀ ~0.4) was

spun down and inoculated into 20 mL of Turbo CGM ($OD_{600} \sim 0.8$). *C. acetobutylicum* previously did not produce enough ethanol at the start of co-culture to support *C. kluyveri*, so Turbo CGM supplemented with 100mM of ethanol in both the *C. kluyveri* control, and in the co-culture. In the pure culture, *C. kluyveri* reached a maximum OD_{600} of 0.96 ± 0.24 at 6 hours of growth and had a maximum pH of 6.4 ± 0.03 at the start of the culture, reaching a pH of 5.91 at 48 hours (Figure 2.3A). In the pure culture control, *C. kluyveri* consumes 27 ± 0.38 mM acetate and 59.9 ± 1.22 mM of ethanol and produces 10.8 ± 0.39 mM of butyrate and 27.7 ± 3.12 mM of hexanoate over 48 hours (Figure 2.3B). The *C. kluyveri* and *C. acetobutylicum* co-culture reached a maximum OD_{600} of 11.4 ± 0.8 at 24 hours of growth, and the pH dropped to 5.12 ± 0.14 and then increased to have a maximum pH of 5.75 ± 0.007 at 48 hours of growth (Figure 2.3C). The co-culture consumes 252.5 ± 23.6 mM glucose, 9.6 ± 1.7 mM of fructose, and produces 26.2 ± 2.1 mM of ethanol, 5.46 ± 0.04 mM of acetate, 154.7 ± 7.5 mM of butanol but no hexanoate over 48 hours (Figure 2.3D) Pure *C. acetobutylicum* culture reached a maximum OD_{600} of 10.1 ± 0.1 at 24 hours of growth, and the pH dropped to 4.91 ± 0.01 and then increased to have a maximum pH of 5.51 ± 0.06 at 48 hours of growth (Figure 2.3E). *C. acetobutylicum* pure culture consumes 257.8 ± 2.8 mM glucose, 11.19 ± 0.01 mM of fructose, and 5.46 ± 0.04 mM of acetate, and produces 26.7 ± 2.0 mM of ethanol and 154.2 ± 1.7 mM of butanol over 48 hours (Figure 2.3F). The co-culture reached an OD_{600} of 11.4 ± 0.8 after 24 hours (Figure 2.3C) while *C. acetobutylicum* reaches an OD_{600} of 10.1 ± 0.1 after 24 hours, possibly indicating the presence of *C. kluyveri* in co-culture, however with no way to confirm strain identity other than metabolite production, the presence of *C. kluyveri* remains unclear. The co-culture profile again resembles that of the *C. acetobutylicum* pure

culture, indicating the more rapid growth of *C. acetobutylicum* could be overtaking *C. kluyveri* in co-culture even when additional *C. kluyveri* is added. It may also be possible that high concentrations of solvents like butanol produced by *C. acetobutylicum* may be inhibiting growth. Butanol has been shown to be inhibitory to growth in *C. acetobutylicum* [108], *Clostridium beijerinckii* [109], and *C. ljungdahlii* [110] at high concentrations, so it is possible that high butanol concentrations can affect *C. kluyveri* growth. Testing whether *C. kluyveri* can grow in the presence of butanol is crucial to successfully creating a syntrophic co-culture between *C. kluyveri* and *C. acetobutylicum*.

2.3.3 *C. kluyveri* can use butanol as the primary source of alcohol for chain elongation

C. kluyveri can produce medium-chain and long-chain fatty acids using the process called chain-elongation. In this process, *C. kluyveri* oxidizes small alcohols like ethanol to Acetyl-CoA, which can then be converted to butyryl-CoA and butyrate. *C. kluyveri* can also further extend fatty acid chain lengths using reverse beta-oxidation by adding an additional acetyl-CoA molecule, extending the chain by 2 carbons. To test whether the high butanol concentration produced by *C. acetobutylicum* is causing *C. kluyveri* growth to be inhibited and to see if a 4C alcohol like butanol can be utilized by *C. kluyveri*, *C. kluyveri* was grown with acetate, and ethanol supplemented with butanol, as well as acetate and only butanol as a source of alcohol. In the DSMZ 52 medium supplemented with 100 mM of ethanol control, *C. kluyveri* reached a maximum OD₆₀₀ of 0.32± 0.01 at 50.5 hours of growth and with a maximum pH of 6.88 ± 0.01 at the start of the culture, dropping to a pH of 6.28 ± 0.04 after 113.5 hours (Figure 2.4A). *C. kluyveri* control in DSMZ 52 with only acetate and

ethanol consumed 26.8 ± 0.1 mM of acetate and 68.7 ± 3.3 mM of ethanol and produced 3.8 ± 0.7 mM of butyrate and 33.6 ± 4.7 mM of hexanoate after 113.5 hours (Figure 2.4B). *C. kluyveri* grown in DSMZ 52 medium supplemented with 30 mM of butanol grew to a maximum OD_{600} of 0.195 ± 0.031 at 113.5 hours, reaching a maximum pH of 7.06 at 24 hours of growth (Figure 2.3C). *C. kluyveri* grown in DSMZ 52 medium supplemented with 30 mM of butanol consumed 14.3 ± 3.3 mM of acetate, 7.5 ± 1.2 of butanol and 3.1 ± 1.3 mM of ethanol, while producing 10.2 ± 1.5 of butyrate and 9.0 ± 4.9 mM of hexanoate over 113.5 hours (Figure 2.4D). *C. kluyveri* grown in DSMZ 52 medium supplemented with 30 mM of butanol and 60 mM of ethanol grew to a maximum OD_{600} of 0.40 ± 0.02 at 24 hours and had a starting pH of 6.88 ± 0.01 at the start of culture, reaching a minimum pH of 6.64 ± 0.02 at 26.5 hours of growth (Figure 2.3E). *C. kluyveri* grown in DSMZ 52 medium supplemented with 30 mM of butanol and 60 mM of ethanol consumed 24.5 ± 1.1 mM of acetate, 4.7 ± 0.1 of butanol and 53.7 ± 3.8 mM of ethanol, while producing 5.2 ± 0.03 of butyrate and 2.2 ± 0.2 mM of hexanoate over 113.5 hours (Figure 2.4F). *C. kluyveri* has been shown to use propanol in chain elongation to produce propionate, valerate, butyrate and hexanoate so *C. kluyveri* has been shown to metabolize other alcohols [107]. Butanol has been detected in co-culture with *C. kluyveri* and *C. ljungdahlii*, however it is not clear whether *C. kluyveri* utilized butanol. More likely, butanol was likely produced due to *C. ljungdahlii* reducing butyrate to butanol [18]. Here we show that *C. kluyveri* can grow in the presence of butanol and that *C. kluyveri* alone can utilize butanol to produce hexanoate. Likely, butanol is oxidized to create butyryl-CoA, which could be used to create hexanoyl-CoA, and subsequently hexanoate.

2.3.4 Increasing the ratio of *C. kluyveri* to *C. acetobutylicum* in co-culture does not enable the co-culture to produce hexanoate

In order to increase the ratio of *C. kluyveri* to *C. acetobutylicum* cells in co-culture, 50 ml of active *C. kluyveri* culture ($OD_{600} \sim 0.600$) was spun down at 5000 rpm and added to 5 mL of active *C. acetobutylicum* culture. Additional 5 mL of *C. acetobutylicum* was spun down at 5000 rpm and the culture supernatant was also added to the co-culture, and the co-culture was allowed to grow for 47 hours. Addition of *C. acetobutylicum* culture supernatant was intended to add metabolites that *C. acetobutylicum* produces so *C. kluyveri* can consume them without overcrowding the co-culture with *C. acetobutylicum* cells. In pure culture, *C. kluyveri* reached a maximum OD_{600} of 3.0 ± 0.2 at 14 hours of growth and had a maximum pH of 6.36 ± 0.01 at the start of the culture, reaching a pH of 5.57 ± 0.58 at 47 hours (Figure 2.5A). In the culture control, *C. kluyveri* consumes 18.9 ± 3.3 mM acetate and 57.8 ± 4.5 mM of ethanol and produces 34.6 ± 4.2 mM of hexanoate over 47 hours (Figure 2.5B). The *C. kluyveri* and *C. acetobutylicum* co-culture reached a maximum OD_{600} of 10.5 ± 0.7 at 23 hours of growth and had a maximum pH of 6.5 at 14 hours of growth (Figure 2.5C). The co-culture consumed 304.9 ± 12.4 mM glucose, and 16.5 ± 0.2 mM of fructose, and produced 40 ± 3.2 mM of ethanol, 31.4 ± 2.9 mM of acetate, 164.3 ± 3.3 mM of butanol but no hexanoate over 47 hours (Figure 2.5D) Pure *C. acetobutylicum* culture reached a maximum OD_{600} of 8.01 ± 0.01 at 39 hours of growth, and had a maximum pH of 5.75 ± 0.08 at 47 hours of growth (Figure 2.5E). *C. acetobutylicum* pure culture consumes 301.0 ± 4.2 mM glucose, and 14.1 ± 1.4 mM of fructose, and produces 32.0 ± 0.8 mM of ethanol, 169.7 ± 6.1 mM of butanol, and 10.4 ± 0.7 of acetate over 47 hours (Figure 2.5F). The *C. kluyveri* pure culture did not reach a very high OD_{600} , only increasing ~ 0.1 over 14 hours and slowly dropping throughout the

fermentation (Figure 2.5A). It is possible that high concentrations of *C. kluyveri* cells inhibit further *C. kluyveri* growth. It is also possible that concentrations of acetate and ethanol are depleted too quickly to support such high OD₆₀₀ for *C. kluyveri*. However, most hexanoate production in pure *C. kluyveri* culture occurs after reaching maximum OD₆₀₀ (Figure 2.5A, 2.5B). Another possibility is that *C. kluyveri* is limited by acidic pH much earlier in the co-culture compared to in pure culture. In pure culture, pH drops to 5.57 ± 0.58 at 47 hours (Figure 2.5A), but in co-culture, the pH reaches 5.52 ± 0.06 after 23 hours (Figure 2.5C). Acidification of pure *C. kluyveri* likely occurs when medium- and long-chain fatty acids are produced, which is limiting to the culture. *C. acetobutylicum* also has 2 phases of growth, acidogenesis and solventogenesis. It is possible that the production of acid like acetate in early culture, and solvent production of ethanol late in culture is incompatible with *C. kluyveri* growth. It has been shown that high concentrations of hexanoate (caproate) can be a limiting factor of cell growth, and acidic conditions in a co-culture of *C. autoethanogenum* and *C. kluyveri* was also shown to be limiting [17]. It was also shown that pH was limiting in a co-culture between *C. ljungdahlii* and *C. kluyveri* [18]. Using bioreactor fermentations where pH is controlled and removing toxic concentrations of hexanoate could help to improve productivity of *C. acetobutylicum* and *C. kluyveri* co-cultures.

2.3.5 A co-culture of *C. acetobutylicum*, *C. ljungdahlii* and *C. kluyveri* produces hexanoate

C. ljungdahlii produces acetate and ethanol which could also be utilized by *C. kluyveri* in co-culture, and *C. ljungdahlii* could also utilize H₂ produced by *C. kluyveri*. It has also been shown that more acetate and isopropanol are produced in *C. acetobutylicum* and *C. ljungdahlii* co-culture than either species alone [24]. To test

whether the addition of *C. ljungdahlii* to a *C. kluyveri* and *C. acetobutylicum* co-culture could help create a more favorable culture environment for fatty acid-chain elongation, *C. ljungdahlii* (OD₆₀₀ ~0.4) and *C. acetobutylicum* (OD₆₀₀ ~0.1) were added to active *C. kluyveri* culture (OD₆₀₀ ~0.7) in Turbo CGM medium supplemented with 80 g/L of glucose and 100 mM of ethanol. Pure *C. kluyveri* grown in DSMZ 52 medium (OD₆₀₀ ~0.3) was spun down at 5000 rpm and inoculated in Turbo CGM to an OD₆₀₀ of ~0.7 supplemented with 100mM of ethanol with no glucose. Pure *C. ljungdahlii* (OD₆₀₀ ~2.0) was passaged into Turbo CGM with no glucose to an OD₆₀₀ of ~0.3, and after 7 hours of growth, was spun down at 5000 rpm and inoculated into Turbo CGM with no glucose to an OD₆₀₀ of ~0.4. Pure *C. acetobutylicum* was grown overnight to an OD of ~7.0 and inoculated into Turbo CGM to an OD₆₀₀ of ~0.1. In pure culture control, *C. kluyveri* consumes 13.2 ± 3.9 mM acetate and 29.5 ± 4.7 mM of ethanol and produces 4.7 ± 1.1 mM of butyrate and 34.0 ± 10.0 mM of hexanoate over 48 hours (Figure 2.6A). In *C. ljungdahlii* pure culture, 31.0 ± 0.01 mM fructose was consumed and 12.9 ± 2.8 mM of ethanol and 105.4 ± 0.6 mM of acetate were produced over 48 hours (Figure 2.6B). *C. acetobutylicum* pure culture consumes 143.6 ± 1.2 mM glucose, and 13.0 ± 0.5 mM of fructose, and produces 17.1 ± 2.9 mM of ethanol, 34.4 ± 0.4 mM of butanol, and 23.6 ± 0.3 of acetate over 48 hours (Figure 2.6C). The *C. kluyveri*, *C. ljungdahlii*, and *C. acetobutylicum* triple co-culture consumes 23.9 ± 1.1 mM glucose, 2.6 ± 0.3 mM of fructose, and 4.2 ± 2.3 mM of ethanol and produces 32.0 ± 0.8 mM of butyrate, 21.4 ± 26.9 mM of butanol, 16.5 ± 2.4 of acetate, 1.97 ± 0.2 mM of isopropanol, $0.7 \text{ mM} \pm 0.1 \text{ mM}$ of 2,3-butanediol and 17.7 ± 1.1 mM of hexanoate over 48 hours (Figure 2.6D). *C. kluyveri* pure culture reached a maximum OD₆₀₀ of 1.01 ± 0.3 at 3 hours of growth, *C. ljungdahlii* pure

culture reached a maximum OD₆₀₀ of 3.2 ± 0.03 at 41.5 hours of growth, *C. acetobutylicum* pure culture reached a maximum OD₆₀₀ of 6.79 ± 0.01 at 17.5 hours of growth, and the co-culture reached a maximum OD₆₀₀ of 2.28 ± 0.28 at 24 hours of growth (Figure 2.6E). *C. kluyveri*, had a maximum pH of 6.33 ± 0.06 at the start of the culture, reaching a pH of 5.94 at 48 hours, and *C. ljungdahlii* had a maximum pH of 6.51 at the start of the culture, reaching a pH of 4.77 at 48 hours, which is consistent with production of acids in both cultures. *C. acetobutylicum* had a maximum pH of 6.4 ± 0.01 at the start of the culture, reaching a pH of 4.66 ± 0.01 at 48 hours. The co-culture had a maximum pH of 6.11 ± 0.05 at the start of the culture, reaching a pH of 4.99 ± 0.06 at 48 hours (Figure 2.6F). Glucose, fructose, and ethanol were consumed, and acetate, butanol, and hexanoate are produced which indicates that *C. acetobutylicum*, *C. ljungdahlii*, and *C. kluyveri* are all present in co-culture (Figure 2.6D). *C. acetobutylicum* activity is confirmed by consumption of glucose, *C. ljungdahlii* activity is confirmed by production of isopropanol and 2,3-butanediol, and *C. kluyveri* activity is confirmed by production of hexanoate in co-culture. The OD₆₀₀ of the co-culture only reached a maximum of 2.28 ± 0.28 at 24 hours (Figure 2.6E) which indicates inhibition of *C. acetobutylicum* growth, which may be why *C. kluyveri* was able to thrive and produce hexanoate. However, pH still seems to be a limiting factor for the co-culture, which reached a pH of 5.0 after 17.5 hours (Figure 2.6F). A better understanding of how co-cultures can work syntrophically on a cell-to-cell level is necessary to further understanding and optimizing an efficient clostridia co-culture system.

2.3.6 Scanning electron microscopy (SEM) of co-cultures of *C. acetobutylicum* and *C. ljungdahlii* show potential fusion events, but similar cell shape and surface texture in SEM makes it difficult to distinguish the two species

It has been recently shown that a co-culture of *C. acetobutylicum* and *C. ljungdahlii* can directly exchange metabolites and electrons to improve carbon yields and produce syntrophically produce isopropanol and 2,3-butanediol through cell-to-cell interactions [24]. To further investigate these cell-to-cell interactions, we used SEM to investigate membrane interactions between the two *Clostridium spp.* in co-culture. The *C. acetobutylicum* and *C. ljungdahlii* co-culture was generated using a 10% inoculum of a 1:5 ratio of *C. acetobutylicum* and *C. ljungdahlii*. Pure *C. acetobutylicum* was grown in Turbo CGM over 24 hours (Figure 2.7A). Pure *C. ljungdahlii* was grown in Turbo CGM without glucose over 48 hours (Figure 2.7B). SEM examination of the *C. acetobutylicum* and *C. ljungdahlii* co-culture shows close contact between cells of slightly varying SEM captured morphology, as indicated in Figure 2.7C with white arrows. However, it is not possible to confirm the identity of each strain using SEM. Using SEM alone we were not able to identify separate species in co-culture. Although *C. ljungdahlii* appears to be larger when compared at the same magnification to *C. acetobutylicum* (Figure 2.7A, 2.7B) and certain cells interacting in co-culture appear to be different sizes (Figure 2.7C), similarity in shape and no distinguishing surface texture does not allow for accurately distinguishing separate species. Fluorescent labeling has been used successfully in several co-cultures to distinguish between species [21-23]. Tagging one or both species with a fluorescent labeling dye or a fluorescent protein would be an ideal way to distinguish between species in co-culture.

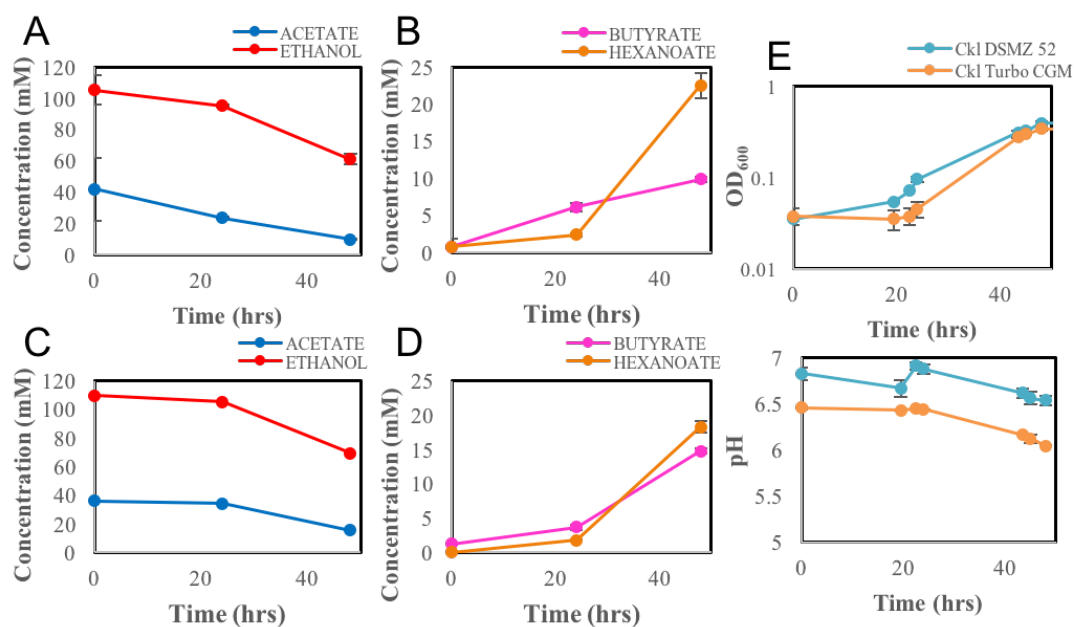


Figure 2.1 - *C. kluyveri* shows a similar growth pattern in the co-culture medium Turbo CGM compared to *C. kluyveri* growth medium DSMZ 52. *A*, *C. kluyveri* ethanol and acetate consumption in DSMZ 52 medium over 48 hours. *B*, *C. kluyveri* butyrate and hexanoate production in DSMZ 52 medium over 48 hours. *C*, *C. kluyveri* ethanol and acetate consumption in Turbo CGM co-culture medium over 48 hours. *D*, *C. kluyveri* butyrate and hexanoate production in Turbo CGM co-culture medium over 48 hours. *E*, *C. kluyveri* growth curves (top) and pH profiles (bottom) in DSMZ 52 (blue) and Turbo CGM (orange). n = 2, error bars: SD.

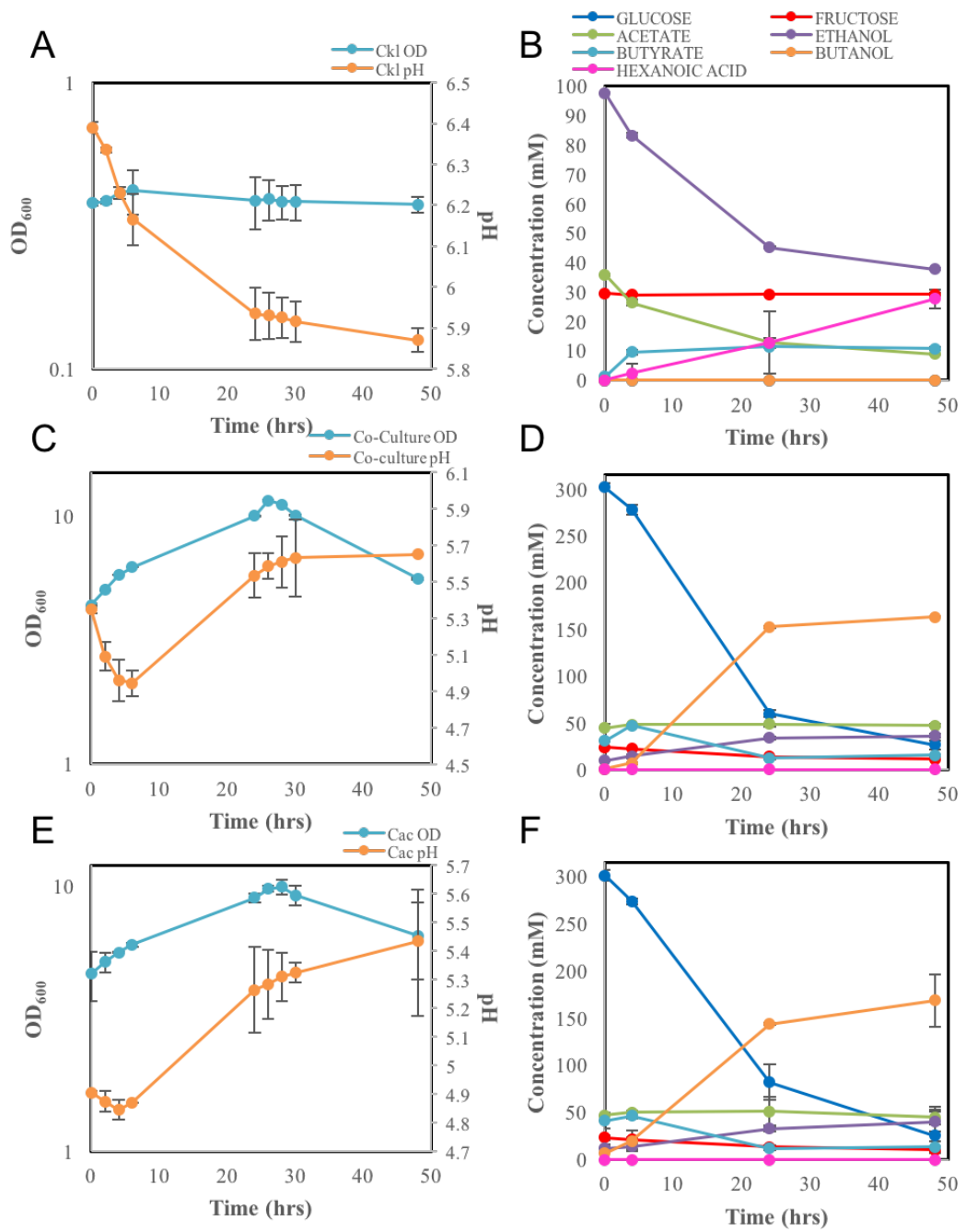


Figure 2.2 - *C. kluyveri* and *C. acetobutylicum* co-culture shows a similar metabolite profile to pure *C. acetobutylicum* co-culture and produces no hexanoate after 20ml of spun down *C. kluyveri* ($\sim OD_{600}$ 0.3) is added to 20ml active *C. acetobutylicum* culture ($\sim OD_{600}$ 4.5). A, *C. kluyveri* pure culture growth curve and pH profile in Turbo CGM without glucose and supplemented with 100mM ethanol over 48 hours. B, *C. kluyveri* metabolite profiles in Turbo CGM without glucose over 48 hours. C, *C. kluyveri* and *C. acetobutylicum* co-culture growth curve and pH profile in Turbo CGM over 48 hours. D, *C. kluyveri* and *C. acetobutylicum* co-culture metabolite profiles in Turbo CGM over 48 hours. E, *C. acetobutylicum* pure culture growth curve and pH profile in Turbo CGM over 48 hours. F, *C. acetobutylicum* pure culture metabolite profiles in Turbo CGM over 48 hours. n = 2, error bars: SD

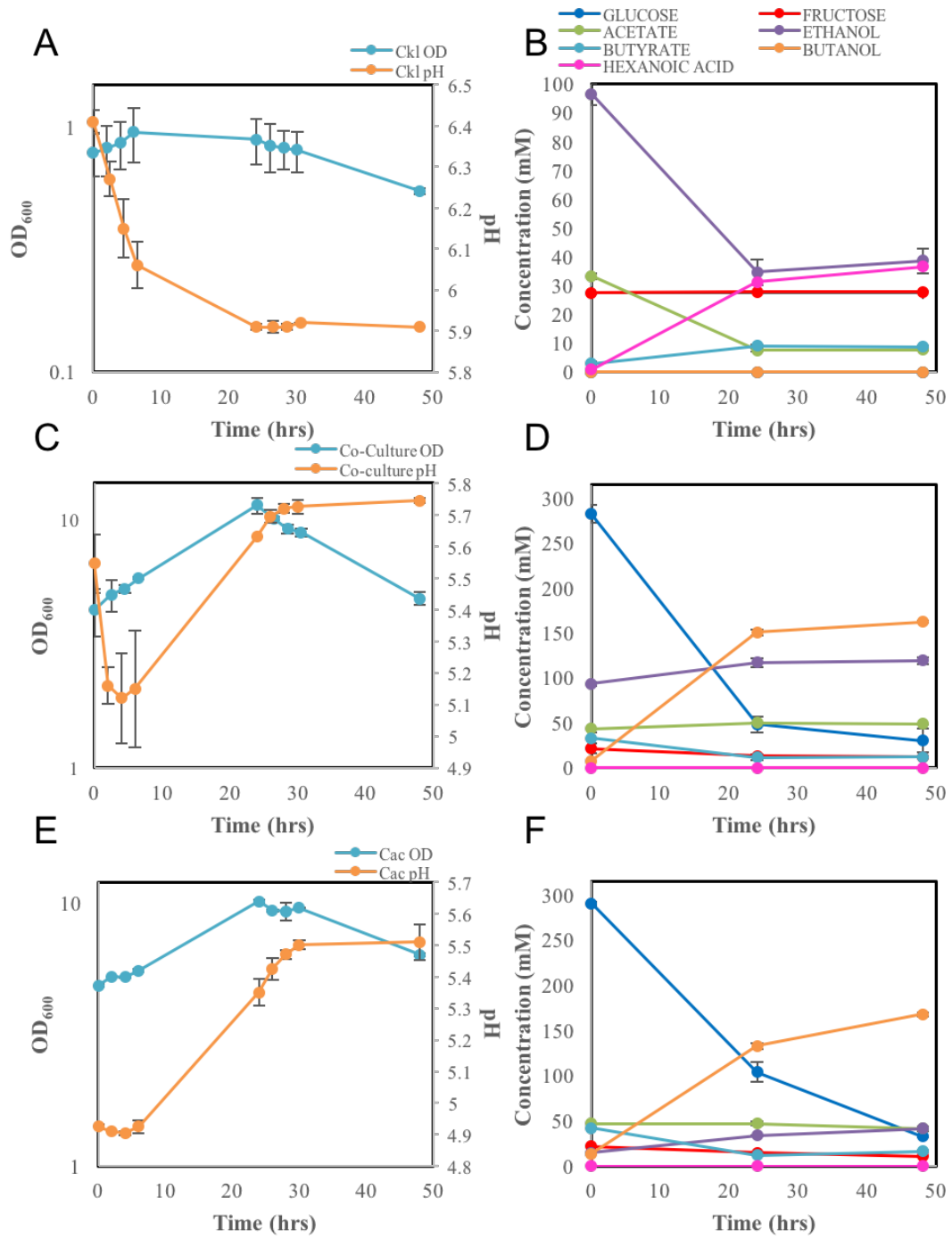


Figure 2.3 - *C. kluyveri* and *C. acetobutylicum* co-culture shows a similar metabolite profile to pure *C. acetobutylicum* co-culture and produces no hexanoate after 40ml of spun down *C. kluyveri* ($\sim OD_{600}$ 0.3) is added to 20ml active *C. acetobutylicum* culture ($\sim OD_{600}$ 4.5). *A*, *C. kluyveri* pure culture growth curve and pH profile in Turbo CGM without glucose and supplemented with 100mM ethanol over 48 hours. *B*, *C. kluyveri* metabolite profiles in Turbo CGM without glucose supplemented with 100mM ethanol over 48 hours. *C*, *C. kluyveri* and *C. acetobutylicum* co-culture growth curve and pH profile in Turbo CGM supplemented with 100mM ethanol over 48 hours. *D*, *C. kluyveri* and *C. acetobutylicum* co-culture metabolite profiles in Turbo CGM supplemented with 100mM ethanol over 48 hours. *E*, *C. acetobutylicum* pure culture growth curve and pH profile in Turbo CGM over 48 hours. *F*, *C. acetobutylicum* pure culture metabolite profiles in Turbo CGM over 48 hours. $n = 2$, error bars: SD

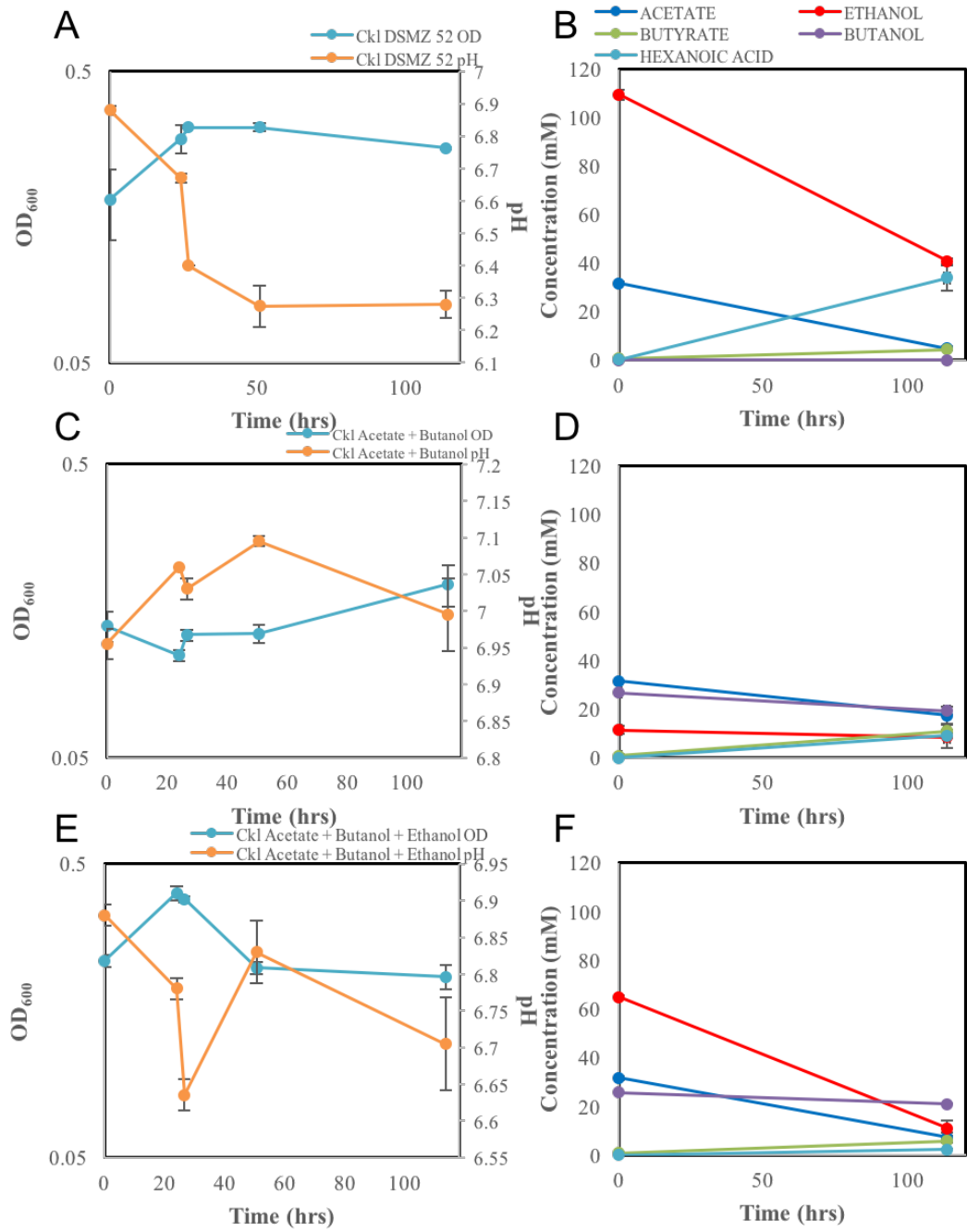


Figure 2.4 - *C. kluyveri* can grow on acetate and butanol and utilize butanol as the primary alcohol in chain elongation. *A*, *C. kluyveri* growth curve and pH profile in DSMZ 52 with 30mM of acetate and 100mM ethanol over 113.5 hours. *B*, *C. kluyveri* metabolite profiles in DSMZ 52 with 30mM of acetate and 100mM ethanol over 113.5 hours. *C*, *C. kluyveri* growth curve and pH profile in DSMZ 52 with 30mM of acetate and 30mM butanol over 113.5 hours. *D*, *C. kluyveri* metabolite profiles in DSMZ 52 with 30mM of acetate and 30mM butanol over 113.5 hours. *E*, *C. kluyveri* growth curve and pH profile in DSMZ 52 with 30mM of acetate, 60mM ethanol, and 30mM butanol over 113.5 hours. *F*, *C. kluyveri* growth curve and pH profile in DSMZ 52 with 30mM of acetate, 60mM ethanol, and 30mM butanol over 113.5 hours. n = 2, error bars: SD

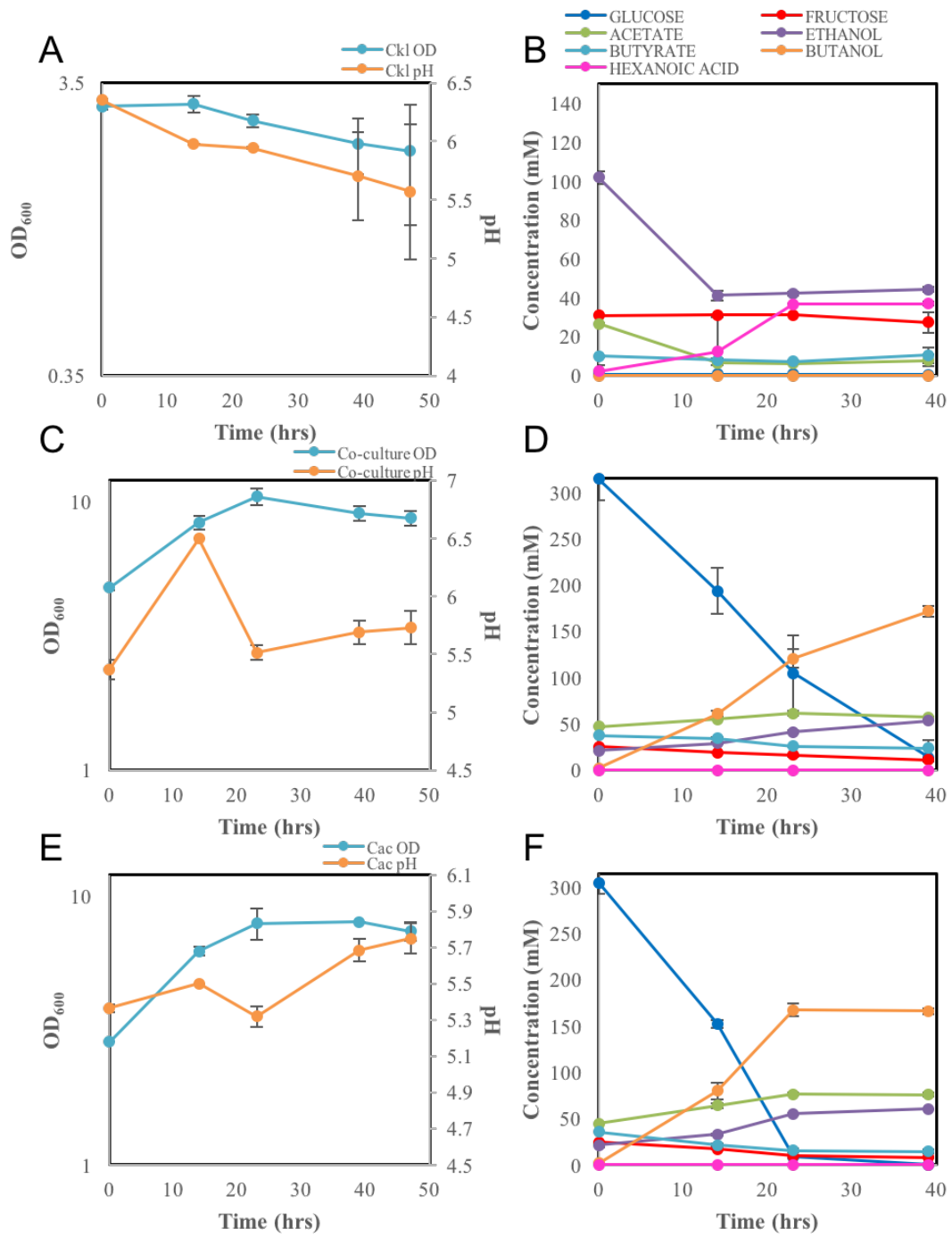


Figure 2.5 - *C. kluyveri* and *C. acetobutylicum* co-culture shows a similar metabolite profile to pure *C. acetobutylicum* co-culture and produces no hexanoate after 50ml of spun down *C. kluyveri* ($\sim OD_{600}$ 0.6) is added to 5ml of active *C. acetobutylicum* culture ($\sim OD_{600}$ 5.0) and 5 ml of *C. acetobutylicum* culture supernatant. *A*, *C. kluyveri* pure culture growth curve and pH profile in Turbo CGM without glucose and supplemented with 100mM ethanol over 48 hours. *B*, *C. kluyveri* metabolite profiles in Turbo CGM without glucose supplemented with 100mM ethanol over 48 hours. *C*, *C. kluyveri* and *C. acetobutylicum* co-culture growth curve and pH profile in Turbo CGM supplemented with 100mM ethanol over 48 hours. *D*, *C. kluyveri* and *C. acetobutylicum* co-culture metabolite profiles in Turbo CGM supplemented with 100mM ethanol over 48 hours. *E*, *C. acetobutylicum* pure culture growth curve and pH profile in Turbo CGM over 48 hours. *F*, *C. acetobutylicum* pure culture metabolite profiles in Turbo CGM over 48 hours. n = 2, error bars: SD

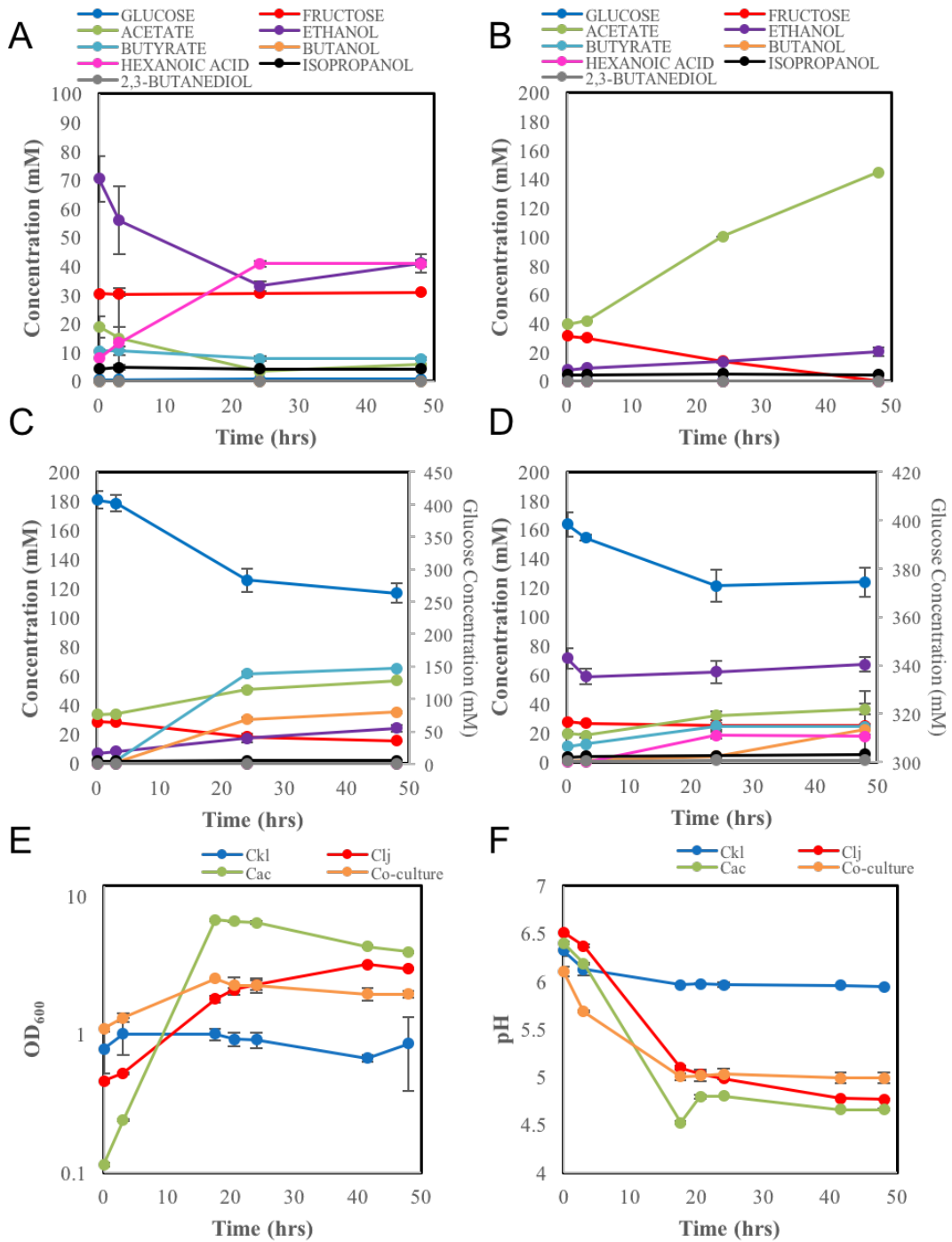


Figure 2.6 - *C. kluyveri*, *C. ljungdahlii* and *C. acetobutylicum* co-culture shows a metabolite profile consistent with growth of all three organisms and produces hexanoate. *A*, *C. kluyveri* pure culture metabolite profiles in Turbo CGM without glucose supplemented with 100mM ethanol over 48 hours. *B*, *C. ljungdahlii* pure culture metabolite profiles in Turbo CGM without glucose. *C*, *C. acetobutylicum* pure culture metabolite profiles in Turbo CGM over 48 hours. *D*, *C. kluyveri*, *C. ljungdahlii* and *C. acetobutylicum* co-culture metabolite profiles in Turbo CGM supplemented with 100mM ethanol over 48 hours. *E*, *C. kluyveri* pure culture (blue), *C. ljungdahlii* pure culture (red), *C. acetobutylicum* pure culture (green), and *C. kluyveri*, *C. ljungdahlii* and *C. acetobutylicum* co-culture (orange) growth curves over 48 hours. *F*, *C. kluyveri* pure culture (blue), *C. ljungdahlii* pure culture (red), *C. acetobutylicum* pure culture (green), and *C. kluyveri*, *C. ljungdahlii* and *C. acetobutylicum* co-culture (orange) pH profiles over 48 hours. n = 2, error bars: SD

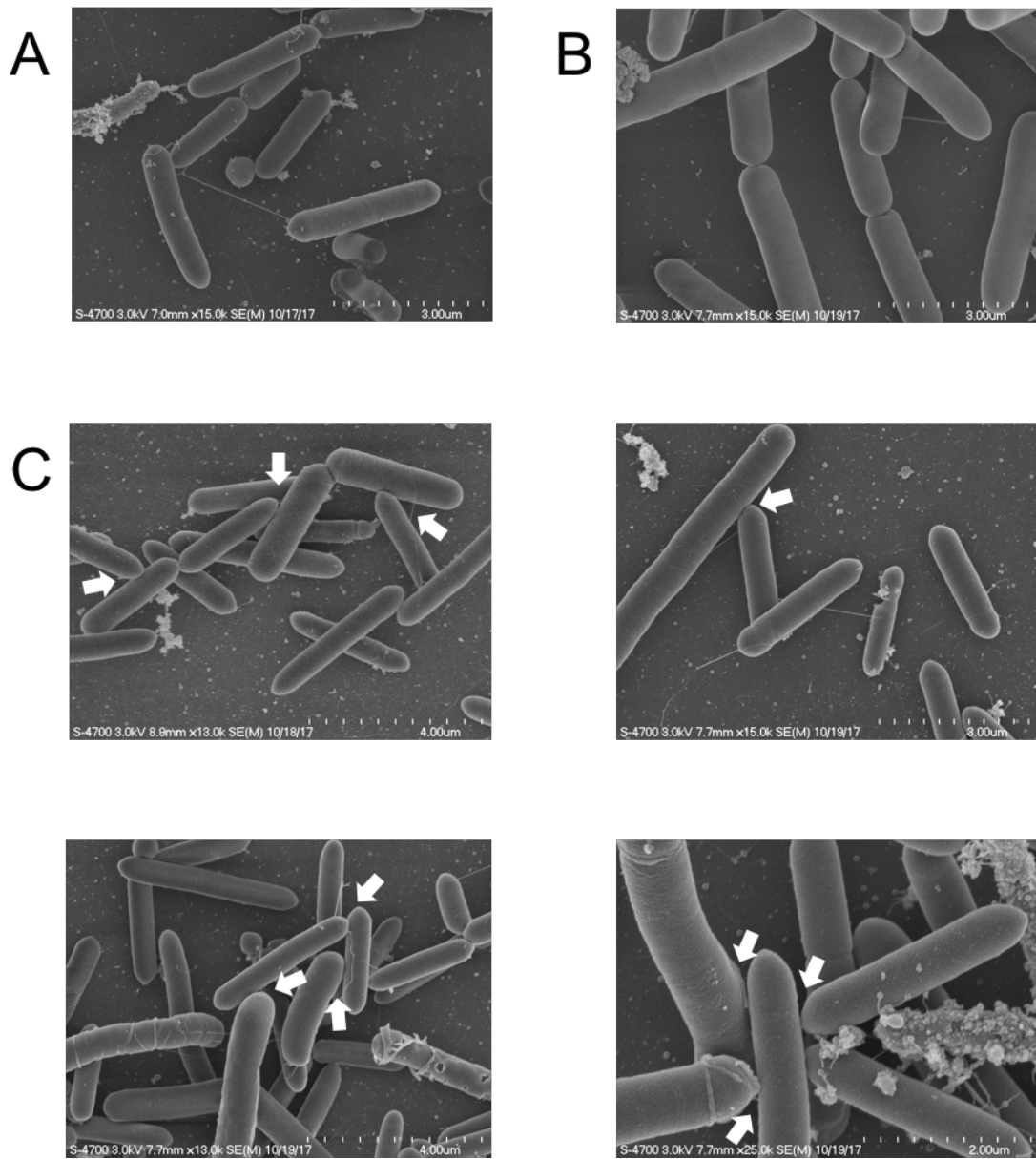


Figure 2.7 - Possible fusion events between *C. ljungdahlii* and *C. acetobutylicum* cells in co-culture using Scanning electron microscopy. A, Pure *C. acetobutylicum* culture after 24 hours of growth. B, Pure *C. ljungdahlii* culture after 48 hours of growth. C, *C. ljungdahlii* and *C. acetobutylicum* co-culture after 24 hours of growth, white arrows represent possible *C. ljungdahlii* and *C. acetobutylicum* fusion events.

Chapter 3

ENGINEERING A FLUORESCENT REPORTER SYSTEM AND VIEWING PROTEIN LOCALIZATION WITH FAST IN *Clostridium acetobutylicum*

3.1 Introduction

Fluorescent proteins (FPs) are an essential tool in molecular biology, but are difficult to utilize in anaerobic bacteria like *Clostridium spp.* The chromophores of traditional FPs like GFP and mCherry require oxygen for maturation [111], which is not possible for live cell imaging in *C. acetobutylicum*. *Clostridium* cells can be fixed and incubated in oxygen to allow for chromophore maturation, but long incubation time and poor expression of large FPs can lead to limitations in reporter studies and microscopy [78].

Anaerobic fluorescent proteins like flavin-binding fluorescent proteins (FbFPs) have been a promising alternative to traditional FPs due to chromophore maturation not requiring the presence of oxygen [86]. FbFPs like phiLOV2.1 have also recently been used as a reporter and fluorescent tag in *Clostridium sp.* [94]. However, in a recent study by Morkada and Heap it was shown that while FbFPs show fluorescence in *E. coli*, in *C. acetobutylicum* phiLOV2.1 and CreiLOV did not show fluorescence above what was shown in the control strain [66].

Another promising alternative to traditional FPs is the fluorescence-activating and absorption-shifting tag (FAST). FAST is a 14-kDa variant on the photoactive yellow protein (PYP) that binds to a fluorogenic ligand to activate fluorescence. FAST has been used successfully in HeLa cells, zebrafish embryos, *S. cerevisiae* and *E. coli*, and this fluorescence activating protein (FAP) does not require oxygen. FAST has been engineered to activate the fluorogenic ligand 4-hydroxy-3-methylbenzylidene-rhodanine (HMBR), and shows brightness and photostability comparable to traditional

FPs [97]. Recently, Monmeyran and colleagues have used the FAST system to study the low oxygen environment of *E. coli* bacterial biofilms. In this study it was shown that FAST and its fluorogens are superior to GFP and mCherry in low oxygen biofilms, and GFP and mCherry did not accurately represent gene expression in an environment with variable oxygen concentrations [103]. Using FAST and the fluorogen HMBR should provide a solution to previous challenges faced by other aerobic and anaerobic fluorescent proteins.

Because of the challenges of current fluorescent proteins in anaerobic bacteria, localization of proteins within bacterial cells have not been as widely investigated as aerobic bacteria. One of the promising candidates for characterizing a fluorescent fusion protein system is a cell division protein involved in the assembly of the “Z ring” in rod shaped bacteria. The “Z ring” is a scaffold of many different proteins involved in the recruitment of components of the cell division machinery, or divisome [112]. One of the most important components of the “Z ring” is the tubulin homologue, FtsZ [113]. FtsZ is a self-activating GTPase that is widely conserved throughout bacteria [114, 115]. Previously FtsZ has been used to characterize the phiLOV fluorescent system in *Clostridioides difficile* (formerly known as *Clostridium difficile*) [94]. One of the many components of Z ring assembly is the Z-ring-associated protein, ZapA. ZapA has been shown to interact with FtsZ during Z ring assembly [116]. ZapA has also been shown to enhance polymerization and stability of FtsZ [113, 116-118]. ZapA has previously been fused with mCherryOpt to show ZapA localization in fixed *C. difficile* cells [78]. Here we examine the FAST and HMBR fluorogen system as a reporter for gene expression, and as a fluorescent tag for viewing protein ZapA localization in *C. acetobutylicum* cells.

3.2 Materials and Methods

3.2.1 Chemicals

All chemicals were purchased from Sigma-Aldrich (St. Louis, MO) unless noted otherwise. *E. coli* NEB 5-alpha, Q5 DNA polymerase and NEBuilder HiFi DNA assembly master mix were purchased from NEB (Ipswich, MA). Restriction endonucleases were purchased from Thermo Fisher Scientific (Waltham, MA). The fluorogen HMBR (4-hydroxy-3-methylbenzylidene-rhodanine) was kindly provided by the lab of Dr. Hanson at the University of Delaware (Newark, DE).

3.2.2 Bacterial Strains, Media and Growth Conditions

All strains and plasmids used in this study are listed in Table B.1 of Appendix B. *E. coli* NEB 5-alpha was used to propagate all plasmids. *E. coli* strains were grown aerobically at 37°C at 250 rpm in liquid LB medium or solid LB agar medium. Appropriate antibiotics were added at the following concentrations: ampicillin, 100 ug/ml; kanamycin, 25 ug/ml. *E. coli* strains were stored at -85°C in 20% glycerol. *C. acetobutylicum* ATCC 824 was grown anaerobically in either liquid 2xYTG medium (16 g/L tryptone, 10 g/L yeast extract, 4 g/L NaCl, and 5 g/L glucose[pH 5.2]), solid 2xYTG medium (pH 5.8), or Turbo CGM medium [24]. Appropriate antibiotics were added at the following concentrations: erythromycin, 40 ug/ml for plates, 100 ug/ml for liquid cultures. Spore forming strains were grown on 2xYTG for at least 5 days, colonies were inoculated in 10 mL of Turbo CGM and heat shocked for 10 minutes at 70-80 °C to kill vegetative cells that may have lost the megaplasmid pSOL1. Optical Density (OD₆₀₀) was measured at 600 nm using a Beckman-Coulter DU370 spectrophotometer.

3.2.3 Genetic Manipulation

All primers used in this study are listed in Table B.2 of Appendix B. The vector p95thlFAST was constructed to express FAST in *C. acetobutylicum* using the strong *Pthl* promoter native to *C. acetobutylicum*. An Integrated DNA Technologies Gblock was created for FAST [97] and was codon optimized for *C. acetobutylicum* using the Integrated DNA Technologies Codon Optimization Tool. The pSOS95_MCS vector [106] was digested using BamHI and the codon optimized FAST gene was cloned into the vector using Gibson Assembly (New England Biolabs). The vector p95thl^{sup}FAST was constructed to express FAST in *C. acetobutylicum* using the optimized *Pthl* promoter 1200-9-9 developed by Yang *et al*, which showed 10-fold higher activity than native *Pthl* [38]. An Integrated DNA Technologies Gblock was created for the *Pthl* promoter 1200-9-9 (*Pthl*^{sup}). The p95thlFAST backbone was amplified using primers and digested with DpnI in order to reduce methylated plasmid background during transformation and PCR purified using the QIAquick PCR Purification Kit (Qiagen). *Pthl*^{sup} was cloned into p95thlFAST using Gibson Assembly (New England Biolabs). The vector p95ptbFAST was constructed to express FAST in *C. acetobutylicum* using the *Pptb* promoter native to *C. acetobutylicum*. The p95thlFAST backbone was amplified using primers and *Pptb* was amplified from the pSOS94_MCS vector [69] using primers. *Pptb* was cloned into p95thlFAST using Gibson Assembly (New England Biolabs). p95ptb^{mod}FAST was constructed to express FAST in *C. acetobutylicum* using the *Pptb* promoter and the p95thl^{sup}FAST backbone. The p95thl^{sup}FAST backbone was amplified using primers and *Pptb* was amplified from the pSOS94_MCS vector using primers. *Pptb* was cloned into p95thl^{sup}FAST using Gibson Assembly (New England Biolabs). The vector p95adcFAST was constructed to express FAST in *C. acetobutylicum* using the *Padc* promoter native to

C. acetobutylicum. The p95thlFAST backbone was amplified using primers and *Padc* was amplified from the pSOS95_MCS vector using primers. The vector p95adc^{mod}FAST was constructed to express FAST in *C. acetobutylicum* using the *Padc* promoter native to *C. acetobutylicum*. The p95thl^{sup}FAST backbone was amplified using primers and *Padc* was amplified from the pSOS95_MCS vector using primers. The plasmid p95ZapA-FAST was created using the *E. coli-Cac* shuttle vector pSOS95_MCS. An Integrated DNA Technologies Gblock was created using the native *thl* promoter and fusing the C-terminal end of ZapA with the N-terminal end of FAST with a short fusion protein linker (GGAGGTGGAAGC). The p95thl^{sup}FAST vector backbone was digested using *SacI* and *EcoRI* enzymes and the *thl*ZapA-FAST Gblock fragment was cloned into the backbone using Gibson Assembly (New England Biolabs).

3.2.4 Vector Transformations

Vectors were transformed into *E. coli* (NEB 5-alpha) and isolated using the QIAprep Spin Miniprep Kit (QIAGEN). Before transforming into *C. acetobutylicum*, vectors were transformed into electrocompetent *E. coli* ER2275 (pAN3) [69] for *in vivo* methylation by the *Bacillus subtilis* phage Φ 3T I methyltransferase contained on the pAN3 vector, as described previously [119]. Vectors were isolated using QIAprep Spin Miniprep Kit (QIAGEN) and transformed into *C. acetobutylicum* using a previously established protocol [120].

3.2.5 Flow Cytometry

Cell fluorescence was analyzed with a BD FACSAria IIu flow cytometer (Becton Dickinson (BD), Franklin Lakes, NJ). A blue solid-state laser (488 nm

excitation) and a 530/30 nm filter was used to measure FAST. FCS files were analyzed and histograms were created using Flowing Software v2.5.1 (Cell Imaging Core, Turku Centre for Biotechnology, Turku, Finland). For *E. coli* flow cytometry sampling, the geometric mean of the FITC-A fluorescence for 10,000 events was taken as the “MFI (A.U.)”. For *C. acetobutylicum* flow cytometry sampling, fluorescent populations of 10,000 events were normalized to *C. acetobutylicum* auto-fluorescence by creating a gate where *C. acetobutylicum* ATCC 824 control without HMBR had fluorescence of <1% and the geometric mean of the FITC-A fluorescence was measured for each fluorescent population as the “MFI (A.U.)”. *E. coli* and *C. acetobutylicum* cells were grown until early to mid-exponential phase of growth (OD₆₀₀ of 0.1-1). *C. acetobutylicum* thl^{sup}FAST cultures were vortexed anaerobically before samples were taken to reduce clumping of cells. Samples were pelleted at 5000 rpm for 15-30 minutes and washed with filtered PBS. Samples were re-suspended to an OD₆₀₀ of 1 in either filtered PBS or filtered 20 uM HMBR in PBS. 5 uL of sample was then added to 500 uL of filtered PBS or filtered 20 uM HMBR in PBS for flow cytometry analysis. Time courses were standardized by normalizing an OD₆₀₀ at hour 10 of growth as previously reported due to long lag growth phases [121].

3.2.6 SpectraMax i3x Microplate Reader

E. coli and *C. acetobutylicum* cells were grown until early to mid-exponential phase of growth (OD₆₀₀ of 0.1-1). *C. acetobutylicum* thl^{sup}FAST cultures were vortexed anaerobically before samples were taken to reduce clumping of cells. Samples were pelleted at 5000 rpm for 15-30 minutes and washed with filtered PBS. Samples were re-suspended to an OD₆₀₀ of 1 in either filtered PBS or filtered 20 uM HMBR in PBS and 100 uL was transferred to black conical-bottom 96-well plates

(BRANDplates[®]). Fluorescence was measured at excitation wavelength of 485 nm and emission wavelength of 535 nm using a SpectraMax i3x Microplate Reader (Molecular Devices, San Jose, CA). *C. acetobutylicum* samples were normalized to *C. acetobutylicum* ATCC 824 re-suspended to an OD₆₀₀ of 1 in filtered PBS. *E. coli* samples were normalized to *E. coli* re-suspended in filtered PBS. Time courses were standardized by normalizing an OD₆₀₀ at hour 10 of growth as previously reported [121].

3.2.7 Confocal Microscopy

Ibidi 8 well μ -Slides (ibidi, Martinsried, Germany) were incubated with 0.1% (w/v) poly-L-lysine in H₂O overnight, then washed with ddH₂O and dried. *E. coli* and *C. acetobutylicum* cells were grown in an overnight culture and samples were pelleted at 5000 rpm for 15-30 minutes and washed with filtered PBS. Samples were re-suspended to an OD₆₀₀ of 1-2 in filtered PBS and 200-300 μ L was transferred to poly-L-lysine coated 8 well μ -Slide and incubated for 1 hour at room temperature. Cells were washed with sterile PBS and 300 μ L of either filtered PBS or filtered 20 μ M HMBR in PBS were added to each well. Cells were imaged using confocal microscopy (Zeiss 880 Multiphoton Confocal Microscope with Airyscan) at the Delaware Biotechnology Institute Bioimaging Center. Images were acquired and processed using ZIESS ZEN – Digital imaging for light microscopy.

3.2.8 Statistical Analysis

Statistical analysis was performed using a two-tailed Student's t-test or means \pm standard deviation (SD) using Microsoft Excel software. Significant differences were considered when $p < 0.05$.

3.3 Results

3.3.1 *E. coli* FAST shows promising fluorescence intensity using flow cytometry, microplate reader, and confocal microscopy

FAST has been shown to be successfully expressed in *E. coli* previously [97]. However, it was crucial to express FAST using an *E. coli* - *C. acetobutylicum* shuttle vector, and under a *C. acetobutylicum* promoter. The shuttle vector pSOS95 was used in NEB 5-alpha *E. coli* to create a strain containing the FAST gene sequence under the native *Pthl* promoter from *C. acetobutylicum*. Flow cytometry analysis shows that expression of FAST in *E. coli* (strain termed *E. coli* FAST) when 20 uM HMBR was added shows high fluorescence during the exponential phase of growth phase with a MFI of 2422.8 ± 86.8 A.U. at 4 hours, increasing to a MFI of 4319.8 ± 50.7 A.U. after 24 hours in the stationary phase of growth. *E. coli* FAST without HMBR showed no fluorescence in both exponential growth and stationary phase of growth (Figure 3.1A). *E. coli* FAST with 20uM HMBR shows a large shift in FITC fluorescence when compared to *E. coli* FAST in filtered PBS (no HMBR control) after 22 hours (Figure 3.1B).

Similarly, using a microplate reader to measure fluorescence intensity, *E. coli* FAST with 20 uM HMBR shows a high fluorescence intensity in exponential growth phase of $2.5 \times 10^7 \pm 1.7 \times 10^6$ A.U. after 4 hours of growth, increasing to $3.3 \times 10^7 \pm 1.7 \times 10^6$ A.U. after 24 hours (Figure 3.1C). *E. coli* FAST shows to be in the exponential phase of growth until after 6 hours, slowing down to late exponential and into stationary phase after 8 hours (Figure 3.1D). After 4 hours of growth, *E. coli* FAST with 20 uM HMBR shows a linear fluorescence expression pattern with a maximum fluorescence intensity of $1.4 \times 10^8 \pm 4.0 \times 10^6$ A.U at an OD⁶⁰⁰ of 10, while after 24 hours of growth, *E. coli* FAST with 20 uM HMBR shows a linear

fluorescence expression pattern with a maximum fluorescence intensity of $2.6 \times 10^8 \pm 2.7 \times 10^7$ A.U. at an OD₆₀₀ of 10 (Figure 3.2A).

E. coli FAST with 20 uM HMBR also shows a bright fluorescent signal using confocal microscopy when compared to *E. coli* FAST in filtered PBS (Figure 3.2B). There is no fluorescent signal in the absence of HMBR, which means that *E. coli* FAST displays no auto-fluorescence.

3.3.2 Expression of FAST in *C. acetobutylicum* using the native thiolase promoter (*Pthl*) results in low HMBR-dependent fluorescence but using a strong mutant *Pthl* promoter improves fluorescent signal

When FAST was expressed in *C. acetobutylicum* under the control of the native *Pthl* using p95thlFAST, only a low fluorescent signal was detected (data not shown). We hypothesized that this was due to low FAST expression. Thus, in order to increase the fluorescent signal, a mutant *Pthl* promoter, super *Pthl* (*Pthl*^{sup}) [38] was used to replace the native *Pthl*. This strain was termed *C. acetobutylicum* thl^{sup}FAST. Using 20 uM HMBR in filtered PBS, FAST expression in this strain resulted in increased fluorescence compared to *C. acetobutylicum* thlFAST or the WT *C. acetobutylicum* control (Figure 3.3).

Using confocal microscopy, *C. acetobutylicum* thl^{sup}FAST with 20 uM HMBR had more frequent and brighter fluorescent cells compared to *C. acetobutylicum* thlFAST, which had fewer brightly fluorescent cells, and overall dimmer fluorescent signal (Figure 3.2B). Control WT *C. acetobutylicum* with 20 uM HMBR shows slight auto-fluorescence (Figure 3.4A). In the absence of HMBR and in resuspended filtered PBS, no fluorescent signal was detected in any of the three WT *C. acetobutylicum*, *C. acetobutylicum* thlFAST or *C. acetobutylicum* thl^{sup}FAST strains using confocal microscopy (Figure 3.4B).

3.3.3 Development of a FAST-based Fluorescent Reporter System for *Clostridium acetobutylicum*

Tummala and colleagues have previously established a beta-galactosidase activity reporter assay for *C. acetobutylicum* using the early growth stage promoters of *Pthl* and *Pptb*, and the late growth stage promoter *Padc*. The *thl* promoter controls the thiolase gene, or acetyl-coenzyme A [CoA] acetyltransferase, which carries out a condensation reaction between 2 molecules of Acetyl-CoA during acidogenesis. The *adc* promoter controls the acetoacetate decarboxylase gene, which catalyzes the decarboxylation acetoacetate to acetone during solvent production. The *ptb* promoter controls the phosphotransbutyrylase gene, which is involved in the production of butyrate in *C. acetobutylicum* during acidogenesis. [34]. Acidogenesis occurs during exponential phase of growth, while solventogenesis occurs in stationary phase of growth. To attempt to establish FAST as a reporter system for clostridia, the previously developed *C. acetobutylicum* thlFAST and thl^{sup}FAST were used and *C. acetobutylicum* adcFAST and ptbFAST were constructed using the native *Padc* and native *Pptb* promoters. Engineered mutants of *Padc* and *Pptb* were not available to test. However, inspired by the optimized spacer between the RBS and start codon developed by Yang and colleagues, the optimized spacer used in *Pthl^{sup}* was used with native *Padc* and *Pptb* promoters to examine the effect of the spacer sequence between the RBS and the start codon on gene expression. This generated p95adc^{mod}FAST and p95ptb^{mod}FAST both were added to *C. acetobutylicum* ATCC 824.

Using flow cytometry, WT control *C. acetobutylicum* with 20 uM HMBR background fluorescence was measured over 37 hours with the highest background fluorescent activity at 9 hours of growth of 304.3 ± 43.2 A.U. and dropping to 229.0 ± 15.4 A.U. after 33 hours. The low WT control *C. acetobutylicum* background

fluorescence is compared to every promoter activity measured with flow cytometry (Figure 3.5A, 3.7A, 3.9A). The *C. acetobutylicum* ATCC 824 control remains in early exponential growth from 9-17.5 hours, reaching late exponential around 33 hours and into stationary phase around 37 hours and is compared to growth curves of all FAST promoter strains used in flow cytometry measurements (Figure 3.5B, 3.7B, 3.9B). The fluorescence intensity of background fluorescence in WT *C. acetobutylicum* was also measured using a microplate reader over 38 hours. Again, background fluorescence was higher early in the culture, with a fluorescence intensity of $2.0 \times 10^5 \pm 3.8 \times 10^4$ A.U. at 10 hours of growth, dropping to $5.7 \times 10^4 \pm 1.0 \times 10^4$ after 18.5 hours and increasing to a maximum of $2.4 \times 10^5 \pm 2.2 \times 10^4$ A.U. after 38 hours. However, this is very low fluorescence activity and WT *C. acetobutylicum* fluorescence is compared to fluorescence intensity of all FAST promoter strains (Figure 3.5C, 3.7C, 3.9C). WT *C. acetobutylicum* growth curve remains in exponential growth from 10-18.5 hours, and reaches stationary phase after 34 hours of growth, and is compared to growth curves of all FAST promoter strains measured by microplate reader (Figure 3.5D, 3.7D, 3.9D).

C. acetobutylicum thlFAST shows higher MFI when compared to WT *C. acetobutylicum*, with a MFI of 597.14 ± 160.4 A.U. after 7 hours of growth, dropping to 446.5 ± 67.0 A.U. after 15.5 hours, and increasing again to 722.3 ± 284.4 A.U. after 35 hours (Figure 3.5A). *C. acetobutylicum* thlFAST also showed a similar growth pattern to WT *C. acetobutylicum*, remaining in exponential growth from 7-15.5 hours, and reaching stationary phase after 31 hours (Figure 3.5B). *C. acetobutylicum* thl^{sup}FAST showed an overall high MFI with the lowest MFI at 8 hours of growth of 1049.4 ± 21.9 A.U. increasing slightly to 1265.5 ± 27.3 A.U. at 12 hours of growth. *C. acetobutylicum* thl^{sup}FAST showed a slight drop in MFI of 1129.4 ± 43.5 A.U., then

increasing to a maximum MFI of 1811.3 ± 160.3 A.U at 36 hours of growth.(Figure 3.5A). The growth curve for *C. acetobutylicum* thl^{sup}FAST was similar to that of the WT *C. acetobutylicum* and samples were vortexed to alleviate severe clumping of cells in culture (Figure 3.5B).

When observing histograms of *C. acetobutylicum* thlFAST, only a small portion of fluorescent cells appear in hours 7-15.5, with a small shift in fluorescent populations at 31 hours, with a slight bimodal population after 31 hours (Figure 3.6A). *C. acetobutylicum* thl^{sup}FAST shows a larger shift in green fluorescence compared to *C. acetobutylicum* thlFAST at 8 hours. After 10 and 14.5 hours, there was not much change in green fluorescence shift, but both showed a bimodal population after 31 hours. At 32 hours, *C. acetobutylicum* thl^{sup}FAST shows the most stable and pronounced shift in green fluorescence, but a large portion of cells as not fluorescent. At 34 hours, the green fluorescence shift is still high, but ~50% of the cell population is not fluorescent (Figure 3.6B). When MFI was measured using flow cytometry, a gate was created to distinguish the fluorescent population from the green background fluorescence found in WT *C. acetobutylicum*. However, this gate only allowed a portion of the cell population to be measured, showing a different fluorescence pattern from what we previously saw using the microplate reader. For both *C. acetobutylicum* thlFAST and *C. acetobutylicum* thl^{sup}FAST, an increase in fluorescence was found after ~16.5 hours of growth, which was not found using a microplate reader (Figure 3.6C). However, when measuring the green fluorescence if the whole population of cells is taken into account for the MFI calculation, we see a pattern more consistent with the data from the microplate measurements in *C. acetobutylicum* thl^{sup}FAST. However, measuring the MFI using the whole population, results in a lower overall

MFI for all strains. *C. acetobutylicum* thl^{sup}FAST showed the highest MFI of 754.7 at 8 hours of growth ± 17.7 A.U., and decreasing over time with the lowest MFI of 264.1 ± 84.3 A.U. after 36 hours. Both WT *C. acetobutylicum* and *C. acetobutylicum* thlFAST showed consistently low MFI over 36 hours (Figure 3.6D).

Using a microplate reader to measure fluorescence intensity, *C. acetobutylicum* thlFAST shows the highest fluorescence intensity in exponential phase at 15.5 hours of growth of $2.1 \times 10^6 \pm 6.7 \times 10^5$ A.U.. Fluorescence intensity then dropped to $1.2 \times 10^6 \pm 8.9 \times 10^5$ A.U. after 35 hours (Figure 3.5C). Again, *C. acetobutylicum* thlFAST shows a similar growth pattern to WT *C. acetobutylicum* remaining in exponential phase through 7-15.5 hours and approaching stationary phase after 31 hours of growth (Figure 3.5D). *C. acetobutylicum* thl^{sup}FAST shows higher fluorescence intensity compared to both WT *C. acetobutylicum* and *C. acetobutylicum* thlFAST, with the highest fluorescence intensity of $4.8 \times 10^6 \pm 1.9 \times 10^6$ A.U. at 10 hours of growth, dropping to $3.1 \times 10^6 \pm 1.6 \times 10^6$ A.U. after 34 hours (Figure 3.5C). Similar to the flow cytometry experiment growth curve, *C. acetobutylicum* thl^{sup}FAST growth dropped after 30 hours due to severe clumping in culture (Figure 3.5D).

C. acetobutylicum adcFAST shows very low MFI in exponential phase of growth, reaching 469.0 ± 4.3 A.U. at 14.5 hours, showing MFI just over WT *C. acetobutylicum* background fluorescence (Figure 3.7A). *C. acetobutylicum* adcFAST shows a similar growth pattern to WT *C. acetobutylicum* and remaining in exponential growth between 6 and 14.5 hours and approaching stationary phase after 30 hours (Figure 3.7B). *C. acetobutylicum* adc^{mod}FAST shows a similar MFI in exponential phase of growth compared to *C. acetobutylicum* adcFAST with the lowest MFI of 407.5 ± 110.0 A.U. at 10 hours of growth, then increasing above the MFI of *C.*

acetobutylicum adcFAST after 30 hours of growth, reaching a maximum MFI of 4248.0 ± 421.1 A.U. at 34 hours of growth (Figure 3.7A). *C. acetobutylicum* adc^{mod}FAST also shows a similar growth pattern to WT *C. acetobutylicum* remaining in exponential growth between 6 and 14.5 hours and approaching stationary phase after 30 hours (Figure 3.7B).

C. acetobutylicum adcFAST shows low green fluorescence shift at 6 and 10 hours of growth and shifting slightly after 14.5 hours. After 30 hours *C. acetobutylicum* adcFAST shows a dramatic shift in the majority of the population, with a small non-fluorescent minority of the population, which is consistent with stationary phase activity of the *adc* promoter. 34 hours shows a similarly dramatic but larger shift in the fluorescent population (Figure 3.8A). *C. acetobutylicum* adc^{mod}FAST shows a similar pattern of fluorescent shift compared to *C. acetobutylicum* adcFAST but with a slightly larger shift in the fluorescent population after 30 hours and a more pronounced bimodal population after 34 hours (Figure 3.8B). When the cell population is gated for green background fluorescence, *C. acetobutylicum* adcFAST and *C. acetobutylicum* adc^{mod}FAST both show higher MFI after 30 hours, which is consistent with our previous microplate experiment (Figure 3.8C). When the MFI of the green fluorescence is calculated using the entire population, we still see this pattern of fluorescence, with a low MFI from 6-14.5 hours in both *C. acetobutylicum* adcFAST and *C. acetobutylicum* adc^{mod}FAST, and a large increase in MFI after 30 hours to a maximum MFI of 1199.2 ± 44.6 A.U. after 34 hours in *C. acetobutylicum* adcFAST. *C. acetobutylicum* adc^{mod}FAST also showed high MFI after 30 hours of growth with a maximum MFI of 1909.6 ± 127.5 A.U. and decreasing to 1488.2 ± 296.2 A.U. after 34 hours (Figure 3.8D).

When using a microplate reader, both *C. acetobutylicum* adcFAST and *C. acetobutylicum* adc^{mod}FAST showed a similar pattern of fluorescence, with low fluorescence intensity at 8 and 12 hours of growth and showed higher fluorescence after 32 hours of growth. *C. acetobutylicum* adcFAST showed a slightly higher fluorescence of $1.6 \times 10^6 \pm 6.6 \times 10^5$ A.U. at 8 hours of growth and increased to a maximum fluorescence intensity of $10.0 \times 10^7 \pm 6.2 \times 10^5$ after 32 hours (Figure 3.7C). *C. acetobutylicum* adc^{mod}FAST showed a lower fluorescence intensity of $5.9 \times 10^5 \pm 2.8 \times 10^4$ A.U. at 8 hours of growth and a maximum fluorescence intensity of $8.4 \times 10^6 \pm 2.9 \times 10^6$ A.U. at 36 hours of growth (Figure 3.7C). Both *C. acetobutylicum* adcFAST and *C. acetobutylicum* adc^{mod}FAST showed a similar growth pattern to WT *C. acetobutylicum* and remained in exponential phase of growth between 8 and 16.5 hours, and reaching stationary phase after 36 hours (Figure 3.7D).

C. acetobutylicum ptbFAST showed a higher MFI in early growth stages, with a maximum MFI of 47.9 ± 26.0 A.U. at 11 hours of growth and decreased to 367.1 ± 15.7 A.U. after 15.5 hours and increasing again to 396.7 ± 31.8 A.U. at 35 hours of growth and showed the closest MFI of all the promoters to WT *C. acetobutylicum* (Figure 3.9A). *C. acetobutylicum* ptbFAST also showed a similar growth pattern to WT *C. acetobutylicum*, it remained in exponential growth from 7 hours to 15.5 hours of growth and reached stationary phase after 31 hours of growth (Figure 3.9B). *C. acetobutylicum* ptb^{mod}FAST showed a similar MFI to *C. acetobutylicum* ptbFAST in early growth, with a MFI of 500.2 ± 81.6 A.U. at 10 hours of growth. Interestingly, *C. acetobutylicum* ptbmodFAST MFI increased over time to a maximum of 840.2 ± 83.5 A.U. after 34 hours of growth (Figure 3.9A). *C. acetobutylicum* ptb^{mod}FAST also

showed a similar growth pattern to WT *C. acetobutylicum* and remained in exponential phase until reaching stationary phase after 34 hours of growth (Figure 3.9B).

Both *C. acetobutylicum* ptbFAST (Figure 3.10A) *C. acetobutylicum* ptb^{mod}FAST (Figure 3.10B) showed a comparable green fluorescence shift pattern in early stages of growth using flow cytometry, and only differed slightly after 30 hours, with *C. acetobutylicum* ptb^{mod}FAST showing a more pronounced shift at 30 hours. Both *C. acetobutylicum* ptbFAST and *C. acetobutylicum* ptb^{mod}FAST showed a large population of non-fluorescent cells after 34 hours (Figure 3.10A, 3.10B). When the cell population is gated for green background fluorescence, *C. acetobutylicum* ptbFAST shows a pattern consistent with microplate reader results, but *C. acetobutylicum* ptb^{mod}FAST shows a large increase in MFI after 30 hours (Figure 3.10C). When the MFI of green fluorescence is calculated using the entire cell population, *C. acetobutylicum* ptbFAST shows a more pronounced pattern consistent with *C. acetobutylicum* ptbFAST microplate results. *C. acetobutylicum* ptb^{mod}FAST shows an increase in MFI of 314.4 ± 33.6 A.U. after 10 hours of growth, and decreases to 235.61 ± 68.1 A.U. However, *C. acetobutylicum* ptb^{mod}FAST increases to a maximum of 318.0 ± 36.8 A.U. at 30 hours of growth, but drops again to 208.1 ± 75.0 A.U. after 34 hours, which is similar to what was observed using the microplate reader. However, spikes in MFI of *C. acetobutylicum* ptb^{mod}FAST appear to be more drastic compared to variations in fluorescence intensity using a microplate reader (Figure 3.10D).

Using a microplate reader to measure fluorescence intensity, *C. acetobutylicum* ptbFAST shows the highest fluorescence intensity at 9 hours of growth of $2.4 \times 10^6 \pm 3.8 \times 10^5$ A.U. and reached a fluorescence intensity of $1.4 \times 10^6 \pm 1.6 \times 10^5$ A.U. after 37

hours of growth (Figure 3.9C). *C. acetobutylicum* ptb^{mod}FAST showed the highest fluorescence intensity of $1.7 \times 10^6 \pm 5.7 \times 10^4$ A.U. at 12 hours, which was slightly lower than *C. acetobutylicum* ptbFAST, and dropped to $1.3 \times 10^6 \pm 4.1 \times 10^5$ A.U. after 16.5 hours and increased again to a fluorescence intensity of $1.5 \times 10^6 \pm 4.1 \times 10^5$ A.U. after 36 hours (Figure 3.9C). Both *C. acetobutylicum* ptbFAST and *C. acetobutylicum* ptb^{mod}FAST showed similar growth patterns to WT *C. acetobutylicum*. *C. acetobutylicum* ptbFAST shows exponential growth between 9 and 17.5 hours and reaches stationary phase after 37 hours, while *C. acetobutylicum* ptb^{mod}FAST showed exponential growth between 8 and 16.5 hours and reaches stationary phase after 36 hours (Figure 3.9D).

3.3.4 *C. acetobutylicum* adcFAST and *C. acetobutylicum* adc^{mod}FAST promoters show highest fluorescence activity compared to other *C. acetobutylicum* FAST promoters

When comparing MFI of the native promoters with flow cytometry, *C. acetobutylicum* thlFAST and *C. acetobutylicum* ptbFAST appear to have similar fluorescence, while *C. acetobutylicum* adcFAST shows a dramatic increase in fluorescence over time (Figure 3.11A). Similarly, when cells are normalized to OD₆₀₀, *C. acetobutylicum* adcFAST still shows a dramatic increase in fluorescence intensity over time, and *C. acetobutylicum* thlFAST and *C. acetobutylicum* ptbFAST show a lower fluorescence intensity but show highest activity in early growth stages (Figure 3.11B). These results are consistent with previous reports of *Pthl*, *Padc*, and *Pptb* activity [34]. Both *C. acetobutylicum* thl^{sup}FAST and *C. acetobutylicum* ptb^{mod}FAST show an increase in MFI over time. However, *C. acetobutylicum* adc^{mod}FAST shows a much more dramatic increase in fluorescence of the cell population over time (Figure 3.11C). When super and modified promoters are normalized to OD₆₀₀, *C.*

acetobutylicum thl^{sup}FAST shows a higher fluorescence intensity in early growth, while *C. acetobutylicum* ptb^{mod}FAST shows only low fluorescence intensity. *C. acetobutylicum* adc^{sup}FAST shows the most dramatic fluorescence intensity pattern after reaching late growth stages (Figure 3.11D).

3.3.5 Development of a Successful Bacterial Cell Division Fusion Protein using FAST and HMBR

There are currently not many options for creating fluorescent fusion proteins in *Clostridium spp.*. Cell fixation and aerobic fluorescence recovery can be time consuming [78], and previously established anaerobic fluorescent proteins have been shown to have low fluorescence expression in clostridia [66]. FAST and fluorogenic ligands have previously been used to create fusion proteins and can be used to successfully observe protein localization in eukaryotic cells [97, 98], but has not been shown in bacteria. To test whether FAST can be used to tag cell division proteins in bacteria, a fusion protein of the hypothetical FtsZ interacting cell division protein ZapA (CAC2355)[122] was designed for *C. acetobutylicum*. The C-terminal end of *C. acetobutylicum* ZapA was fused to the N-terminal end of FAST using a small protein linker to try and avoid steric hindrance of the N-terminal, bundling associated, head of ZapA [113, 123]. ZapA-FAST was first introduced to *E. coli* where fluorescently labeled proteins appeared to aggregate toward the center of dividing cells. *E. coli* cells containing ZapA-FAST also appeared to be elongated (Figure 3.12). After ZapA-FAST localization was observed in *E. coli*, ZapA-FAST was added to *C. acetobutylicum*. *C. acetobutylicum* cells containing ZapA-FAST showed localization of proteins at opposite poles of cells, as well as at the center of two dividing cells (Figure 3.13).

3.4 Discussion

The goal of this study was to establish an oxygen-independent fluorescent reporter system using FAST, and to show that FAST fusion proteins can be functional in *C. acetobutylicum*. We investigated the fluorescence activating protein, FAST and the fluorogenic ligand, HMBR, developed by Plamont and colleagues. FAST binds to the fluorogen HMBR to activate, allowing for fluorescence to occur without the need for oxygen for chromophore maturation [97]. Tummala and colleagues have previously established a beta-galactosidase reporter system using the promoters *Pthl*, *Padc* and *Pptb*. It was shown that using these promoters upstream of *lacZ* were able to show different promoter activities, with *Pptb* and *Pthl* showing high activity in exponential growth, and *Padc* showing high activity in stationary phase of growth in batch cultures without pH control [34].

Microplate readers are one of the most widely available resources for fluorescence intensity measurement, so we developed a method to measure the expression *C. acetobutylicum* promoters using FAST. *C. acetobutylicum* thlFAST, *C. acetobutylicum* adcFAST, and *C. acetobutylicum* ptbFAST all show patterns of activity using this method, indicating FAST can be used to study promoter activity over time. However, some promoters seem to be more stable when expressed. *C. acetobutylicum* adcFAST showed the highest activity of all promoters and reached highest fluorescence intensity during stationary phase of growth, which is consistent with *adc* promoter activity. While *C. acetobutylicum* thlFAST and *C. acetobutylicum* ptbFAST also show fluorescence intensity consistent with *ptb* and *thl* promoter activity, in exponential phase, these promoters show activity much lower than *C. acetobutylicum* adcFAST (Figure 3.11C).

C. acetobutylicum thl^{sup}FAST was able to increase the expression of FAST (Figure 3.3), and showed highest fluorescence intensity in exponential phase of growth (Figure 3.5C), so we attempted to generate strong *Padc* and *Pptb* promoters using the optimized spacer created by Yang and colleagues [38]. *C. acetobutylicum* adc^{mod}FAST and *C. acetobutylicum* ptb^{mod}FAST both showed activity corresponding to each respective promoter. However, *C. acetobutylicum* adc^{mod}FAST showed similar activity to the native *adc* promoter but did not show an increase in fluorescence intensity compared to *C. acetobutylicum* adcFAST (Figure 3.7C). *C. acetobutylicum* ptb^{mod}FAST also did not increase in fluorescence intensity, and actually showed lower fluorescence intensity in exponential growth compared to *C. acetobutylicum* ptbFAST (Figure 3.9C). Based in this information, we have concluded that the optimized spacer is promoter dependent. The development of FAST expression systems using native promoters from other *Clostridium spp.* would be useful for further characterization of FAST as an expression reporter. The use of an inducible promoter could be particularly useful in the construction of fusion proteins with FAST. This could reduce the toxicity of overexpressed *Clostridium* genes/proteins in both *E. coli* before transformation into *C. acetobutylicum*, and in *C. acetobutylicum*, and for controlling when FAST will be expressed for optimal confocal microscopy imaging.

The spacer between the RBS and start codon have been well researched in *E. coli*, with an optimal spacer being 5 nucleotides using a weak promoter [124]. An optimized spacer has also suggested that spacer length greater or less than 5 nucleotide distorts the 30S subunit of the ribosome, and decreases translation initiation rate in *E. coli* [125]. However, the optimized spacer varies between different species [6]. Yang and colleagues previously investigated the RBS spacer when attempting to improve

solventogenic clostridia by strengthening the biotin synthetic pathway and found that a *thl* promoter with a shortened spacer had low strength, but improved growth and solvent production [126]. Investigation of the sequence of the spacer between the RBS and start codon could further improve protein expression [6]. Using weak promoters like *Pptb* to further investigate an optimized spacer could also potentially improve understanding of the spacer in *Clostridium spp.*

Flow cytometry is a high-throughput method for detecting and measuring several physical, chemical and biological characteristics of single cells [127]. By measuring the MFI of FITC signal with flow cytometry, we hoped to further validate that FAST can be used as a fluorescent reporter in *C. acetobutylicum*. However, in almost all promoter strains, the MFI increased over time, even in strains where promoter activity should be highest in exponential phase (Figure 3.5A, 3.7A, 3.9A). This is likely due to the appearance of non-fluorescent cells in the population later in culture. While gating allows us to only calculate the MFI of highly fluorescent cells, the microplate reader shows an average MFI based on the whole population. This is likely why we see more prominent promoter activity patterns and consistency with microplate reader fluorescence measurements when the MFI of the whole population is measured (Figure 3.6D, 3.8D, 3.10D). It has been suggested previously that due to differences in cell differentiation and morphogenesis, sporulating bacterial populations, including *Clostridia*, have heterogeneous populations when observed with flow cytometry [127].

However, the high-throughput technique demonstrated here could be applied to generating quick variants of promoters. Rohlhill and colleagues have previously demonstrated a sort-seq method for sorting variants of a formaldehyde-inducible *E.*

coli promoter (*P_{frm}*). In this study a library of mutant promoters was generated and sorted via fluorescence-activated cell sorting (FACS) and mutations were identified using high-throughput sequencing [128]. This method could also be adapted to quickly sort mutant promoters in *Clostridia spp.* now that a fluorescent reporter system has been developed that does not require oxygen for chromophore maturation.

We chose a hypothetical cell division protein to view protein localization in *C. acetobutylicum* because the localization pattern has already been established in other systems [113, 116, 129, 130]. Overexpression of ZapA-FAST in *E. coli* appears to localize to the Z-ring and may potentially replace the native ZapA. This could be what caused the elongated cell morphology in *E. coli* (Figure 3.12), which is consistent with overexpression of the native *E. coli* ZapA [130]. *C. acetobutylicum* ZapA-FAST appeared to localize in the center of dividing cells, as well as to opposite poles of dividing cells (Figure 3.13). This is consistent with the updated mechanism of endospore forming Firmicutes, *B. subtilis*, proposed by Eswaramoorthy and colleagues. This mechanism shows the localization cell division associated protein, DivIVA. In this study DivIVA was shown to localize midcell as well as at cell poles [131]. Creating ZapA-FAST has confirmed cell division localization in *C. acetobutylicum* as well as showed that FAST can be used to fluorescently tag proteins in *C. acetobutylicum*, which has not been shown previously in live cells.

The development of a fluorescent reporter system in *C. acetobutylicum* using FAST has allowed us to distinguish between auto-fluorescence and fluorescent signal, which previously was shown to not be possible using other oxygen-independent fluorescent proteins [66]. This study has also showed that FAST and HMBR can be used to fluorescently label proteins in *C. acetobutylicum* and have the possibility to

shed light on other uncharacterized protein localization in *Clostridium spp.*. FAST and HMBR could also be utilized in developing fluorescent reporter systems in other *Clostridia spp.* as well as other anaerobic bacteria.

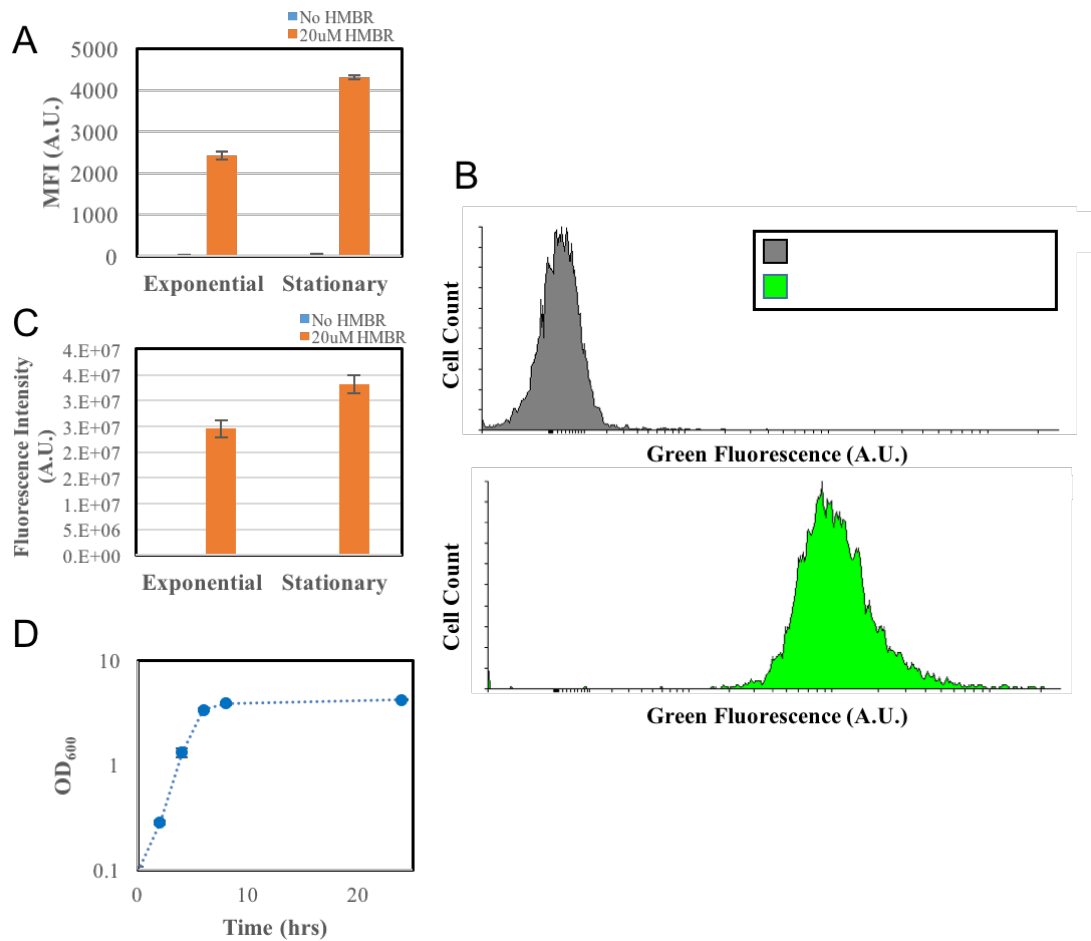


Figure 3.1 - *E. coli* thlFAST shows promising fluorescence using flow cytometry and microplate reader. *A*, *E. coli* thlFAST MFI (A.U.) in LB medium + ampicillin after 4 hours (exponential) and 24 hours (stationary) using flow cytometry. *B*, Histograms showing *E. coli* thlFAST with No HMBR added (grey) and *E. coli* thlFAST with 20uM HMBR added (green) after ~22 hours. *C*, *E. coli* thlFAST fluorescence intensity in LB medium + after 4 hours (exponential) and 24 hours (stationary) using SpectraMax i3x Microplate Reader. *D*, *E. coli* thlFAST growth curve in LB medium + ampicillin over 24 hours. n = 2, error bars: SD.

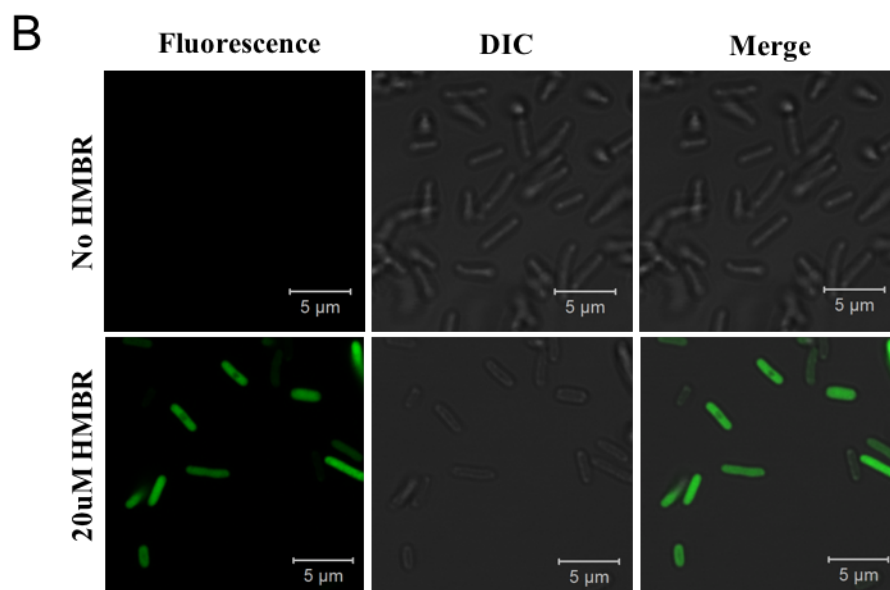
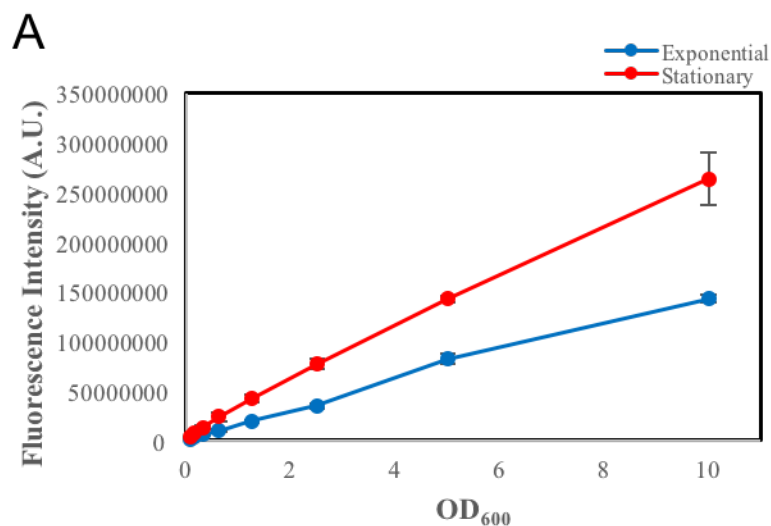


Figure 3.2 - *E. coli* thlFAST shows stable linear fluorescence expression pattern in exponential and stationary phases of growth, shows higher fluorescence intensity in stationary phase of growth (red) compared to exponential phase of growth, and shows bright fluorescence using confocal microscopy. *A*, *E. coli* thlFAST fluorescence measured by microplate reader at 4 hours of growth (blue) and 24 hours of growth (red) resuspended in filtered PBS from OD₆₀₀ 0.078 to OD₆₀₀ 10. *B*, Confocal microscopy of *E. coli* thlFAST with No HMBR (top) and 20uM HMBR (bottom), fluorescence (left) differential interference contrast (middle) and merge (right). n = 2, error bars: SD.

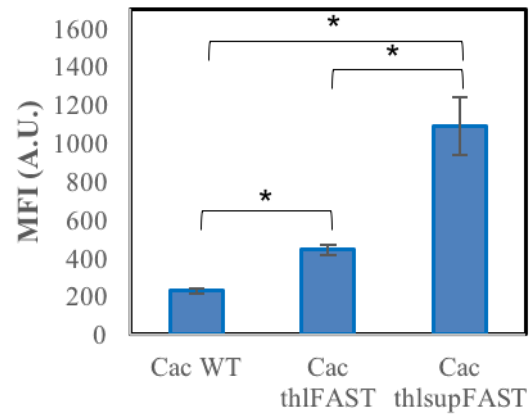


Figure 3.3 - *C. acetobutylicum* thl^{sup}FAST shows improved fluorescence when compared to *C. acetobutylicum* thlFAST and *C. acetobutylicum* ATCC 824 using flow cytometry *A*, Geometric mean fluorescence of *C. acetobutylicum* ATCC 824, *C. acetobutylicum* thlFAST, and *C. acetobutylicum* thl^{sup}FAST after ~10 hours at an OD₆₀₀ of ~1.0. n = 2, student's t-test, error bars: SD *p<0.05.

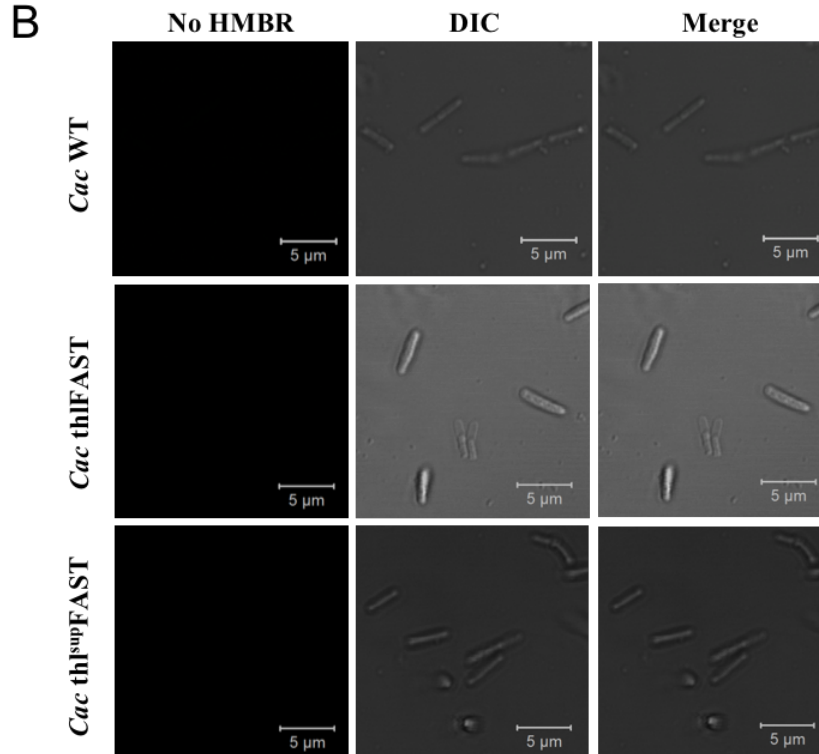
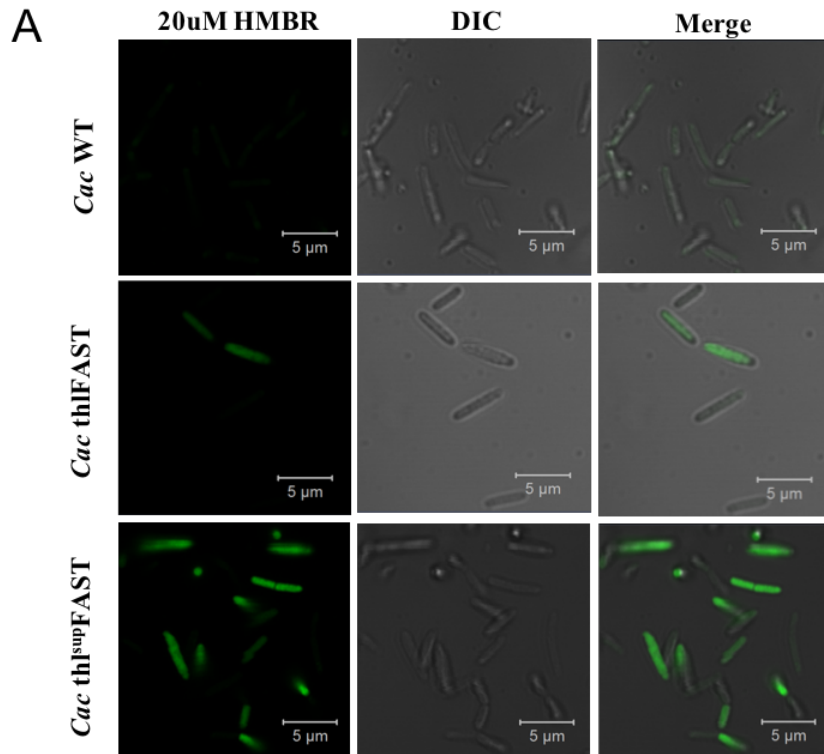


Figure 3.4 - *C. acetobutylicum* thl^{sup}FAST shows improved fluorescence when compared to *C. acetobutylicum* thlFAST and *C. acetobutylicum* ATCC 824 using confocal microscopy. *A*, Confocal microscopy of *C. acetobutylicum* ATCC 824 (top), *C. acetobutylicum* thlFAST (middle), and *C. acetobutylicum* thl^{sup}FAST (bottom) with 20uM HMBR (left), differential interference contrast (middle), and merge (right) after ~30 hours. *B*, Confocal microscopy controls of *C. acetobutylicum* ATCC 824 (top), *C. acetobutylicum* thlFAST (middle), and *C. acetobutylicum* thl^{sup}FAST (bottom) with No HMBR (left), differential interference contrast (middle), and merge (right) after ~30 hours.

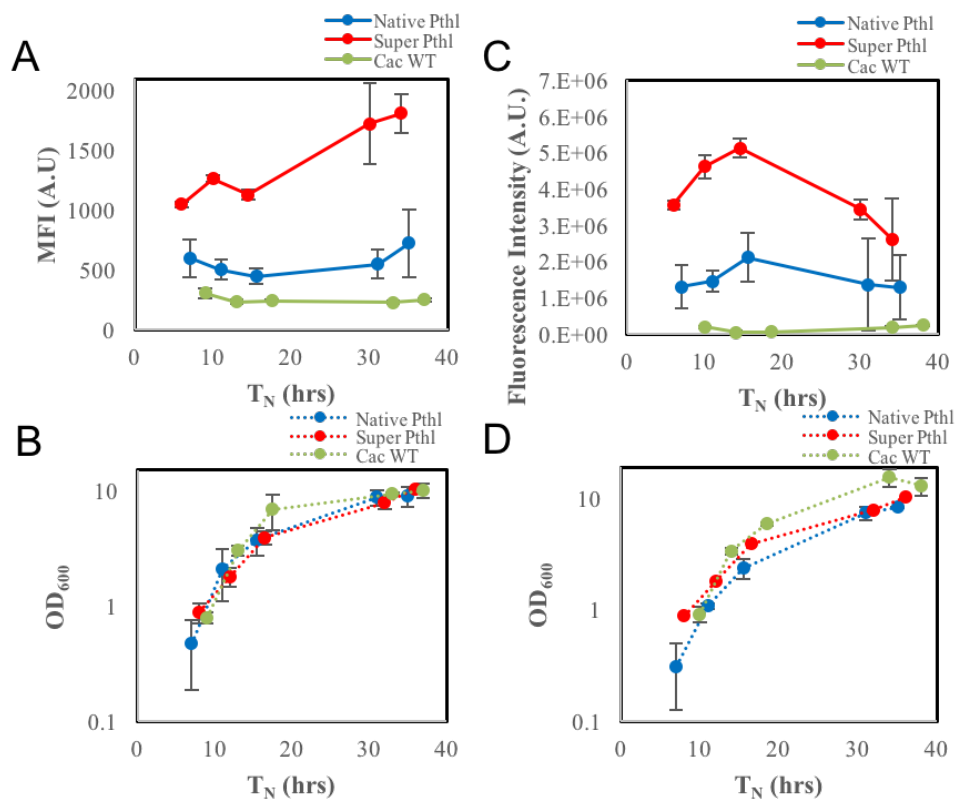


Figure 3.5 - *C. acetobutylicum* thl^{SUP}FAST shows improved fluorescence over time compared to *C. acetobutylicum* thlFAST using flow cytometry and both *C. acetobutylicum* thl^{SUP}FAST and *C. acetobutylicum* thlFAST show a fluorescence pattern consistent with promoter growth phase activity. A, *C. acetobutylicum* thl^{SUP}FAST (red), *C. acetobutylicum* thlFAST (blue), and *C. acetobutylicum* WT (green) geometric means over ~37 hours using flow cytometry. WT n = 3, thlFAST n = 4, thl^{SUP}FAST n = 3. B, Flow cytometry experiment *C. acetobutylicum* thl^{SUP}FAST (red), *C. acetobutylicum* thlFAST (blue), and *C. acetobutylicum* WT (green) growth curve in Turbo CGM + erythromycin or Turbo CGM over ~37 hours. WT n = 3, thlFAST n = 4, thl^{SUP}FAST n = 3. C, *C. acetobutylicum* thl^{SUP}FAST (red), *C. acetobutylicum* thlFAST (blue), and *C. acetobutylicum* WT (green) fluorescence intensity over ~38 hours using SpectraMax i3x Microplate Reader. WT n = 2, thlFAST n = 2, thl^{SUP}FAST n = 3. D, Microplate reader experiment *C. acetobutylicum* thl^{SUP}FAST (red), *C. acetobutylicum* thlFAST (blue), and *C. acetobutylicum* WT (green) growth curve in Turbo CGM + erythromycin over ~38 hours. WT n = 2, thlFAST n = 2, thl^{SUP}FAST n = 3, error bars: SD.

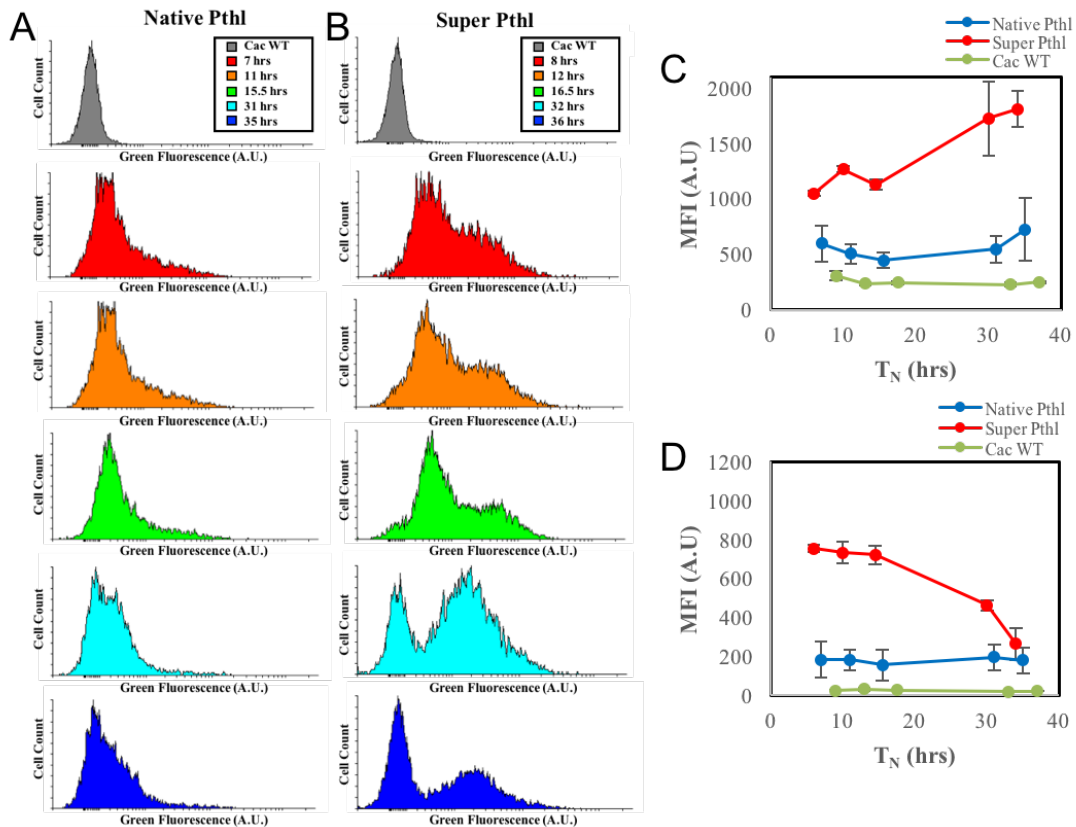


Figure 3.6 - Histograms of thlFAST and thl^{SUP}FAST over time show improvement in fluorescence shift over time. *A*, Histograms showing *C. acetobutylicum* thlFAST (left column) after 7 hours (red), 11 hours (orange), 15.5 hours (green), 31 hours (light blue) and 35 hours (dark blue). *B*, Histograms showing *C. acetobutylicum* thl^{SUP}FAST (right column) after 6 hours (red), 10 hours (orange), 14.5 hours (green), 30 hours (light blue) and 34 hours (dark blue), compared with *C. acetobutylicum* WT (grey) after 9 hours of growth. *C*, *C. acetobutylicum* thl^{SUP}FAST (red), *C. acetobutylicum* thlFAST (blue), and *C. acetobutylicum* WT (green) geometric means over ~37 hours with measuring only green fluorescent population. *D*, *C. acetobutylicum* thl^{SUP}FAST (red), *C. acetobutylicum* thlFAST (blue), and *C. acetobutylicum* WT (green) geometric means over ~37 hours measuring green fluorescence of entire population. Error bars: SD.

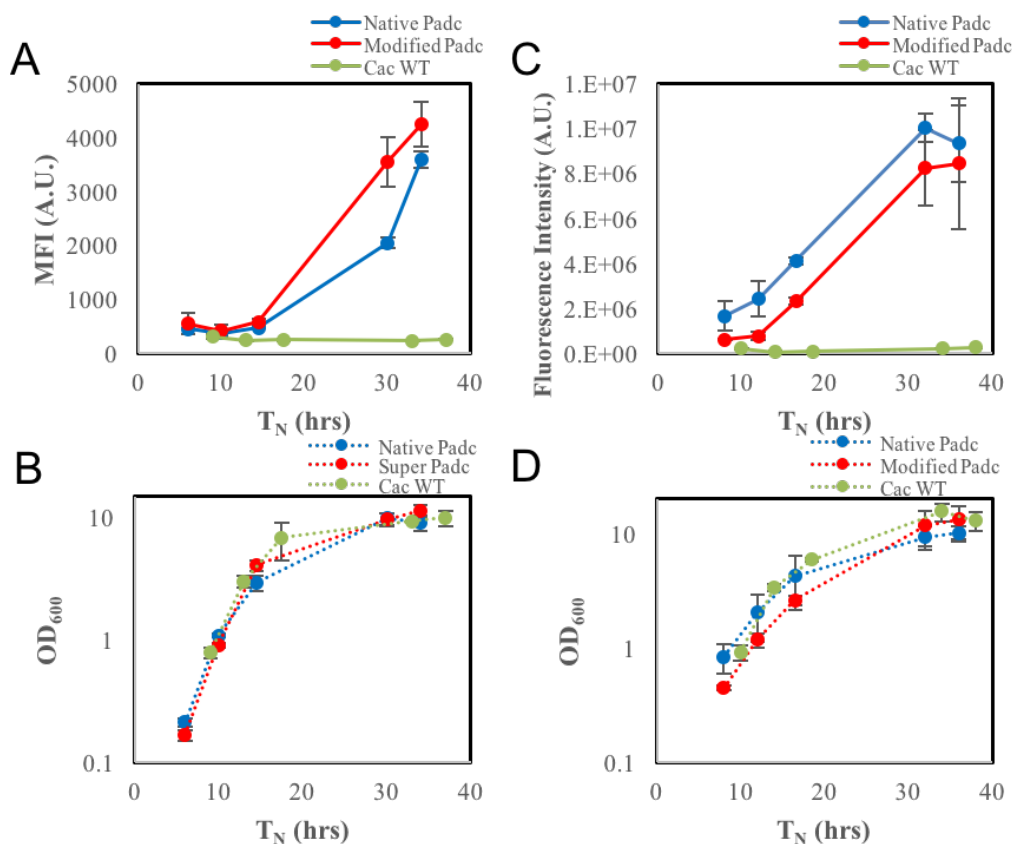


Figure 3.7 - *C. acetobutylicum* $adc^{mod}FAST$ shows improved fluorescence over time compared to *C. acetobutylicum* $adcFAST$ using flow cytometry and both *C. acetobutylicum* $adc^{mod}FAST$ and *C. acetobutylicum* $adcFAST$ show a fluorescence pattern consistent with promoter growth phase activity. A, *C. acetobutylicum* $adc^{mod}FAST$ (red), *C. acetobutylicum* $adcFAST$ (blue), and *C. acetobutylicum* WT (green) geometric means over ~35 hours using flow cytometry. WT n = 3, $adcFAST$ n = 2, $adc^{mod}FAST$ n = 3. B, Flow cytometry experiment *C. acetobutylicum* $adc^{mod}FAST$ (red), *C. acetobutylicum* $adcFAST$ (blue), and *C. acetobutylicum* WT (green) growth curve in Turbo CGM + erythromycin or Turbo CGM over ~35 hours. WT n = 3, $adcFAST$ n = 2, $adc^{mod}FAST$ n = 3. C, *C. acetobutylicum* $adc^{mod}FAST$ (red), *C. acetobutylicum* $adcFAST$ (blue), and *C. acetobutylicum* WT (green) fluorescence intensity over ~35 hours using using SpectraMax i3x Microplate Reader. n = 2. D, Microplate reader experiment *C. acetobutylicum* $adc^{mod}FAST$ (red), *C. acetobutylicum* $adcFAST$ (blue), and *C. acetobutylicum* WT (green) growth curve in Turbo CGM + erythromycin or Turbo CGM over ~35 hours. n = 2, error bars: SD.

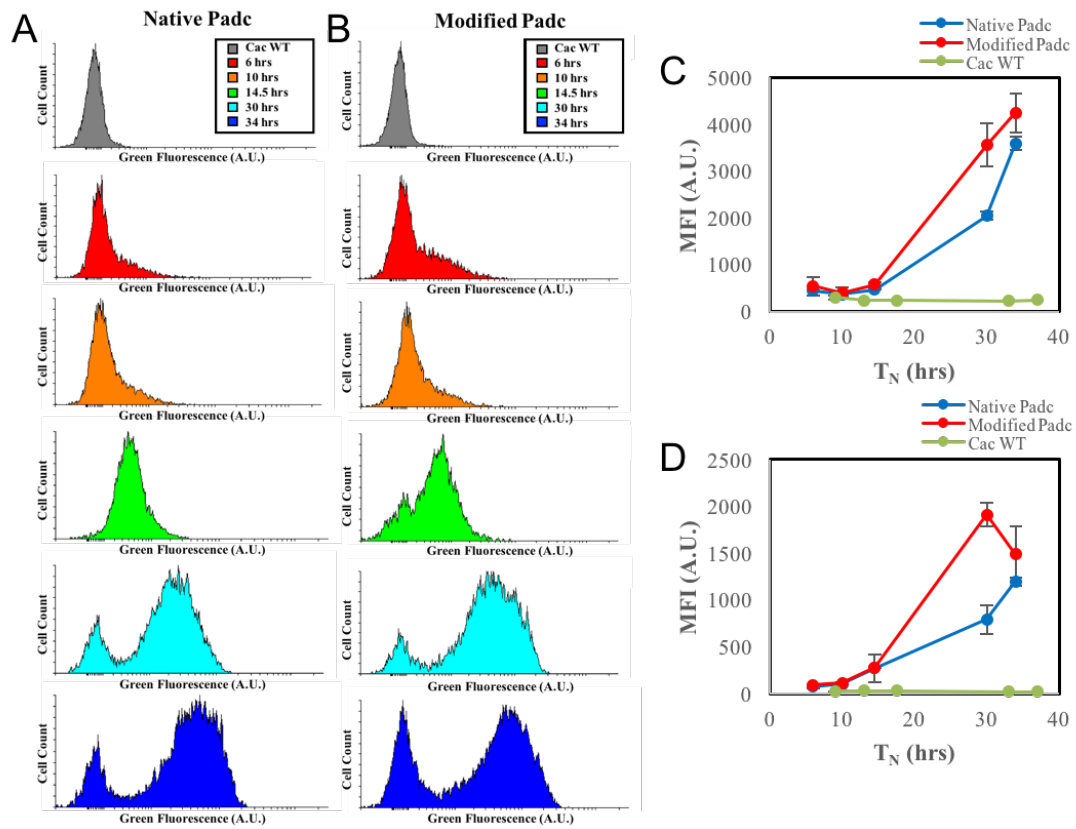


Figure 3.8 - Histograms of *adcFAST* and *adc^{mod}FAST* over time show slight improvement in fluorescence shift over time. *A*, Histograms showing *C. acetobutylicum* *adcFAST* (left column) after 6 hours (red), 10 hours (orange), 14.5 hours (green), 30 hours (light blue) and 34 hours (dark blue). *B*, Histograms showing *C. acetobutylicum* *adc^{mod}FAST* (right column) after 6 hours (red), 10 hours (orange), 14.5 hours (green), 30 hours (light blue) and 34 hours (dark blue), compared with *C. acetobutylicum* WT (grey) after 9 hours of growth. *C*, *C. acetobutylicum* *adc^{mod}FAST* (red), *C. acetobutylicum* *adcFAST* (blue), and *C. acetobutylicum* WT (green) geometric means over ~ 37 hours with measuring only green fluorescent cell population. *D*, *C. acetobutylicum* *adc^{mod}FAST* (red), *C. acetobutylicum* *adcFAST* (blue), and *C. acetobutylicum* WT (green) geometric means over ~ 37 hours measuring green fluorescence of entire population. Error bars: SD.

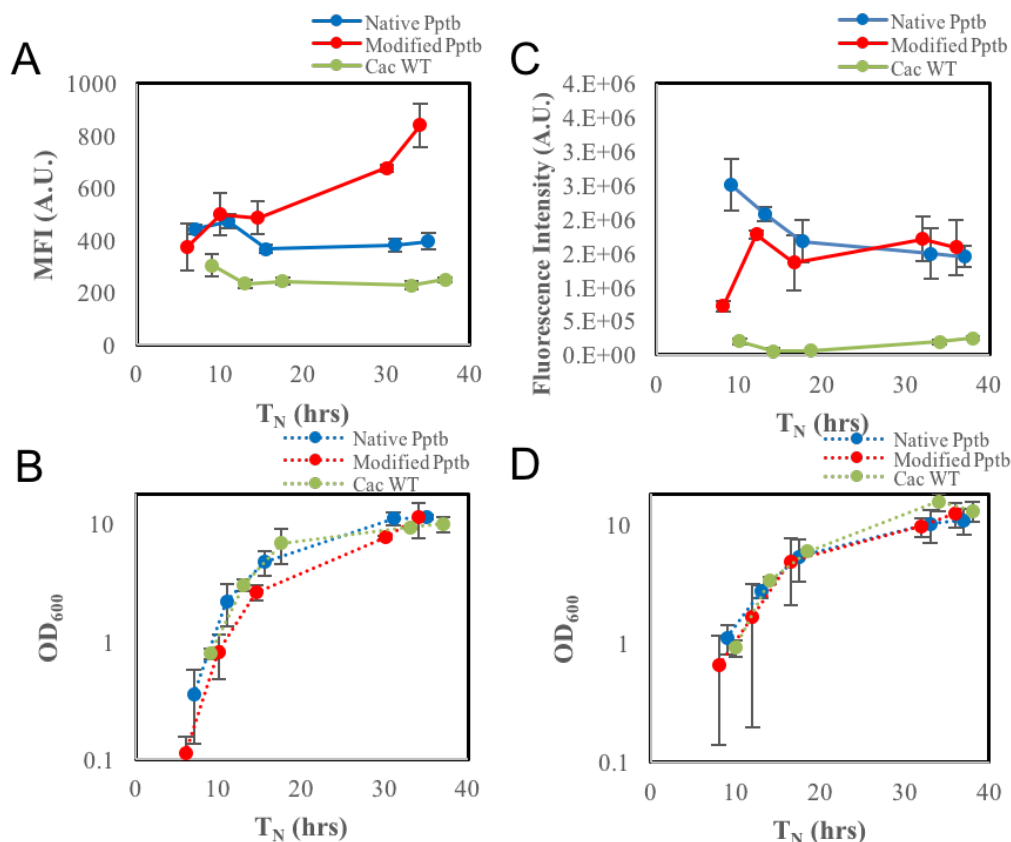


Figure 3.9 - *C. acetobutylicum* ptb^{mod} FAST shows improved fluorescence over time compared to *C. acetobutylicum* ptb FAST using flow cytometry and both *C. acetobutylicum* ptb^{mod} FAST and *C. acetobutylicum* ptb FAST show a fluorescence pattern consistent with promoter growth phase activity. *A*, *C. acetobutylicum* ptb^{mod} FAST (red), *C. acetobutylicum* ptb FAST (blue), and *C. acetobutylicum* WT (green) geometric means over ~35 hours using flow cytometry. WT $n = 3$, ptb FAST $n = 3$, ptb^{mod} FAST $n = 2$. *B*, Flow cytometry experiment *C. acetobutylicum* ptb^{mod} FAST (red), *C. acetobutylicum* ptb FAST (blue), and *C. acetobutylicum* WT (green) growth curve in Turbo CGM + erythromycin or Turbo CGM over ~35 hours. WT $n = 3$, ptb FAST $n = 3$, ptb^{mod} FAST $n = 2$. *C*, *C. acetobutylicum* ptb^{mod} FAST (red), *C. acetobutylicum* ptb FAST (blue), and *C. acetobutylicum* WT (green) fluorescence intensity over ~35 hours using using SpectraMax i3x Microplate Reader. $n = 2$. *D*, Microplate reader experiment *C. acetobutylicum* ptb^{mod} FAST (red), *C. acetobutylicum* ptb FAST (blue), and *C. acetobutylicum* WT (green) growth curves in Turbo CGM + erythromycin or Turbo CGM over ~35 hours. $n = 2$, error bars: SD.

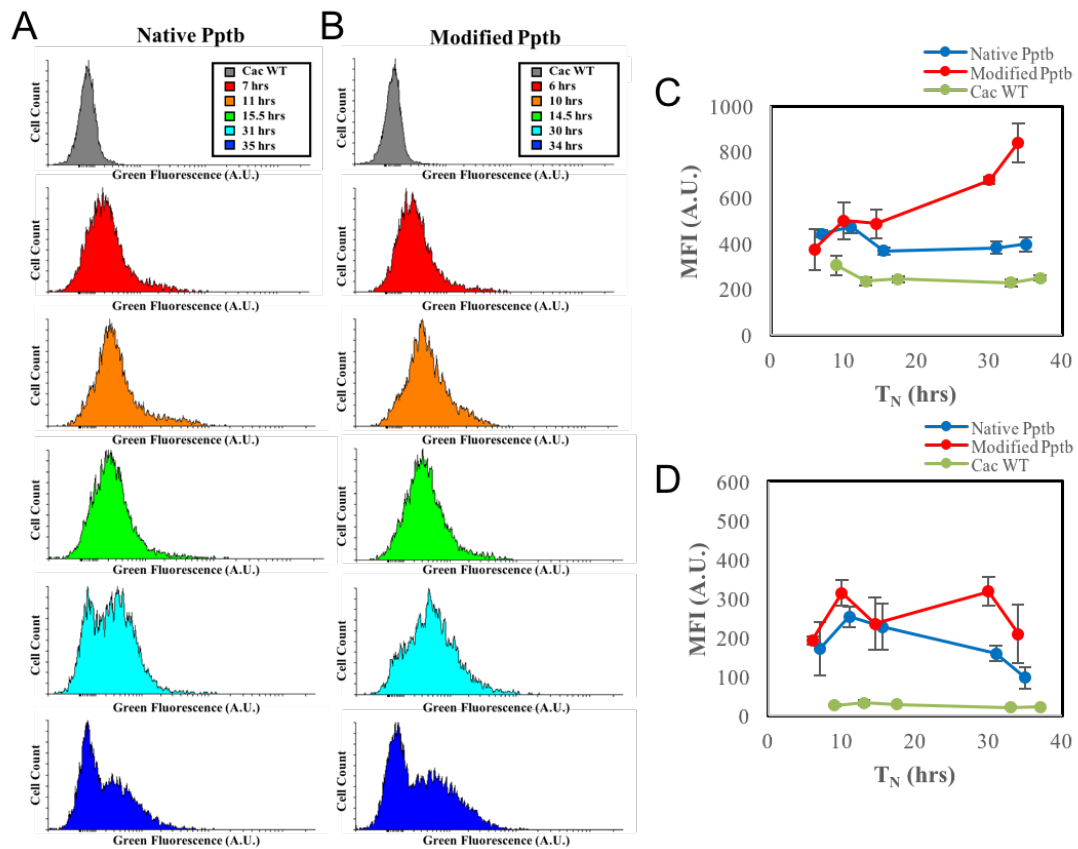


Figure 3.10 - Histograms of *ptb*FAST and *ptb*^{mod}FAST over time show little difference in fluorescence shift over time. *A*, Histograms showing *C. acetobutylicum* *ptb*FAST (left column) after 7 hours (red), 11 hours (orange), 15.5 hours (green), 31 hours (light blue) and 35 hours (dark blue). *B*, Histograms showing *C. acetobutylicum* *ptb*^{mod}FAST (right column) after 6 hours (red), 10 hours (orange), 14.5 hours (green), 30 hours (light blue) and 34 hours (dark blue), compared with *C. acetobutylicum* WT (grey) after 9 hours of growth. *C*, *C. acetobutylicum* *ptb*^{mod}FAST (red), *C. acetobutylicum* *ptb*FAST (blue), and *C. acetobutylicum* WT (green) geometric means over ~37 hours with measuring only green fluorescent population. *D*, *C. acetobutylicum* *ptb*^{mod}FAST (red), *C. acetobutylicum* *ptb*FAST (blue), and *C. acetobutylicum* WT (green) geometric means over ~37 hours measuring green fluorescence of entire population. Error bars: SD.

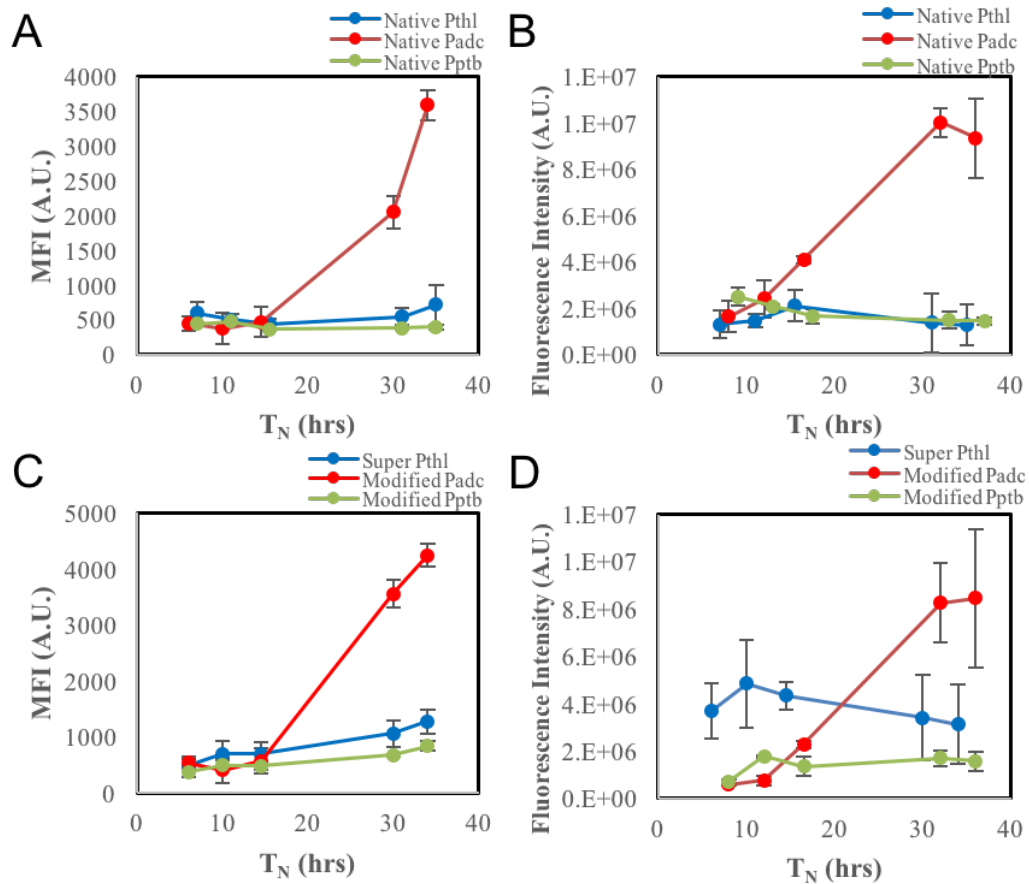


Figure 3.11 - *C. acetobutylicum* $adc^{mod}FAST$ and *C. acetobutylicum* $adcFAST$ show strongest activity compared to *C. acetobutylicum* $thlFAST$, *C. acetobutylicum* $thl^{sup}FAST$, *C. acetobutylicum* $ptbFAST$, and *C. acetobutylicum* $ptb^{mod}FAST$ using flow cytometry and microplate reader. *A*, *C. acetobutylicum* $thlFAST$ (blue), *C. acetobutylicum* $adcFAST$ (red), *C. acetobutylicum* $ptbFAST$ (green) geometric means over ~ 35 hours using flow cytometry. $thlFAST$ $n = 4$, $adcFAST$ $n = 2$, $ptbFAST$ $n = 3$. *B*, *C. acetobutylicum* $thlFAST$ (blue), *C. acetobutylicum* $adcFAST$ (red), *C. acetobutylicum* $ptbFAST$ (green) geometric means over ~ 35 hours using microplate reader. $n = 2$. *C*, *C. acetobutylicum* $thl^{sup}FAST$ (blue), *C. acetobutylicum* $adc^{sup}FAST$ (red), *C. acetobutylicum* $ptb^{sup}FAST$ (green) geometric means over ~ 35 hours using flow cytometry. $thl^{sup}FAST$ $n = 3$, $adc^{mod}FAST$ $n = 3$, $ptb^{mod}FAST$ $n = 2$. *D*, *C. acetobutylicum* $thl^{sup}FAST$ (blue), *C. acetobutylicum* $adc^{sup}FAST$ (red), *C. acetobutylicum* $ptb^{sup}FAST$ (green) geometric means over ~ 35 hours using microplate reader. $thl^{sup}FAST$ $n = 3$, $adc^{mod}FAST$ $n = 2$, $ptb^{mod}FAST$ $n = 2$, error bars: SD.

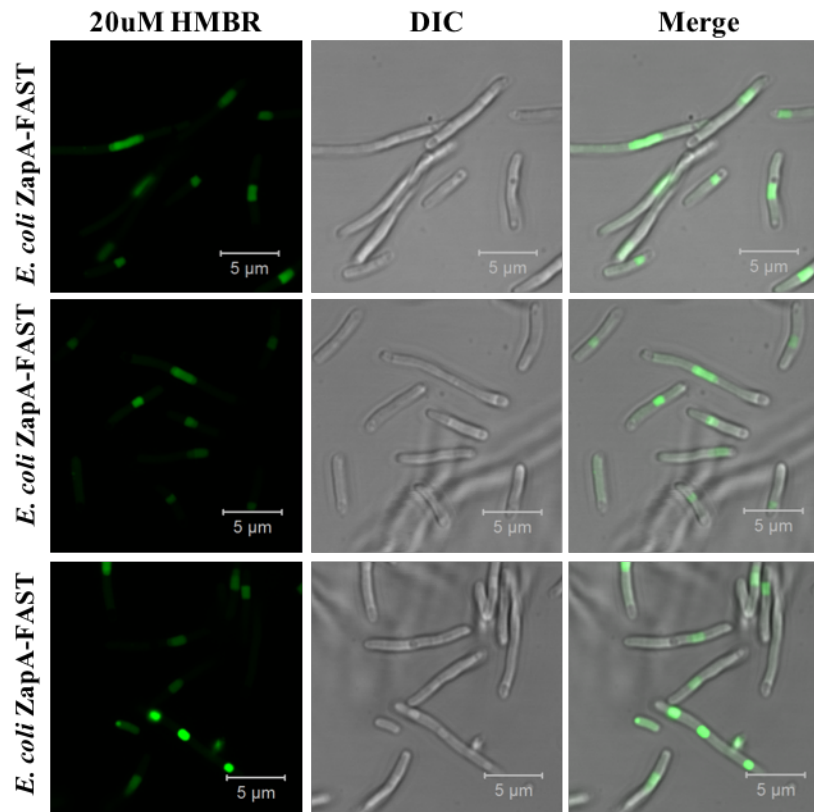


Figure 3.12 - FAST and HMBR are an efficient system to view protein localization within *E. coli* cells. *E. coli ZapA-FAST* with 20uM HMBR (left) differential interference contrast (middle) and merge (right) using confocal microscopy.

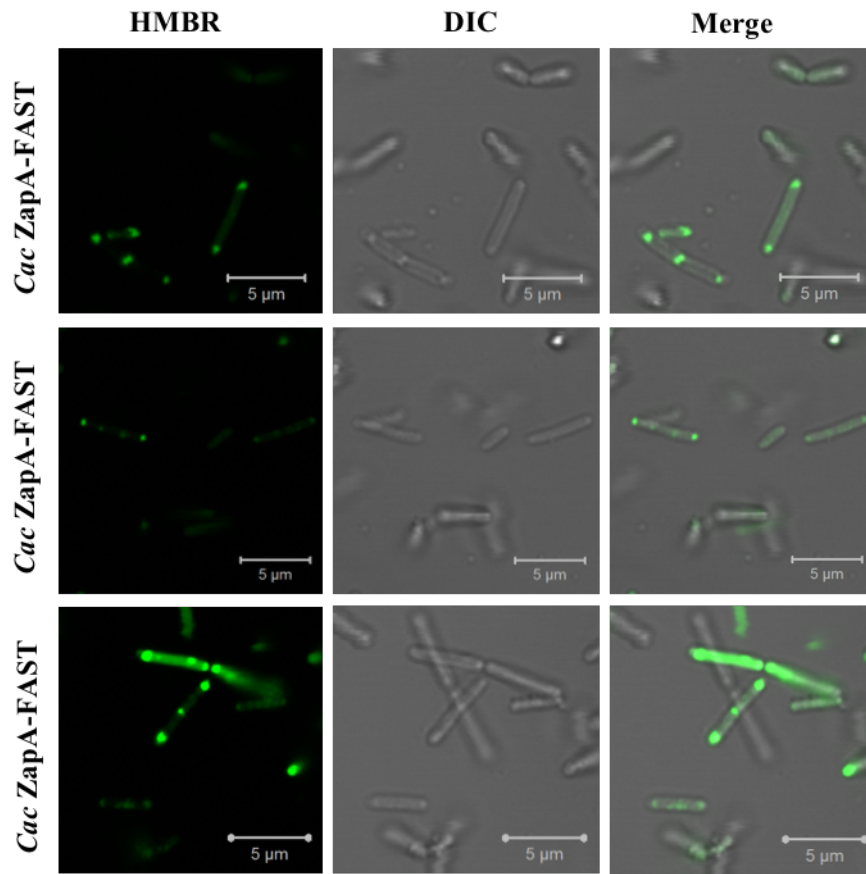


Figure 3.13 - FAST and HMBR are an efficient system to view protein localization within *C. acetobutylicum* cells. *C. acetobutylicum* ZapA-FAST with 20uM HMBR (left) differential interference contrast (middle) and merge (right) using confocal microscopy.

Chapter 4

CONCLUSIONS AND FUTURE DIRECTIONS

The purpose of this study was to explore the metabolism of syntrophic clostridia co-culture, and to develop an anaerobic, highly-fluorescent protein labeling system for characterization in clostridia in order to better understand cell-to-cell interactions in the future. Our lab has previously established a syntrophic relationship between the acetogen, *C. ljungdahlii* and the solventogen, *C. acetobutylicum* [24]. This study aimed to explore metabolic interactions of other *Clostridium spp.* with these two already established syntrophic organisms. We aimed to develop a synthetic syntrophic co-culture capable of producing industrially valuable chemicals, in particular, the C6 carboxylic acid, hexanoate. Additionally, the fluorescent labeling system of FAST and the fluorogen, HMBR, was examined in order to better understand the syntrophic interactions between *Clostridium spp.*, which has previously been unsuccessful.

4.1 Overall Conclusions

After several attempts at designing a synthetic co-culture of *C. kluyveri* and *C. acetobutylicum*, it appears that these *Clostridium spp.* are need further optimization for synthetic co-culture. It has been previously shown that an ethanol:acetate ratio of 3:1 results in more efficient production of hexanoate in *C. kluyveri* culture [132]. However, in co-culture, *C. acetobutylicum* does not produce ethanol and acetate at this optimal ratio. Another problem with *C. kluyveri* and *C. acetobutylicum* is pH range incompatibility. *C. kluyveri* prefers a more neutral pH [132], while *C. acetobutylicum* grows in more acidic conditions [4]. *C. kluyveri* has also been shown to only be compatible with other *Clostridium spp.* in narrow pH ranges [17, 18]. Increasing the

amount of *C. kluyveri* to *C. acetobutylicum*, and the addition of ethanol to the co-culture to increase the ethanol ratio did not result in the production of hexanoate. It is possible that a *C. acetobutylicum* and *C. kluyveri* co-culture cannot work together syntrophically without constant pH control in culture.

The ability of *C. kluyveri* to produce hexanoate from butanol as a main source of alcohol has not been previously shown. Butanol has been detected in co-cultures containing *C. kluyveri* [17, 18], but impure cultures make it difficult to distinguish between metabolites produced by each species unless they are known metabolites. An alcohol is required for chain elongation to occur and for hexanoate to be produced. In pure *C. kluyveri* fed butanol and ethanol as alcohol substrate, a decrease in butanol concentration over time suggests that *C. kluyveri* can utilize butanol to produce hexanoate. It should be noted that *C. kluyveri* appears to grow slowly in the presence of butanol which has been shown previously [107]. Growth with butanol as the only alcohol was also tested in this study but no growth of *C. kluyveri* was reported. It is possible that, like ethanol, a certain ratio of butanol to acetate is required for optimal growth. This may be another reason that *C. kluyveri* cannot grow syntrophically with *C. acetobutylicum*. Butanol titers produced by *C. acetobutylicum* exceed the concentration of butanol tested for *C. kluyveri* growth in this study, so it is possible that high concentrations of butanol may be toxic to *C. kluyveri*.

The *C. kluyveri*, *C. ljungdahlii*, and *C. acetobutylicum* co-culture was shown to work syntrophically. A small amount of isopropanol and 2,3-butanediol were both produced in co-culture, suggesting that *C. acetobutylicum* and *C. ljungdahlii* were interacting syntrophically. Hexanoate was also produced in co-culture, which indicated that *C. kluyveri* can utilize the metabolites from *C. acetobutylicum* and *C. ljungdahlii*.

It is unclear if *C. kluyveri* can utilize acetone and ethanol from *C. acetobutylicum* or *C. ljungdahlii* individually, or from both simultaneously. However, the acidic environment of the co-culture needs to be addressed to ensure a productive co-culture and to allow each *Clostridium spp.* to utilize each syntrophic metabolite efficiently. *C. acetobutylicum* appears only utilize and produce a small amount of metabolites in co-culture. This leads us to believe that the growth conditions of *C. acetobutylicum* was not optimal in co-culture. The small amount of isopropanol and 2,3-butanediol also show that *C. ljungdahlii* did not perform optimally in co-culture. The metabolite profiles that suggest growth of *C. acetobutylicum* and *C. ljungdahlii* are not consistent with what has been shown previously with the two species in co-culture [24]. It is possible that utilization of electrons by *C. kluyveri* interferes with the previously established co-culture phenotype of only *C. acetobutylicum* and *C. ljungdahlii*.

While evidence of syntrophic interactions has been shown by our lab, more evidence is needed to better understand cell-to-cell interactions in co-culture. One of the ways that different species can be distinguished in co-culture is through fluorescent labeling [21-23]. However, characterization of an anaerobic fluorescent reporter system was required before attempting to label anaerobically grown cells like *C. acetobutylicum*. Traditional FP labeling systems have been previously used in clostridia, however, cell fixation and aerobic incubation was required [78]. This is not ideal for high-throughput techniques or for viewing fluorescence in live cells. In this study we show that FAST and the fluorogenic ligand, HMBR can be used in *C. acetobutylicum* as a successful, oxygen-independent, fluorescent system. Original expression of FAST with the native *Pthl* promoter resulted in a low fluorescent signal, however, the addition of the mutant *Pthl* promoter, *Pthl^{sup}* was able to significantly

increase the MFI of FAST with HMBR. *Pthl^{sup}* also resulted in *C. acetobutylicum* cells that showed higher fluorescence and more fluorescent cells with confocal microscopy.

Using a the widely available tool for measuring fluorescence, the microplate reader, it was possible to distinguish between different native promoters in *C. acetobutylicum*. The strong promoter, *Pthl*, showed fluorescence distinguishable from WT *C. acetobutylicum* auto-fluorescence and was detected in exponential phase of growth. *Pthl* activity in exponential growth is consistent with what has been shown previously [34]The weak promoter, *Pptb*, also showed exponential growth phase activity consistent with what has been previously reported [34]. This shows that FAST can be used to detect even weak promoter activity in *C. acetobutylicum* cells. The *adc* promoter showed the highest activity of all native promoters and had the strongest fluorescence intensity during stationary phase of growth. This pattern of activity is also consistent with what has been shown previously [34].

As a proof of concept, a cell division associated protein was chosen to view protein localization of FAST in *C. acetobutylicum*. It is known that cell division proteins like FtsZ and ZapA localize to midcell in *E. coli* and *B. subtilis* [133, 134]. Hypothetical *C. acetobutylicum* protein, ZapA, fused to FAST in *E. coli* showed localization and cell morphology of ZapA overexpression consistent with overexpression of the native *E. coli* ZapA [130]. *C. acetobutylicum* ZapA-FAST also showed localization between dividing cells, which showed that FAST can be used for creating fusion proteins in *C. acetobutylicum*. FAST fusions have potential for use in all oxygen-sensitive *Clostridium spp.* and for further investigation of *C. acetobutylicum* protein localization.

4.2 Recommendations for Future Work

The *C. kluyveri*, *C. ljungdahlii*, and *C. acetobutylicum* co-culture was the most successful co-culture in this study. One way to approach future experiments would be to perform co-cultures in a pH-controlled bioreactor experiment. Keeping the co-culture from becoming too acidic could assist in keeping *C. kluyveri* alive in co-culture so that it can utilize the metabolites produced by *C. acetobutylicum* and *C. ljungdahlii*. Keeping a more neutral co-culture pH could also be combined with removal of toxic hexanoate from co-culture through in-line product extraction.

C. kluyveri could also be adapted to be more compatible with *C. acetobutylicum* and *C. ljungdahlii* by passaging *C. kluyveri* in acidic medium. Each passage could slowly decrease the pH until *C. kluyveri* can grow in more acidic conditions along with *C. acetobutylicum*. Similarly, if *C. kluyveri*, *C. ljungdahlii* and *C. acetobutylicum* are adapted to tolerate high concentrations of hexanoate, this could also create a more productive co-culture. Testing the co-culture in a closed headspace should also be explored so that different gas mixtures can be tested for potential effects on each of the organisms. Our lab has previously created *C. acetobutylicum* that can produce higher ethanol titers [121], so further engineering of *C. acetobutylicum* to suit *C. kluyveri*'s metabolic needs is possible.

We demonstrated the highly-fluorescent reporter system using FAST, in this study, and further studies could use FAST to characterize other genes and promoters in *C. acetobutylicum* and other *Clostridium spp.*. The FAST system could be further utilized in *Clostridium spp.* by tagging species in syntrophic co-cultures. Using *C. acetobutylicum* thl^{SUP}FAST in a co-culture of fluorescent stained *C. kluyveri* could help us understand under what conditions *C. kluyveri* and *C. acetobutylicum* can interact. This could also be used to check to see if *C. kluyveri* is actually able to grow in the

presence of *C. acetobutylicum*. FAST could also be used for high-throughput analysis using flow cytometry for detection of strong gene expression and could potentially be used for fluorescence-activated cell sorting (FACS) of mutant promoters.

It could be interesting to explore the assembly of the divisome in *Clostridium* spp. Not much is known about the *Clostridium* divisome, besides homology studies that identified potential proteins in clostridia genomes. It could be possible to test the ZapA-FAST plasmid in other *Clostridium* spp. with *C. acetobutylicum* ZapA homologs. It is likely that localization would occur in other *Clostridium* spp. because of localization of *C. acetobutylicum* ZapA-FAST that was shown in *E. coli* in this study, whose native ZapA is not very homologous to *C. acetobutylicum* ZapA.

Another exciting opportunity for FAST is the creation of additional fusion proteins in *C. acetobutylicum*. One group of proteins that are of particular interest are ferredoxins (Fd). *C. acetobutylicum* Fd is used involved in hydrogen production and transfer of electrons [135]. The confirmed syntrophic co-culture of *C. acetobutylicum* and *C. ljungdahlii* by our lab has been speculated to involve the transfer of electrons between species. It is possible that Fd in *C. acetobutylicum* is what drives this transfer of electron to *C. ljungdahlii*. Now that we have established that FAST can be used to create fusion proteins, we can attempt to tag *C. acetobutylicum* Fd. If Fd is involved in the *C. acetobutylicum* – *C. ljungdahlii* co-culture, we should see localization of Fd-FAST to areas where *C. acetobutylicum* and *C. ljungdahlii* membranes interact. *C. ljungdahlii* and *C. kluyveri* also contain Fd [11, 13], which could also be tagged with FAST to view localization in co-culture.

REFERENCES

1. Rainey, F.A., B.J. Hollen, and A. Small, *Genus I. Clostridium Prazmowski 1880, 23AL*, in *Bergey's Manual of Systematic Bacteriology: The Firmicutes*, P. de Vos, et al., Editors. 2009, Springer-Verlag: New York, NY. p. 738-864.
2. Tracy, B.P., et al., *Clostridia: the importance of their exceptional substrate and metabolite diversity for biofuel and biorefinery applications*. *Current Opinion in Biotechnology*, 2012. **23**(3): p. 364-381.
3. Papoutsakis, E.T., *Reassessing the Progress in the Production of Advanced Biofuels in the Current Competitive Environment and Beyond: What Are the Successes and Where Progress Eludes Us and Why*. *Industrial & Engineering Chemistry Research*, 2015. **54**(42): p. 10170-10182.
4. Jones, D.T. and D.R. Woods, *Acetone-Butanol Fermentation Revisited*. *Microbiological Reviews*, 1986. **50**(4): p. 484-524.
5. Papoutsakis, E.T., *Engineering solventogenic clostridia*. *Current Opinion in Biotechnology*, 2008. **19**(5): p. 420-429.
6. Gyulev, I.S., et al., *Part by Part: Synthetic Biology Parts Used in Solventogenic Clostridia*. *ACS Synthetic Biology*, 2017.
7. Gheshlaghi, R., et al., *Metabolic pathways of clostridia for producing butanol*. *Biotechnology Advances*, 2009. **27**(6): p. 764-781.
8. Charubin, K., et al., *Engineering Clostridium Organisms as Microbial Cell-Factories: Challenges & Opportunities*. *Metabolic Engineering*, 2018.
9. Kerby, R. and J.G. Zeikus, *Catabolic Enzymes of the Acetogen Butyribacterium methylotrophicum Grown on Single-carbon Substrates*. *Journal of Bacteriology*, 1987. **169**(12): p. 5605-5609.
10. Maru, B.T., et al., *Fixation of CO₂ and CO on a diverse range of carbohydrates using anaerobic, non-photosynthetic mixotrophy*. *Fems Microbiology Letters*, 2018. **365**(8): p. 8.
11. Kopke, M., et al., *Clostridium ljungdahlii represents a microbial production platform based on syngas*. *Proceedings of the National Academy of Sciences of the United States of America*, 2010. **107**(29): p. 13087-13092.

12. Barker, H.A. and S.M. Taha, *Clostridium kluyverii*, an organism concerned in the formation of caproic acid from ethyl alcohol. *Journal of Bacteriology*, 1942. **43**(3): p. 347-363.
13. Seedorf, H., et al., *The genome of Clostridium kluyveri*, a strict anaerobe with unique metabolic features. *Proceedings of the National Academy of Sciences of the United States of America*, 2008. **105**(6): p. 2128-2133.
14. Steinbusch, K.J.J., et al., *Biological formation of caproate and caprylate from acetate: fuel and chemical production from low grade biomass*. *Energy & Environmental Science*, 2011. **4**(1): p. 216-224.
15. Spirito, C.M., et al., *Chain elongation in anaerobic reactor microbiomes to recover resources from waste*. *Current Opinion in Biotechnology*, 2014. **27**: p. 115-122.
16. Salimi, F. and R. Mahadevan, *Characterizing metabolic interactions in a clostridial co-culture for consolidated bioprocessing*. *Bmc Biotechnology*, 2013. **13**: p. 9.
17. Diender, M., A.J.M. Stams, and D.Z. Sousa, *Production of medium-chain fatty acids and higher alcohols by a synthetic co-culture grown on carbon monoxide or syngas*. *Biotechnology for Biofuels*, 2016. **9**: p. 11.
18. Richter, H., et al., *A Narrow pH Range Supports Butanol, Hexanol, and Octanol Production from Syngas in a Continuous Co-culture of Clostridium ljungdahlii and Clostridium kluyveri with In-Line Product Extraction*. *Frontiers in Microbiology*, 2016. **7**: p. 1773.
19. Haas, T., et al., *Technical photosynthesis involving CO₂ electrolysis and fermentation*. *Nature Catalysis*, 2018. **1**(1): p. 32-39.
20. Summers, Z.M., et al., *Direct Exchange of Electrons Within Aggregates of an Evolved Syntrophic Coculture of Anaerobic Bacteria*. *Science*, 2010. **330**(6009): p. 1413-1415.
21. Dubey, G.P. and S. Ben-Yehuda, *Intercellular Nanotubes Mediate Bacterial Communication*. *Cell*, 2011. **144**(4): p. 590-600.
22. Pande, S., et al., *Metabolic cross-feeding via intercellular nanotubes among bacteria*. *Nature Communications*, 2015. **6**: p. 13.

23. Benomar, S., et al., *Nutritional stress induces exchange of cell material and energetic coupling between bacterial species*. Nature Communications, 2015. **6**: p. 10.
24. Charubin, K. and E.T. Papoutsakis, *Direct cell-to-cell exchange of matter in a synthetic Clostridium syntrophy enables CO₂ fixation, superior metabolite yields, and an expanded metabolic space*. Metabolic Engineering, 2019. **52**: p. 9-19.
25. Lovley, D.R., *Happy together: microbial communities that hook up to swap electrons*. Isme Journal, 2017. **11**(2): p. 327-336.
26. Joseph, R.C., N.M. Kim, and N.R. Sandoval, *Recent Developments of the Synthetic Biology Toolkit for Clostridium*. Frontiers in Microbiology, 2018. **9**: p. 13.
27. Shaw, W.V., [57] *Chloramphenicol acetyltransferase from chloramphenicol-resistant bacteria*, in *Methods in Enzymology*. 1975, Academic Press. p. 737-755.
28. Sebald, M. and G. Brefort, *Transfer of a tetracycline-chloramphenicol plasmid in Clostridium perfringens*. Comptes Rendus Hebdomadaires Des Seances De L Academie Des Sciences Serie D, 1975. **281**(4): p. 317-319.
29. Steffen, C. and H. Matzura, *Nucleotide sequence analysis and expression studies of a chloramphenicol-acetyltransferase-coding gene from Clostridium perfringens*. Gene, 1989. **75**(2): p. 349-354.
30. Bullifent, H.L., A. Moir, and R.W. Titball, *The construction of a reporter system and use for the investigation of Clostridium perfringens gene expression*. Fems Microbiology Letters, 1995. **131**(1): p. 99-105.
31. Feustel, L., S. Nakotte, and P. Durre, *Characterization and development of two reporter gene systems for Clostridium acetobutylicum*. Applied and Environmental Microbiology, 2004. **70**(2): p. 798-803.
32. Sanders, R.E., *The Lactose Operon of Escherichia coli*, in *Bacteria, Bacteriophages, and Fungi: Volume 1*, R.C. King, Editor. 1974, Springer US: Boston, MA. p. 163-168.
33. Burchhardt, G. and H. Bahl, *Cloning and analysis of the beta-galactosidase-encoding gene from Clostridium thermosulfurogenes EMI*. Gene, 1991. **106**(1): p. 13-19.

34. Tummala, S.B., N.E. Welker, and E.T. Papoutsakis, *Development and characterization of a gene expression reporter system for Clostridium acetobutylicum ATCC 824*. Applied and Environmental Microbiology, 1999. **65**(9): p. 3793-3799.
35. Wiesenborn, D.P., F.B. Rudolph, and E.T. Papoutsakis, *Phosphotransbutyrylase from Clostridium acetobutylicum ATCC 824 and its role in acidogenesis*. Applied and Environmental Microbiology, 1989. **55**(2): p. 317-322.
36. Wiesenborn, D.P., F.B. Rudolph, and E.T. Papoutsakis, *Thiolase from Clostridium acetobutylicum ATCC 824 and Its Role in the Synthesis of Acids and Solvents*. Applied and Environmental Microbiology, 1988. **54**(11): p. 2717-2722.
37. Petersen, D.J. and G.N. Bennett, *Purification of Acetoacetate Decarboxylase from Clostridium acetobutylicum ATCC 824 and Cloning of the Acetoacetate Decarboxylase Gene in Escherichia coli*. Applied and Environmental Microbiology, 1990. **56**(11): p. 3491-3498.
38. Yang, G., et al., *Rapid Generation of Universal Synthetic Promoters for Controlled Gene Expression in Both Gas-Fermenting and Saccharolytic Clostridium Species*. ACS Synthetic Biology, 2017. **6**(9): p. 1672-1678.
39. Adcock, P.W. and C.P. Saint, *Rapid confirmation of Clostridium perfringens by using chromogenic and fluorogenic substrates*. Applied and Environmental Microbiology, 2001. **67**(9): p. 4382-4384.
40. Tan, Y., et al., *Comparative transcriptome analysis between csrA-disruption Clostridium acetobutylicum and its parent strain*. Molecular Biosystems, 2015. **11**(5): p. 1434-1442.
41. Jefferson, R.A., S.M. Burgess, and D. Hirsh, *Beta-Glucuronidase from Escherichia coli as a gene-fusion marker*. Proceedings of the National Academy of Sciences of the United States of America, 1986. **83**(22): p. 8447-8451.
42. Jefferson, R.A., *The GUS reporter gene system*. Nature, 1989. **342**(6251): p. 837-838.
43. Ravagnani, A., et al., *Spo0A directly controls the switch from acid to solvent production in solvent-forming clostridia*. Molecular Microbiology, 2000. **37**(5): p. 1172-1185.

44. Girbal, L., et al., *Development of a sensitive gene expression reporter system and an inducible promoter-repressor system for Clostridium acetobutylicum*. Applied and Environmental Microbiology, 2003. **69**(8): p. 4985-4988.
45. Mani, N., B. Dupuy, and A.L. Sonenshein, *Isolation of RNA polymerase from Clostridium difficile and characterization of glutamate dehydrogenase and rRNA gene promoters in vitro and in vivo*. Journal of Bacteriology, 2006. **188**(1): p. 96-102.
46. Dong, H., et al., *Development of an anhydrotetracycline-inducible gene expression system for solvent-producing Clostridium acetobutylicum: A useful tool for strain engineering*. Metabolic Engineering, 2012. **14**(1): p. 59-67.
47. Stewart, G.S.A.B. and P. Williams, *lux genes and the applications of bacterial bioluminescence*. Journal of General Microbiology, 1992. **138**: p. 1289-1300.
48. Phillips-Jones, M.K., *Bioluminescence (lux) expression in the anaerobe Clostridium perfringens*. Fems Microbiology Letters, 1993. **106**(3): p. 265-270.
49. Phillips-Jones, M.K., *Use of a lux reporter system for monitoring rapid changes in alpha-toxin gene expression in Clostridium perfringens during growth*. Fems Microbiology Letters, 2000. **188**(1): p. 29-33.
50. Davis, T.O., et al., *Development of a transformation and gene reporter system for group II, non-proteolytic Clostridium botulinum type B strains*. Journal of Molecular Microbiology and Biotechnology, 2000. **2**(1): p. 59-69.
51. Sabathe, F., et al., *amyP, a reporter gene to study strain degeneration in Clostridium acetobutylicum ATCC 824*. Fems Microbiology Letters, 2002. **210**(1): p. 93-98.
52. Paiva, A.M.O., et al., *The Signal Sequence of the Abundant Extracellular Metalloprotease PPEP-I Can Be Used to Secrete Synthetic Reporter Proteins in Clostridium difficile*. Acs Synthetic Biology, 2016. **5**(12): p. 1376-1382.
53. Quixley, K.W.M. and S.J. Reid, *Construction of a reporter gene vector for Clostridium beijerinckii using a Clostridium endoglucanase gene*. Journal of Molecular Microbiology and Biotechnology, 2000. **2**(1): p. 53-57.

54. Oh, Y.H., et al., *Construction of heterologous gene expression cassettes for the development of recombinant Clostridium beijerinckii*. Bioprocess and Biosystems Engineering, 2016. **39**(4): p. 555-563.
55. Pearce, B.J., Y.B. Yin, and H.R. Masure, *Genetic identification of exported proteins in Streptococcus pneumoniae*. Molecular Microbiology, 1993. **9**(5): p. 1037-1050.
56. Lee, M.H., et al., *Characterization of Enterococcus faecalis alkaline phosphatase and use in identifying Streptococcus agalactiae secreted proteins*. Journal of Bacteriology, 1999. **181**(18): p. 5790-5799.
57. Edwards, A.N., et al., *An alkaline phosphatase reporter for use in Clostridium difficile*. Anaerobe, 2015. **32**: p. 98-104.
58. Dave, G.A., *A rapid qualitative assay for detection of Clostridium perfringens in canned food products*. Acta Biochimica Polonica, 2017. **64**(2): p. 207-213.
59. Pyne, M.E., et al., *Technical guide for genetic advancement of underdeveloped and intractable Clostridium*. Biotechnology Advances, 2014. **32**(3): p. 623-641.
60. Heap, J.T., et al., *The ClosTron: A universal gene knock-out system for the genus Clostridium*. Journal of Microbiological Methods, 2007. **70**(3): p. 452-464.
61. Heap, J.T., et al., *The ClosTron: Mutagenesis in Clostridium refined and streamlined*. Journal of Microbiological Methods, 2010. **80**(1): p. 49-55.
62. Nariya, H., et al., *Development and Application of a Method for Counters selectable In-Frame Deletion in Clostridium perfringens*. Applied and Environmental Microbiology, 2011. **77**(4): p. 1375-1382.
63. Nakayama, S.I., et al., *Metabolic engineering for solvent productivity by downregulation of the hydrogenase gene cluster hupCBA in Clostridium saccharoperbutylacetonicum strain NI-4*. Applied Microbiology and Biotechnology, 2008. **78**(3): p. 483-493.
64. Tolonen, A.C., A.C. Chilaka, and G.M. Church, *Targeted gene inactivation in Clostridium phytofermentans shows that cellulose degradation requires the family 9 hydrolase Cphy3367*. Molecular Microbiology, 2009. **74**(6): p. 1300-1313.

65. Teng, L., et al., *Flavin mononucleotide (FMN)-based fluorescent protein (FbFP) as reporter for promoter screening in Clostridium cellulolyticum*. *Journal of Microbiological Methods*, 2015. **119**: p. 37-43.
66. Mordaka, P. and J.T. Heap, *Stringency of synthetic promoter sequences in Clostridium revealed and circumvented by tuning promoter library mutation rates*. *ACS Synthetic Biology*, 2018.
67. Nuyts, S., et al., *The use of radiation-induced bacterial promoters in anaerobic conditions: A means to control gene expression in Clostridium-mediated therapy for cancer*. *Radiation Research*, 2001. **155**(5): p. 716-723.
68. Hartman, A.H., H.L. Liu, and S.B. Melville, *Construction and Characterization of a Lactose-Inducible Promoter System for Controlled Gene Expression in Clostridium perfringens*. *Applied and Environmental Microbiology*, 2011. **77**(2): p. 471-478.
69. Al-Hinai, M.A., A.G. Fast, and E.T. Papoutsakis, *Novel System for Efficient Isolation of Clostridium Double-Crossover Allelic Exchange Mutants Enabling Markerless Chromosomal Gene Deletions and DNA Integration*. *Applied and Environmental Microbiology*, 2012. **78**(22): p. 8112-8121.
70. Banerjee, A., et al., *Lactose-Inducible System for Metabolic Engineering of Clostridium ljungdahlii*. *Applied and Environmental Microbiology*, 2014. **80**(8): p. 2410-2416.
71. Zhang, J., et al., *A novel arabinose-inducible genetic operation system developed for Clostridium cellulolyticum*. *Biotechnology for Biofuels*, 2015. **8**: p. 13.
72. Heim, R., D.C. Prasher, and R.Y. Tsien, *Wavelength mutations and posttranslational autoxidation of green fluorescent protein*. *Proceedings of the National Academy of Sciences of the United States of America*, 1994. **91**(26): p. 12501-12504.
73. Lippincott-Schwartz, J., E. Snapp, and A. Kenworthy, *Studying protein dynamics in living cells*. *Nature Reviews Molecular Cell Biology*, 2001. **2**(6): p. 444-456.
74. Gross, L.A., et al., *The structure of the chromophore within DsRed, a red fluorescent protein from coral*. *Proceedings of the National Academy of Sciences of the United States of America*, 2000. **97**(22): p. 11990-11995.

75. Shaner, N.C., et al., *Improved monomeric red, orange and yellow fluorescent proteins derived from Discosoma sp red fluorescent protein*. Nature Biotechnology, 2004. **22**(12): p. 1567-1572.
76. Day, R.N. and F. Schaufele, *Fluorescent protein tools for studying protein dynamics in living cells: a review*. Journal of Biomedical Optics, 2008. **13**(3): p. 6.
77. Zhang, C., X.-H. Xing, and K. Lou, *Rapid detection of a gfp-marked Enterobacter aerogenes under anaerobic conditions by aerobic fluorescence recovery*. FEMS Microbiology Letters, 2005. **249**(2): p. 211-218.
78. Ransom, E.M., C.D. Ellermeier, and D.S. Weiss, *Use of mCherry Red Fluorescent Protein for Studies of Protein Localization and Gene Expression in Clostridium difficile*. Applied and Environmental Microbiology, 2015. **81**(5): p. 1652-1660.
79. Pinilla-Redondo, R., L. Riber, and S.J. Sorensen, *Fluorescence Recovery Allows the Implementation of a Fluorescence Reporter Gene Platform Applicable for the Detection and Quantification of Horizontal Gene Transfer in Anoxic Environments*. Applied and Environmental Microbiology, 2018. **84**(6).
80. Keppler, A., et al., *A general method for the covalent labeling of fusion proteins with small molecules in vivo*. Nature Biotechnology, 2003. **21**(1): p. 86-89.
81. Regoes, A. and A.B. Hehl, *SNAP-tag (TM) mediated live cell labeling as an alternative to GFP in anaerobic organisms*. Biotechniques, 2005. **39**(6): p. 809-+.
82. Nicolle, O., et al., *Development of SNAP-tag-mediated live cell labeling as an alternative to GFP in Porphyromonas gingivalis*. Fems Immunology and Medical Microbiology, 2010. **59**(3): p. 357-363.
83. Los, G.V., et al., *HaloTag: A novel protein labeling technology for cell imaging and protein analysis*. Acs Chemical Biology, 2008. **3**(6): p. 373-382.
84. Martincova, E., et al., *Live Imaging of Mitosomes and Hydrogenosomes by HaloTag Technology*. Plos One, 2012. **7**(4): p. 6.

85. Li, C., A.G. Tebo, and A. Gautier, *Fluorogenic Labeling Strategies for Biological Imaging*. International Journal of Molecular Sciences, 2017. **18**(7): p. 11.
86. Drepper, T., et al., *Reporter proteins for in vivo fluorescence without oxygen*. Nature Biotechnology, 2007. **25**(4): p. 443-445.
87. Drepper, T., et al., *Flavin Mononucleotide-Based Fluorescent Reporter Proteins Outperform Green Fluorescent Protein-Like Proteins as Quantitative In Vivo Real-Time Reporters*. Applied and Environmental Microbiology, 2010. **76**(17): p. 5990-5994.
88. Lobo, L.A., C.J. Smith, and E.R. Rocha, *Flavin mononucleotide (FMN)-based fluorescent protein (FbFP) as reporter for gene expression in the anaerobe Bacteroides fragilis*. FEMS microbiology letters, 2011. **317**(1): p. 67-74.
89. Potzkei, J., et al., *Real-time determination of intracellular oxygen in bacteria using a genetically encoded FRET-based biosensor*. BMC Biology, 2012. **10**: p. 13.
90. Landete, J.M., et al., *Anaerobic green fluorescent protein as a marker of Bifidobacterium strains*. International Journal of Food Microbiology, 2014. **175**: p. 6-13.
91. Landete, J.M., et al., *Use of anaerobic green fluorescent protein versus green fluorescent protein as reporter in lactic acid bacteria*. Applied Microbiology and Biotechnology, 2015. **99**(16): p. 6865-6877.
92. Chapman, S., et al., *The photoreversible fluorescent protein iLOV outperforms GFP as a reporter of plant virus infection*. Proceedings of the National Academy of Sciences of the United States of America, 2008. **105**(50): p. 20038-20043.
93. Christie, J.M., et al., *Structural Tuning of the Fluorescent Protein iLOV for Improved Photostability*. Journal of Biological Chemistry, 2012. **287**(26): p. 22295-22304.
94. Buckley, A.M., et al., *Lighting Up Clostridium Difficile: Reporting Gene Expression Using Fluorescent Lov Domains*. Scientific Reports, 2016. **6**.

95. Seo, S.O., et al., *Development of an oxygen-independent flavin mononucleotide-based fluorescent reporter system in Clostridium beijerinckii and its potential applications*. Journal of Biotechnology, 2018. **265**: p. 119-126.
96. Jullien, L. and A. Gautier, *Fluorogen-based reporters for fluorescence imaging: a review*. Methods and Applications in Fluorescence, 2015. **3**(4): p. 12.
97. Plamont, M.-A., et al., *Small fluorescence-activating and absorption-shifting tag for tunable protein imaging in vivo*. Proceedings of the National Academy of Sciences, 2016. **113**(3): p. 497-502.
98. Li, C.G., et al., *Dynamic multicolor protein labeling in living cells*. Chemical Science, 2017. **8**(8): p. 5598-5605.
99. Pimenta, F.M., et al., *Chromophore Renewal and Fluorogen-Binding Tags: A Match Made to Last*. Scientific Reports, 2017. **7**: p. 8.
100. Emanuel, G., J.R. Moffitt, and X.W. Zhuang, *High-throughput, image-based screening of pooled genetic-variant libraries*. Nature Methods, 2017. **14**(12): p. 1159-+.
101. Kim, J.K., et al., *Phenolic Pyrogallol Fluorogen for Red Fluorescence Development in a PAS Domain Protein*. Chemistry of Materials, 2018. **30**(5): p. 1467-1471.
102. Li, C.E., et al., *Fluorogenic Probing of Membrane Protein Trafficking*. Bioconjugate Chemistry, 2018. **29**(6): p. 1823-1828.
103. Monmeyran, A., et al., *The inducible chemical-genetic fluorescent marker FAST outperforms classical fluorescent proteins in the quantitative reporting of bacterial biofilm dynamics*. Scientific Reports, 2018. **8**: p. 11.
104. Carlson, E.D. and E.T. Papoutsakis, *Heterologous Expression of the Clostridium carboxidivorans CO Dehydrogenase Alone or Together with the Acetyl Coenzyme A Synthase Enables both Reduction of CO₂ and Oxidation of CO by Clostridium acetobutylicum*. Applied and Environmental Microbiology, 2017. **83**(16): p. 15.
105. Jones, S.W., et al., *CO₂ fixation by anaerobic non-photosynthetic mixotrophy for improved carbon conversion*. Nature Communications, 2016. **7**: p. 9.

106. Fast, A.G. and E.T. Papoutsakis, *Functional Expression of the Clostridium ljungdahlii Acetyl-Coenzyme A Synthase in Clostridium acetobutylicum as Demonstrated by a Novel In Vivo CO Exchange Activity En Route to Heterologous Installation of a Functional Wood-Ljungdahl Pathway*. Applied and Environmental Microbiology, 2018. **84**(7): p. 15.
107. Kenealy, W.R. and D.M. Waselefsky, *Studies on the substrate range of Clostridium kluyveri; the use of propanol and succinate*. Archives of Microbiology, 1985. **141**(3): p. 187-194.
108. Baer, S.H., H.P. Blaschek, and T.L. Smith, *Effect of Butanol Challenge and Temperature on Lipid Composition and Membrane Fluidity of Butanol-Tolerant Clostridium acetobutylicum*. Applied and Environmental Microbiology, 1987. **53**(12): p. 2854-2861.
109. Huffer, S., et al., *Role of Alcohols in Growth, Lipid Composition, and Membrane Fluidity of Yeasts, Bacteria, and Archaea*. Applied and Environmental Microbiology, 2011. **77**(18): p. 6400-6408.
110. Ramio-Pujol, S., et al., *Effect of ethanol and butanol on autotrophic growth of model homoacetogens*. Fems Microbiology Letters, 2018. **365**(10): p. 4.
111. Remington, S.J., *Fluorescent proteins: maturation, photochemistry and photophysics*. Current Opinion in Structural Biology, 2006. **16**(6): p. 714-721.
112. Goehring, N.W. and J. Beckwith, *Diverse paths to midcell: Assembly of the bacterial cell division machinery*. Current Biology, 2005. **15**(13): p. R514-R526.
113. Adams, D.W. and J. Errington, *Bacterial cell division: assembly, maintenance and disassembly of the Z ring*. Nature Reviews Microbiology, 2009. **7**(9): p. 642-653.
114. Margolin, W., *Themes and variations in prokaryotic cell division*. Fems Microbiology Reviews, 2000. **24**(4): p. 531-548.
115. Deboer, P., R. Crossley, and L. Rothfield, *The essential bacterial cell-division protein FtsZ is a GTPase*. Nature, 1992. **359**(6392): p. 254-256.
116. Gueiros, F.J. and R. Losick, *A widely conserved bacterial cell division protein that promotes assembly of the tubulin-like protein FtsZ*. Genes & Development, 2002. **16**(19): p. 2544-2556.

117. Low, H.H., M.C. Moncrieffe, and J. Lowe, *The crystal structure of ZapA and its modulation of FtsZ polymerisation*. Journal of Molecular Biology, 2004. **341**(3): p. 839-852.
118. Small, E., et al., *FtsZ polymer-bundling by the Escherichia coli ZapA orthologue, YgfE, involves a conformational change in bound GTP*. Journal of Molecular Biology, 2007. **369**(1): p. 210-221.
119. Mermelstein, L.D. and E.T. Papoutsakis, *In vivo methylation in Escherichia coli by the Bacillus subtilis phage phi 3T I methyltransferase to protect plasmids from restriction upon transformation of Clostridium acetobutylicum ATCC 824*. Applied and Environmental Microbiology, 1993. **59**(4): p. 1077-1081.
120. Mermelstein, L.D., et al., *Expression of cloned homologous fermentative genes in Clostridium acetobutylicum ATCC 824*. Bio-Technology, 1992. **10**(2): p. 190-195.
121. Sillers, R., M.A. Al-Hinai, and E.T. Papoutsakis, *Aldehyde-Alcohol Dehydrogenase and/or Thiolase Overexpression Coupled With CoA Transferase Downregulation Lead to Higher Alcohol Titrers and Selectivity in Clostridium acetobutylicum Fermentations*. Biotechnology and Bioengineering, 2009. **102**(1): p. 38-49.
122. Nolling, J., et al., *Genome sequence and comparative analysis of the solvent-producing bacterium Clostridium acetobutylicum*. Journal of Bacteriology, 2001. **183**(16): p. 4823-4838.
123. Roach, E.J., M.S. Kimber, and C.M. Khursigara, *Crystal Structure and Site-directed Mutational Analysis Reveals Key Residues Involved in Escherichia coli ZapA Function*. Journal of Biological Chemistry, 2014. **289**(34): p. 23276-23286.
124. Chen, H.Y., et al., *Determination of the optimal aligned spacing between the Shine-Dalgarno sequence and the translation initiation codon of Escherichia coli in mRNAs*. Nucleic Acids Research, 1994. **22**(23): p. 4953-4957.
125. Salis, H.M., E.A. Mirsky, and C.A. Voigt, *Automated design of synthetic ribosome binding sites to control protein expression*. Nature Biotechnology, 2009. **27**(10): p. 946-U112.

126. Yang, Y.P., et al., *Improving the performance of solventogenic clostridia by reinforcing the biotin synthetic pathway*. *Metabolic Engineering*, 2016. **35**: p. 121-128.
127. Tracy, B.P., S.M. Gaida, and E.T. Papoutsakis, *Flow cytometry for bacteria: enabling metabolic engineering, synthetic biology and the elucidation of complex phenotypes*. *Current Opinion in Biotechnology*, 2010. **21**(1): p. 85-99.
128. Rohlhill, J., N.R. Sandoval, and E.T. Papoutsakis, *Sort-Seq Approach to Engineering a Formaldehyde-Inducible Promoter for Dynamically Regulated Escherichia coli Growth on Methanol*. *Acs Synthetic Biology*, 2017. **6**(8): p. 1584-1595.
129. Galli, E. and K. Gerdes, *Spatial resolution of two bacterial cell division proteins: ZapA recruits ZapB to the inner face of the Z-ring*. *Molecular Microbiology*, 2010. **76**(6): p. 1514-1526.
130. Galli, E. and K. Gerdes, *FtsZ-ZapA-ZapB Interactome of Escherichia coli*. *Journal of Bacteriology*, 2012. **194**(2): p. 292-302.
131. Eswaramoorthy, P., et al., *Cellular Architecture Mediates DivIVA Ultrastructure and Regulates Min Activity in Bacillus subtilis*. *Mbio*, 2011. **2**(6).
132. Gildemyn, S., et al., *Upgrading syngas fermentation effluent using Clostridium kluyveri in a continuous fermentation*. *Biotechnology for Biofuels*, 2017. **10**.
133. Anderson, D.E., F.J. Gueiros-Filho, and H.P. Erickson, *Assembly dynamics of FtsZ rings in Bacillus subtilis and Escherichia coli and effects of FtsZ-regulating proteins*. *Journal of Bacteriology*, 2004. **186**(17): p. 5775-5781.
134. Jensen, S.O., L.S. Thompson, and E.J. Harry, *Cell division in bacillus subtilis: FtsZ and FtsA association is Z-ring independent, and FtsA is required for efficient midcell Z-ring assembly*. *Journal of Bacteriology*, 2005. **187**(18): p. 6536-6544.
135. Guerrini, O., et al., *Characterization of two 2 4Fe4S ferredoxins from Clostridium acetobutylicum*. *Current Microbiology*, 2008. **56**(3): p. 261-267.

Appendix A

SYNTROPHIC INTERACTIONS IN CLOSTRIDIA CO-CULTURES

Table A.1 Strains and plasmids used in this study

Strain	Relevant Characteristics	Source
<i>C. acetobutylicum</i>		
ATCC 824	Wild-type strain	ATCC
<i>C. ljungdahlii</i>		
ATCC 55383	Wild-type strain	ATCC
<i>C. kluyveri</i>		
ATCC 8527	Wild-type strain	ATCC

Appendix B

ENGINEERING A FLUORESCENT REPORTER SYSTEM AND VIEWING PROTEIN LOCALIZATION WITH FAST IN *Clostridium acetobutylicum*

Table B.1 Strains and Plasmids used in this study

Strain	Relevant Characteristics	Source
<i>E. coli</i>		
NEB 5-alpha	<i>fhuA2 Δ(argF-lacZ)U169 phoA glnV44 Φ80 Δ(lacZ)M15 gyrA96 recA1 relA1 endA1 thi-1 hsdR17</i>	NEB
ER2275	<i>hsdR mcrA recA1 endA1</i>	NEB
<i>C. acetobutylicum</i>		
ATCC 824	Wild-type strain	ATCC
Plasmids		
pAN3	<i>Km^r ; Φ3T I gene</i>	Al-Hinai <i>et al.</i> 2012
pSOS94_MCS	<i>ptb promoter, Amp^r MLS^r ColE1 Ori repL, MCS</i>	Al-Hinai <i>et al.</i> 2012
pSOS95_MCS	<i>thl promoter, Amp^r MLS^r ColE1 Ori repL, MCS</i>	Fast and Papoutsakis 2018
p95thlFAST	<i>thl promoter, Amp^r MLS^r ColE1 Ori repL FAST</i>	This study
p95thl ^{sup} FAST	<i>thl^{sup} promoter, Amp^r MLS^r ColE1 Ori repL FAST</i>	This study
p95adcFAST	<i>adc promoter, Amp^r MLS^r ColE1 Ori repL FAST</i>	This study
p95adc ^{mod} FAST	<i>adc^{mod} promoter, Amp^r MLS^r ColE1 Ori repL FAST</i>	This study
p95ptbFAST	<i>ptb promoter, Amp^r MLS^r ColE1 Ori repL FAST</i>	This study
p95ptb ^{mod} FAST	<i>ptb^{mod} promoter, Amp^r MLS^r ColE1 Ori repL FAST</i>	This study
p95ZapA-FAST	<i>thl promoter, ZapA, Amp^r MLS^r ColE1 Ori repL ZapA FAST</i>	This study

Table B.2 Primers used in this study. Binding regions are indicated by uppercase.
Homology regions are indicated by lowercase.

Number	Primer ID	Sequence 5'-3'
1	p95_FAST_F	ATGGAACACGTCAGCATTG
2	p95_FAST_R	CACGCCATTCCAACCAATAG
3	p95_thlFAST_F	CAGGAGGTAGTCTATATGGAACAC
4	p95_thlFAST_R	AAAAAATAAAGAGGGTTATAATGAAC
5	p95_thlsupFAST_F	AGGAGGTTAGGATCCATGG
6	p95_thlsupFAST_R	AAAAAATAAAGAGGGTTATAATGAAC
7	ptb_F	ttcattataaccctctttatcttCCTCCTTAT AAAATTAGTATAATTATAGC
8	ptb_R	cggttccatagactacctcctgCATTTATATTTT AACAAACTTTTCACATG
9	mod_ptb_F	ttcattataaccctctttatcttCCTCCTTATAAAAT TAGTATAATTATAGC
10	mod_ptb_R	cggttccatggatcctaaccctcctCATTTATATTTT AACAAACTTTTCACATG
11	adc_F	ttcattataaccctctttatcttCCTCCTTATAAAAT TAGTATAATTATAGC
12	adc_R	cggttccatagactacctcctgAAAAGTCACCTT CCTAAATTTAATAATG
13	mod_adc_F	ttcattataaccctctttatcttCCTCCTTATAAAAT TAGTATAATTATAGC
14	mod_adc_R	cggttccatggatcctaaccctcctAAAAGTCACCT TCCTAAATTTAATAATG